

Europa Surface and Atmospheric Sample Probe
“Minos Probe”
Team 4
Final Design Report



Ian Pylkkanen, John Keis, Michael Kern, Matthew Okay, Botao Zhao, DigVijay Ghule

Under the Direction of Professor K.S. Anderson
MANE 4850 Space Vehicle Design Capstone

December 9, 2019
Rensselaer Polytechnic Institute

Table of Contents

Acknowledgements	4
Contributions	4
Executive Summary	5
List of Terms, Acronyms, and Abbreviations	6
List of Tables	8
List of Figures	9
1 Introduction and Background	10
1.1 Past Missions	10
1.2 Mission Purpose	10
2 Scope	10
2.1 Customer Requirements	10
2.2 Objectives	11
2.3 Considerations	11
2.3.1 Technical Issues	11
2.3.2 Time Constraints	11
2.3.3 Environmental Constraints	11
2.3.4 Political Constraints	12
2.3.5 Cost Constraints	12
3 Design	12
3.1 Power	12
3.1.1 Power Requirements & Scheduling	12
3.1.2 Radioisotope Thermoelectric Generator	12
3.1.3 Battery Characteristics & Sizing	13
3.1.4 Power Control, Monitoring, & Regulation System	14
3.1.5 Future Work	16
3.2 Propulsion	16
3.2.1 Trajectory Overview	16
3.2.2 Computational Analysis	16
3.2.3 Propellant	18
3.2.4 Attitude Control	19
3.2.5 Main Engine	20

3.2.6	Future Work	21
3.3	Structures	21
3.3.1	Design Overview	21
3.3.2	Materials	21
3.3.3	Chassis Structure	23
3.3.4	Landing Legs	24
3.3.5	Final Assembly	25
3.3.6	Finite Element Analysis	27
3.3.7	Future Work	29
3.4	Mechanisms/Deployables	30
3.4.1	Landing Mechanisms/Deployables	30
3.4.2	Scientific Payload	31
3.4.3	Communication Deployables	32
3.4.4	Future Work	35
3.5	Command and Data	35
3.5.1	Hardware	36
3.5.2	In Transit to Europa	36
3.5.3	Landing	36
3.5.4	Initial Deployments	38
3.5.5	Sample Collection	38
3.5.6	Window of Communication	41
3.5.7	Communication	42
3.5.8	Failure Mitigation	42
3.5.9	Power Consumption	43
3.5.10	Future Work	43
3.6	Communications	43
3.6.1	Communications System Overview	43
3.6.2	Communications Window	43
3.6.3	UHF System	44
3.6.4	X-Band System	46
3.6.5	Future Communication Work	47
3.7	Thermal Control	48

3.7.1	Preliminary Design	48
3.7.2	Heating	48
3.7.3	Internal Heat Transfer	49
3.7.4	Thermal Radiation	50
3.7.5	Future Work	50
4	Budgets Summary	51
4.1	Mass Budget	51
4.2	Power Budget	51
4.3	Propulsion Budget	51
5	Risks	52
5.1	Public Health, Environmental, Social, Cultural, and Economic Risks	52
5.2	Mission Risks	52
5.3	Power Risks and Mitigations	52
5.4	Propulsion Risks and Mitigations	53
5.5	Structures Risks and Mitigation	53
5.6	Mechanisms/Deployables Risks and Mitigations	54
5.7	Command and Data Risks and Mitigations	54
5.8	Communications Risks and Mitigations	55
5.9	Thermal Control Risks and Mitigations	55
6	Timeline and Planning	56
7	Conclusion	57
	References	58
	Appendix A	62
	Deliverables	62
	Risk Tables	62
	Appendix B	66
	Appendix C	69
	Appendix D	72
	Appendix E	74

Acknowledgements

As a team, we would like to thank Dr. Kurt Anderson. As a professor and associate dean in the Mechanical, Aerospace and Nuclear Engineering department at Rensselaer Polytechnic Institute, his insight and teachings from his many years of experience in the space industry have been invaluable.

Contributions

Team 4 Contributions		
	Section	Contributor
-	Report Structure and Formatting	Ian Pylkanen, John Keis
-	Executive Summary	Ian Pylkanen, John Keis
1	Introduction and Background	Ian Pylkanen, John Keis
2	Scope	Matthew Okay
3.1	Power Systems	DigVijay Ghule
3.2	Propulsion	Michael Kern
3.3	Chassis	Botao Zhao
3.4	Mechanisms/Deployables	Ian Pylkanen
3.5	Command and Data	Matthew Okay
3.6	Communications	John Keis
3.7	Thermal Control	Justin Weiss
4	Budgets	All members
5	Risks	All Members
6	Timeline and Planning	Botao Zhao
7	Conclusion	Ian Pylkanen, Michael Kern

Executive Summary

This report outlines the final design of the Minos Probe (MP) given the scope of the class. All major subsystems have been decided and analysis performed. The systems have been designed for the MP to travel to Europa on-board the Rhadamanthus-Orbiter (RO). Once RO reaches Europa, the Minos Probe will be jettisoned and perform a powered descent onto the surface of Europa performing a soft landing. Once on the surface of Europa, the Minos Probe will collect valuable data on the composition of the atmosphere and surface ice, as well as take pictures of the landscape of the landing site. It is hoped that the MP's landing site will be near one of Europa's geysers, allowing for analysis of material from below Europa's surface. The data that is collected will be transmitted back to RO and subsequently on to Earth. The Minos Probe will not be stationary and will not leave the surface of Europa.

This report touches on past missions that allowed for a better understanding of the overall purpose and influences of the current planned mission. Customer requirements have been outlined to provide a guide of the project objectives, considerations, requirements, and risks. The design of the Minos Probe will be detailed in its seven sub-systems: power, propulsion, chassis, deployables, command and data, communications, and thermal control. Basic engineering analysis will also be discussed for each subsystem. A risk analysis has been performed for all sub-systems, as well as the mission as a whole. A timeline for current and future development has also been provided.

It is important to note due to the scope of the class, the limited time, and the limited resources that are available to the team, this final design report lies more in line with what a preliminary design report for an actual aerospace engineering firm would be. Future work has been addressed for each subsystem in the hypothetical scenario that the limitations stated above were overcome.

The Preliminary Design Report produced on 10/21/2019 is referenced frequently throughout this report and can be found in Appendix E.

List of Terms, Acronyms, and Abbreviations

BAE - British Aerospace

CPU - Central Processing Unit

EEPROM - Electrically Erasable Programmable Read-Only Memory

EPS - Electrical Power System

ESA - European Space Agency

GPHS-RTG - General-Purpose Heat Source Radioisotope Thermoelectric Generator

HGA – High Gain Antenna

JPL - Jet Propulsion Lab

K – Kelvin

Kbps – Kilobits per second

LEO – Low Earth Orbit

MB - Mega Bites

MHW-RTG - Multihundred-Watt Radioisotope Thermoelectric Generator

MLI - Multilayer Insulation

MMH - Monomethyl hydrazine

MMRTG - Multi-Mission Radioisotope Thermoelectric Generator

MP - Minos Probe

MSL - Mars Science Laboratory

NASA- National Aeronautics and Space Administration

REASON - Radar for Europa Assessment and Sounding: Ocean to Near-Surface

RHU - Radioisotope Heating Units

RO- Rhadamanthus-Orbiter

RTG - Radioisotope Thermal Generator

SAM - Sample Analysis at Mars

SC1s – Scientific Chambers next to the RTG

SC2s – Scientific Chambers next to the communications

SDST – Small Deep Space Transponder

SNAP-19 - Systems Nuclear Auxiliary POWER 19

SSPA – Solid State Power Amplifier

SUDA - Surface Dust Analyzer

TCS - Thermal Control System

TDA – Terminal Descent Altitude

UHF - Ultra-High Frequency (300 MHz to 3 GHz)

X-Band - 8 – 12 GHz

List of Tables

Table 1: Material Selection Matrix	22
Table 2: Mechanical Properties of 2219-T87 Aluminum Alloy [42]	23
Table 3: Mesh Characteristics.....	29
Table 4: Scientific Payload Mass and Power Usage.....	32
Table 5: Acceptable Temperature Ranges	48
Table 6: Desired Temperatures by Compartment	49
Table 7: Thermal Strap Cross-sectional Areas	50
Table 8: Mass Budget	51
Table 9: Power Budget.....	51
Table 10: Propulsion Budget	51
Table 11: Course Deliverables.....	62
Table 12: Mission Risk Table	62
Table 13: Power System Risk Table.....	63
Table 14: Propulsion System Risk Table.....	63
Table 15: Chassis Risk Table.....	63
Table 16: Mechanisms/Deployables System Risk Table.....	64
Table 17: Command and Data System Risk Table	64
Table 18: Communications System Risk Table.....	65
Table 19: Thermal System Risk Table.....	65
Table 20: MER X-band and UHF Mass and Input Power Summary [17].....	66
Table 21: MRO Telecom Mass and Power Summary [22].....	67
Table 22: STK Communications Simulation	68

List of Figures

Figure 1: Diagram of an MMRTG [1]	13
Figure 2: Lithium Ion Battery Assembly Unit.....	14
Figure 3: Battery Control Board [6].....	15
Figure 4: Interpoint SMFLHP DC-DC Converter [8].....	15
Figure 5: Hohmann-Transfer (Note: Not to scale) [Appendix C].....	16
Figure 6: TDA and Vertical Descent (Note: Not to scale) [Appendix C]	17
Figure 7: MATLAB Output [Appendix C].....	18
Figure 8: Bi-Propellant System.....	19
Figure 9: Cold Gas Thruster Arrangement	19
Figure 10: Triad Thruster [9]	20
Figure 11: R-42 Engine [10]	20
Figure 12: Strength of 2024 Aluminum [4]	22
Figure 13: Chassis Octagonal Design.....	24
Figure 14: Landing Leg Design	24
Figure 15: Section View of a Shock Absorber [27].....	25
Figure 16: Lander Configuration	25
Figure 17: Lander 2-D Sketch.....	26
Figure 18: Lander Configuration (folded)	26
Figure 19: Lander 2-D Sketch (folded).....	27
Figure 20: Mesh Type and Total Number.....	28
Figure 21: Maximum Displacement	28
Figure 22: Maximum Principal Stress	29
Figure 23: Crushable Legs Dimensions (dimensions in mm).....	30
Figure 24: Two-Axis Gimbal [15]	34
Figure 25: High-Gain Gimbal Design [16].....	34
Figure 26: Gimbal Pin-Puller Configuration [16].....	35
Figure 27: Landing Command Scheme	36
Figure 28: Cold Thrusters Command Scheme.....	37
Figure 29: Initial Deployables Command Scheme	38
Figure 30: Atmospheric Readings Command Scheme	39
Figure 31: Mastcam-Z Command Scheme	40
Figure 32: Ice Analysis Command Scheme	41
Figure 33: Communication Command Scheme	42
Figure 34: STK simulated orbit and communications between the RO and MP.....	44
Figure 35: C/TT-505 Transceiver being used on the Minos Probe ^[21]	45
Figure 36: UHG antenna pattern [17]	45
Figure 37: SDST being used on the Minos Probe [17].....	46
Figure 38: High gain antenna mounted to 2-axis gimbal being used on the Minos Probe.	47

1 Introduction and Background

1.1 Past Missions

Key missions in the past, present, and future are briefly described in the bullet points that follow.

- 1973, 1974: Pioneer 10 and 11 become the first orbiters to image Europa during their flybys of Jupiter.
- 1979: Voyager 1 and 2 take higher resolution images of Europa during their flybys of Jupiter. Icy surface observed. Speculation of ocean underneath.
- 1995-2003: Galileo takes the most detailed images of Europa.
- 2007: New Horizons images Europa on its way to Pluto.
- 2013: NASA's Hubble Telescope observes what is theorized to be plumes of water spouting from geysers on Europa's surface.
- Europa Clipper is a future mission to orbit Jupiter and take detailed images and data of Europa's surface.

1.2 Mission Purpose

Human kind greatly values life and knows how vast it can be in all of its forms. We are a curious species by nature and have an inherent gene for exploration. For centuries we have wondered what is beyond Earth and is it possible that life could exist elsewhere. This mission is an exploratory mission designed to further study Jupiter's moon, Europa. The hope is to analyze the composition of Europa's atmosphere and surface to discover if it contains any of the elements we know are associated with the presence of life. This mission would be the first to land and analyze physical samples Europa. This mission will provide some of these answers and provide a framework for future missions to the surface of Europa.

2 Scope

2.1 Customer Requirements

The National Aeronautics and Space Administration (NASA) and the European Space Agency (ESA) have outlined a need for further investigation of Europa. The customer requires that a probe be delivered to the surface of Europa and conduct atmospheric and surface analysis. This requires a need to (1) deliver the scientific payload to Europa/Jupiter orbit, (2) successfully deploy the probe and land on the surface and, (3) take the required measurements that can then be transmitted to the orbiter and then to earth.

2.2 Objectives

This report details the design and development of the probe, which will be capable of safely landing on the surface and conducting analysis to be transmitted to the orbiter. This project consists of a design phase, followed by a development phase. The design was divided into seven subsystems; power, propulsion, chassis, mechanisms/deployables, command and data, communications, and thermal control.

2.3 Considerations

2.3.1 Technical Issues

An unmanned landing in Europa's harsh environmental conditions is extremely challenging. It will require state of the art propulsion and command systems to ensure a safe descent.

Due to high amounts of radiation, communication windows to the orbiter will be limited. A significant delay between the Minos Probe and Earth will need to be accounted for. This could potentially cause a problem with the probe to go unnoticed on earth until it is too late to try and reprogram.

Surface temperatures on Europa are exceptionally cold, averaging around 110 Kelvin. To combat this, a strong thermal control system must be utilized, with minimal room for failure, making the design of a high functioning thermal control system a top priority. Additionally, at low temperatures optical distortion can occur, and can make imaging a more difficult task.

2.3.2 Time Constraints

NASA has not defined any specific time requirements at this time. Depending on the trajectory taken, it could take the RO and Minos Probe several years to reach Europa. The Minos Probe is currently being designed to have a life span of around one year on the surface of Europa. The only time requirements at the moment are due to the launch window. Deep space travel requires departing the Earth at a time when Jupiter and Earth are at their closest.

2.3.3 Environmental Constraints

The environmental constraints occur in two different environments, one on Earth and one on Europa. On earth, the environmental constraints are mostly concerned with the launch of the spacecraft. Due to the probe's design, there will be a large amount of radioactive material aboard, between the Radioisotope Thermal Generator (RTG) power source and the Radioisotope Heating Units (RHU). A launch failure can result in mandated quarantine zone due to large amount of radiation that can be released upon a crash. Furthermore, even if the radioactive units are protected, a crash with leaked propellant can cause environmental damage.

On Europa, the largest environmental constraints come from data collection. During landing, if the thrusters are not turned off at an adequate position, there is a possibility of propellant

contamination. It is also possible that the scientific instrumentation can become contaminated from substances on Earth, and skew the data in an untruthful way.

2.3.4 Political Constraints

A mission of this magnitude can have a large array of political consequences. Due to highly radioactive materials, there can be skepticism from political constituents on the risk-reward practicality of the mission. There can be further skepticism in this regard for the high cost of the mission, that will have to come from taxpayers, and may not be considered worth the price. The last majorly political issue will regard if the mission discovers possibilities of life, and how this may affect the fundamental human understanding of the universe.

2.3.5 Cost Constraints

The cost constraints of this mission will involve the specific agencies funding the mission. This may vary due to different government policies, and geopolitical climates in the countries funding the mission.

3 Design

3.1 Power

3.1.1 Power Requirements & Scheduling

An early estimate of the power requirements allocated 150-200 W to run all systems at maximum load. A full breakdown of the power requirements by subsystem is located in Section 4.2. Since the thermal control system does not require power for its functions, the power generated from the source will be allocated between the mechanisms/deployables system (scientific instruments) and the communications system in an alternating schedule in order to provide each with the necessary power to complete its functions. The command/data system will receive continuous power for the duration of the mission due to its significance to the life of the MP spacecraft.

3.1.2 Radioisotope Thermoelectric Generator

For the power source of the MP spacecraft, a radioisotope thermoelectric generator (RTG) was chosen in order to provide the vehicle with steady and continuous electrical power for the duration of the mission. The RTG will also allow the spacecraft to be fully independent from sunlight as it does lack intensity on the surface of Europa. The model of RTG that was selected is the Multi-Mission Radioisotope Thermoelectric Generator (MMRTG) developed by Aerojet Rocketdyne and Teledyne Energy Systems [1]. This model was most famously used on the 2011 Mars Science Laboratory (MSL) mission, or Curiosity rover, which saw great success in terms of its expansion on the overall lifespan of the mission. The MMRTG is powered by plutonium-238 (^{238}Pu) and consists of eight general-purpose heat source (GPHS) modules, provided by the Department of Energy [2]. The heat from radioactive decay within the GPHS modules is then converted to

electricity using 16 thermoelectric modules of 48 PbTe/TAGS thermoelectric couples connected to a heat sink [2]. The MMRTG will generate 110 W of electric power and 2000 W of thermal power beginning of life (BOL), while only dropping to 100 W of electric power at end of life (EOL) [2]. Also, with a mass of 45 kg, the MMRTG provides 2.4 W/kg of electric power at BOL [2]. The dimensions of the MMRTG are 64 cm in diameter (fin-tip to fin-tip) by 66 cm tall [2]. Ample shielding in the form of a 2.5 mm lead sheet will be used in order to block the electronics within the spacecraft from radiation damage. Furthermore, the MMRTG will also be an integral part of the thermal control system with the use of aluminum thermal straps that transmit waste heat from the RTG fins to the rest of the spacecraft. Figure 1 below represents a diagram of an MMRTG.

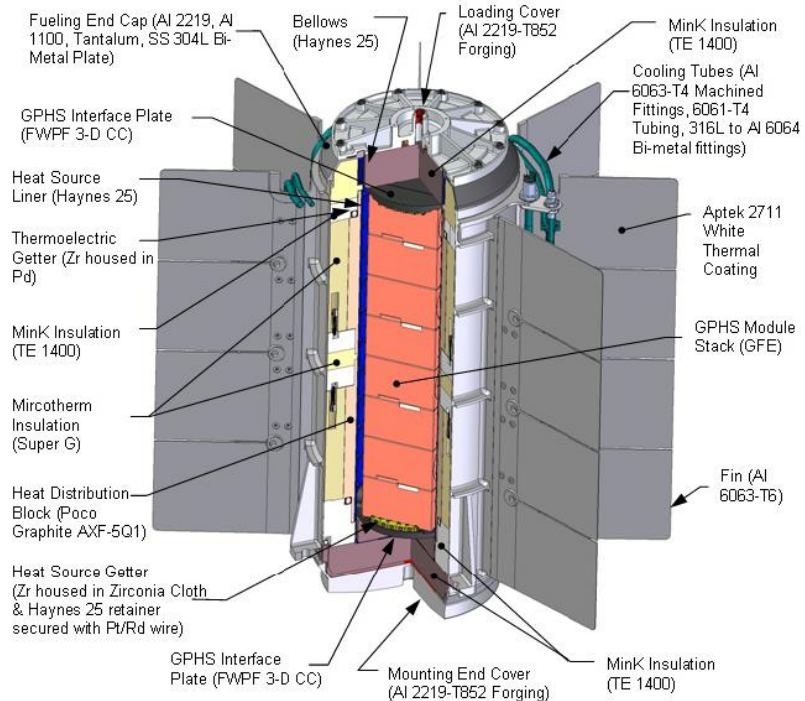


Figure 1: Diagram of an MMRTG [1]

3.1.3 Battery Characteristics & Sizing

For the power storage of the MP spacecraft, lithium-ion (Li-Ion) batteries were chosen as the rechargeable, secondary battery. In particular, the “heritage” MCMB-LiNiCoO₂ cell chemistry manufactured by Yardney Technical Products (EaglePicher Technologies, LLC) will be utilized in the Li-Ion batteries, where nickel-cobalt oxide (NCO) will be used as the cathode, meso-carbon microbeads (MCMB) will be used as the anode, and the low-temperature electrolyte will be based on a ternary mixture of carbonate solvents, developed at NASA Jet Propulsion Laboratory (JPL) [3] [4]. The MP battery assembly configuration will consist of two parallel 8-cell batteries (8s2p) [3]. The batteries will feature a 43 Ah prismatic cell design and the cell size or model will be NCP 43-1, seen previously on the MSL Curiosity rover [3]. The operating voltage range for the batteries

will be 24-32.8 V [3]. The batteries will also have a cycle life greater than 1,000 cycles at 100% depth of discharge (DOD) [3]. Also, the operating temperature range for the batteries will be -20°C to 30°C [3]. At -20°C, the batteries are capable of delivering about 75% of their ambient-temperature capacity [4]. The mass of the battery assembly will be 26.5 kg with a specific energy of 104 Wh/kg [3]. The following image, Figure 2, is a Li-Ion battery assembly unit which was also used on the Curiosity rover.



Figure 2: Lithium Ion Battery Assembly Unit

3.1.4 Power Control, Monitoring, & Regulation System

Furthermore, since the MP spacecraft does not include any solar arrays and only consists of an RTG as its primary power source, the vehicle does not require internal source control in the form of direct energy transfer (DET) and peak power tracking (PPT) systems which both incorporate the shunt regulator into their designs. The RTG will produce electricity at a constant rate as long as heat is generated from the radioactive decay of ^{238}Pu . As a result, the power generated from the RTG will be controlled externally through the energy storage control system and the power management and distribution (PMAD) system. For energy storage control, the MP will have an onboard battery management system (BMS) in order to monitor and balance the voltages, temperature, and DOD within the individual cells contained in the battery assembly unit [5]. The BMS will also protect the batteries from overcharge and over-discharge and provide cell balance [5]. In the case of the BMS, the cell voltage will be kept at 3.5 V and the battery assembly unit will be at the bus voltage of 28 V at discharge [6]. The batteries will be kept at a temperature of 20°C in order to optimize its performance. The batteries will be also limited to 50% DOD during the main mission on the surface of Europa to prevent cell performance degradation over this 12-month lifespan [6].

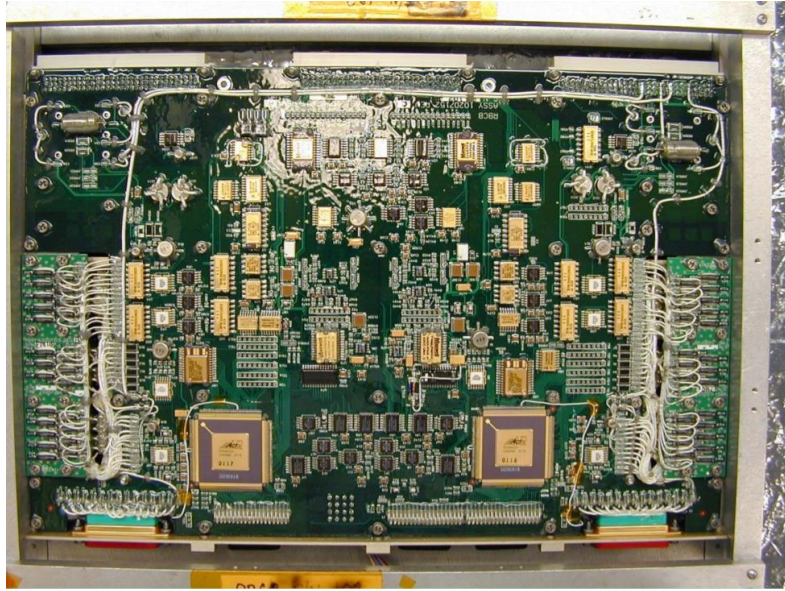


Figure 3: Battery Control Board [6]

In addition, there are three main components of the PMAD system; Fault Detection, Isolation, and Recovery, Management and Control, and Distribution and Transmission [7]. Firstly, the MP will feature autonomous fault detection and isolation algorithms in order to detect faults in the power system and protect the main bus from any catastrophic failures which would impact the mission [7]. Secondly, the MP will use tantalum wet-slug capacitors as input and output filter capacitors of DC-DC converters in order to store energy in the form of a separated electrical charge [3]. Finally, the MP will contain a series of DC-DC converters in order to convert a source of direct current from one voltage to another. This is required to transmit power from the power source to the scientific instruments and equipment. The MP will include various Interpoint DC-DC converters and EMI filter modules such as the SMFLHP, SMRT, SMHF, and SFME, developed by Crane Aerospace & Electronics [8].



Figure 4: Interpoint SMFLHP DC-DC Converter [8]

3.1.5 Future Work

In future iterations of this project, more specific and detailed analysis will be performed using the exact load demands of the system. The exact configuration of the RTG, Li-Ion batteries, and power control system within the chassis of the MP will be determined. Also, a complete functional block diagram will be completed for the power control systems. Furthermore, a complete power schedule for the entire mission lifespan must be computed. Finally, the wiring between the power source, storage, and control systems must be designed.

3.2 Propulsion

3.2.1 Trajectory Overview

Starting from an estimated 100 km circular parking orbit, the Minos Probe (MP) will perform a series of retrograde burns and a gravity-assisted turn in order to land on the surface of Europa. The first retrograde burn will result in an elliptical trajectory to initiate a Hohmann-transfer maneuver. Next, the MP will execute a gravity-assisted turn to increase vertical velocity and a retrograde burn to reduce horizontal velocity to zero. During terminal descent, vertical velocity and acceleration will be regulated by the main engine to ensure that loads on the spacecraft remain within allowable levels. Zero vertical velocity and engine shutdown will occur at an altitude of two meters.

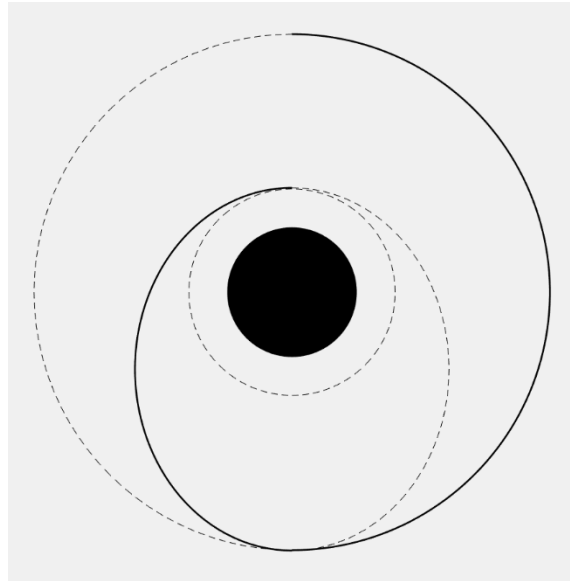


Figure 5: Hohmann-Transfer (Note: Not to scale) [Appendix C]

3.2.2 Computational Analysis

A MATLAB script was written to compare estimated ΔV requirements for a range of landing profiles [Appendix C]. The solution is constrained by a need for vehicle safety as well as fuel efficiency. These two criteria are at odds with each other, as a Hohmann transfer alone would result in a dangerously high velocity at low altitudes. Conversely, a direct descent consumes significantly more fuel.

The following equations were used to estimate the ΔV required for the MP to land on the surface of Europa from an altitude of 100 km. ΔV changes were assumed instantaneous and finite burn losses were considered negligible. The calculation was simplified to Hohmann-Transfer ΔV added to the ΔV gain of an object falling to the surface from TDA. Atmospheric drag was neglected given Europa's incredibly thin atmosphere.

$$(\Delta V)^2 = 2g(\text{altitude}) \quad \text{Eq. 2.1}$$

$$V = \frac{h}{r} \quad \text{Eq. 2.2}$$

$$V_{circle} = \sqrt{\mu/r_{orbit}} \quad \text{Eq. 2.3}$$

$$h = \sqrt{2\mu} \sqrt{\frac{r_a r_b}{r_a + r_b}} \quad \text{Eq. 2.4}$$

$$\mu = 3201$$

$$r_{\text{europa}} = 1561$$

$$g = 1.315$$

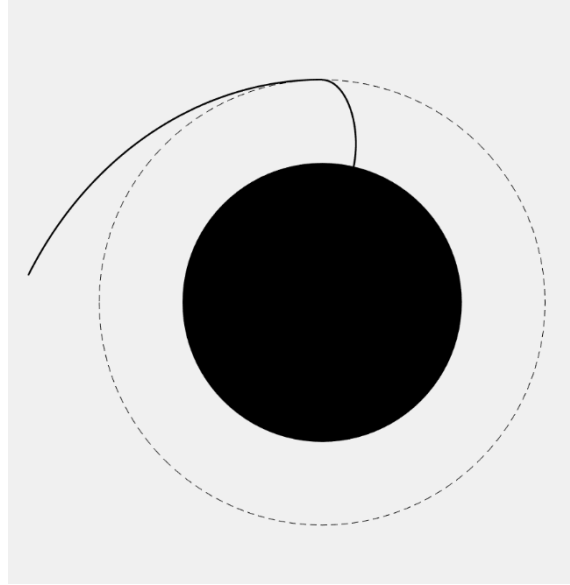


Figure 6: TDA and Vertical Descent (Note: Not to scale) [Appendix C]

Based on simulation data and comparisons to Apollo flightpaths, TDA was determined to be optimal at 15 km. The resulting trajectory reduces the risk of impact, offers room to maneuver, and requires less fuel. The margin of error for retrograde ΔV is 18%. This was determined by calculating the ΔV required to induce a transfer orbit that intersects the surface of Europa. From 15 km, terminal descent duration can preserve fuel efficiency in the range of 20-60 seconds. A TDA of 15km requires 20% less ΔV than a direct descent alone, improving the fuel to weight ratio of the MP.

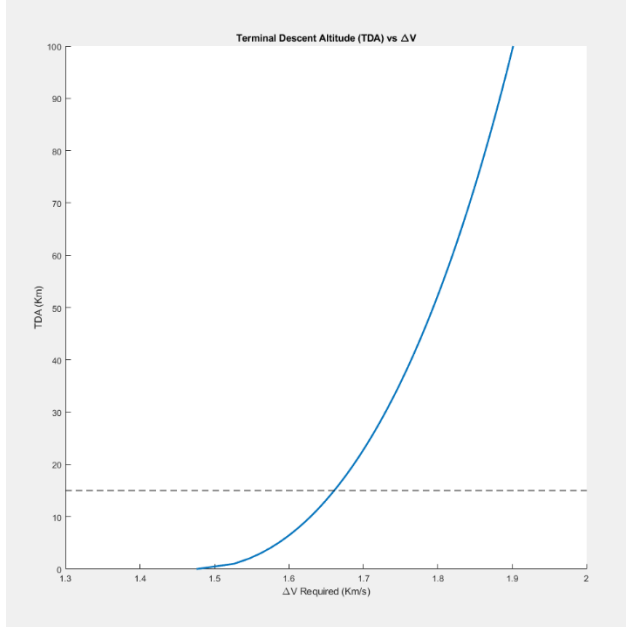


Figure 7: MATLAB Output [Appendix C]

The ΔV corresponding to a TDA of 15 km is approximately 1.66 km/s. A solar system ΔV map [Appendix C] was consulted to compare results. ΔV is listed as 1.45 between Europa and a 100 km orbit. Acknowledging that the model involved significant simplifications; ΔV output of the MP was increased by 20% to 2 km/s. This added margin will also increase the MP's maneuverability during terminal descent. The following equation is used to calculate the mass ratio

$$\Delta V = I_{SP} g_0 \ln \frac{m_0}{m_f} \quad Eq. 2.5$$

$$I_{SP, MMH} = 303$$

$$g_0 = 0.00981$$

3.2.3 Propellant

The main engine is a bi-propellant system using Monomethyl hydrazine (MMH) and Nitrogen Tetroxide. MMH is a hydrazine variant with a lower freezing temperature than hydrazine. Frozen fuel is a significant concern for the mission given the frigid environment. Taking advantage of MMH's relative thermal advantage over Hydrazine, it was selected for this mission despite its lower specific impulse. The mass ratio for the MP is 1.96. Probe mass is estimated to be 380 kg resulting in a total launch mass of the MP is 745 kg.

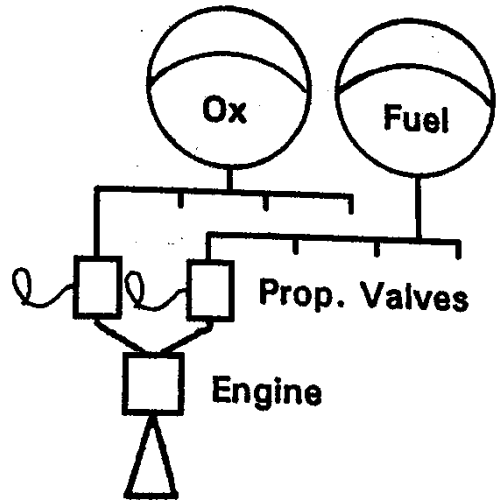


Figure 8: Bi-Propellant System

Selecting MMH for fuel had thermal benefits but came at the cost of added mass. While hydrazine can utilize a dual-mode propulsion system, MMH must have a secondary system for attitude control. An arrangement of four nitrogen gas thrusters was selected for this purpose.

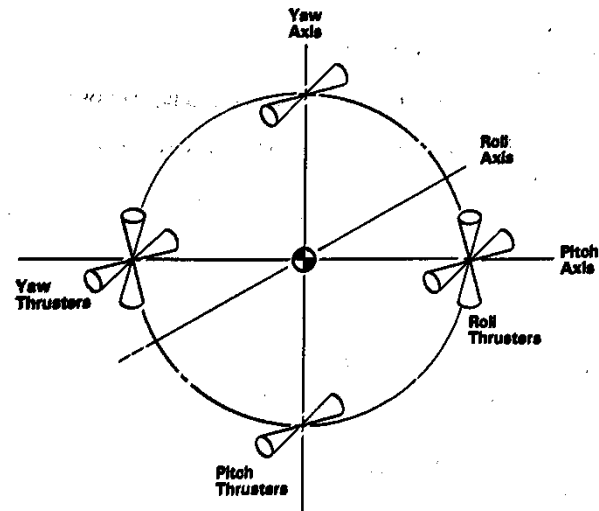


Figure 9: Cold Gas Thruster Arrangement

3.2.4 Attitude Control

The flight-proven Vacco 2 lbf cold gas triad thruster from NASA's Manned Maneuvering Unit (MMU) is used to provide attitude control. Nitrogen gas is stored in a spherical tank at 220 PSI. The command and data subsystem controls solenoid function to maintain an upright orientation throughout descent.

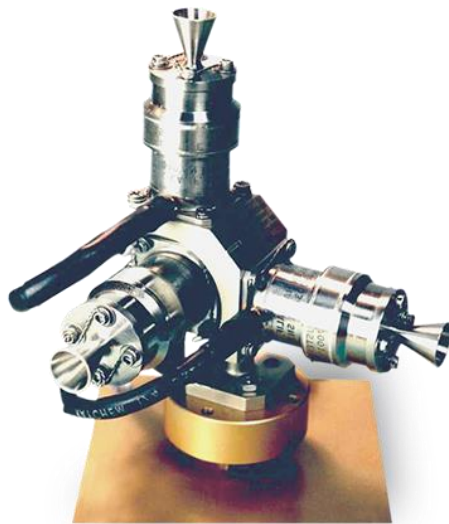
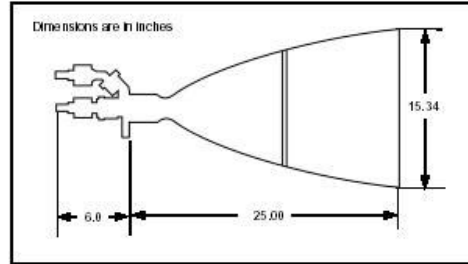


Figure 10: Triad Thruster [9]

3.2.5 Main Engine

R-42 - 890N (200 lbf) BIPROPELLANT ROCKET ENGINE



Design Characteristics

- Propellant MMH/NTO(MON-3)
 - Thrust/Steady State..... 890 N (200 lbf)
 - Inlet Pressure Range..... 29.3-6.9 Bar (425-100 psia)
 - Chamber Pressure*..... 7.1 Bar (103 psia)
 - Expansion Ratio 160:1
 - Flowrate*..... 300 g/sec (0.66 lbm/sec)
 - Valve Aerojet Solenoid, Single Coil, Single Seat
 - Valve Power 46 Watts @ 28 Vdc
 - Mass..... 4.53 kg (10.0 lbm)
- *at rated thrust

Performance

- Specific Impulse* sec (lbf-sec/lbm)..... 303
- Total Impulse..... 24,271,000 N-sec (5,456,700 lbf-sec)
- Total Pulses 134
- Minimum Impulse Bit 44.48 N-sec (10.0 lbf-sec)
- Steady State Firing Cumulative (sec) 27,000
- Steady State Firing (Single Firing) (sec) 3,940

Rev. Date: 4/02/03

11411 139th PL NE • P.O. BOX 97009 • REDMOND, WA 98073-9709
(425) 885-5000 FAX (425) 882-5747

Approved for public release and export

AEROJET

Figure 11: R-42 Engine [10]

An R-42 Aerojet engine was selected for the MP main engine. It provides 890N of thrust and is the high-power variant of the R-4 engine used on the Apollo Command Module.

3.2.6 Future Work

Future work for the propulsion system will entail an advanced computational analysis and design of flight trajectory. Fuel storage management and tank design will also be further analyzed. Lastly, attitude control signals processing will be developed. This will help solidify the amount of Nitrogen gas to carry onboard the probe, the size of associated tanks, and the remaining structural mass.

3.3 Structures

3.3.1 Design Overview

The structures subsystem consists of two parts: the lander body structure and the landing legs. The lander body will contain all of the scientific equipment and provide structural connections to the landing leg assemblies. As one of the most critical components throughout the entire mission, the design of the lander body will not only affect the lander's performance, but also influence the arrangement and the operating modes of the instruments. The landing legs will provide structural support for a stable landing and absorb most of the impact energy during the touchdown process. Therefore, for the landing legs' material selection and structural design, the characteristic of energy absorbing ability and buffering mechanism must be taken into account.

3.3.2 Materials

For the material selection, five main factors were considered: density, Young's Modulus (stiffness), tensile stress (strength), elongation, and cost. Since one important goal for the design is to make the lander as light as possible, while keeping the high structural strength and integrity, the materials with good mechanical properties and low density should be considered and compared. In order to fulfill the design requirements, five possible materials were selected for constructing the chassis and the landing legs. The materials are 2024-T4 Aluminum Alloy, 2219-T87 Aluminum Alloy, 6061-T6 Aluminum Alloy, and 7075-T73 Aluminum Alloy. Only aluminum alloys were considered because aluminum is a solid and robust material, having a relatively low density and would not get brittle in an extremely low temperature environment. In fact, the strength of aluminum increases with the decrease of the temperature, which means the lander's mechanical properties will not be affected by the extreme weather on Europa. The relevant mechanical properties at different temperatures are shown below:

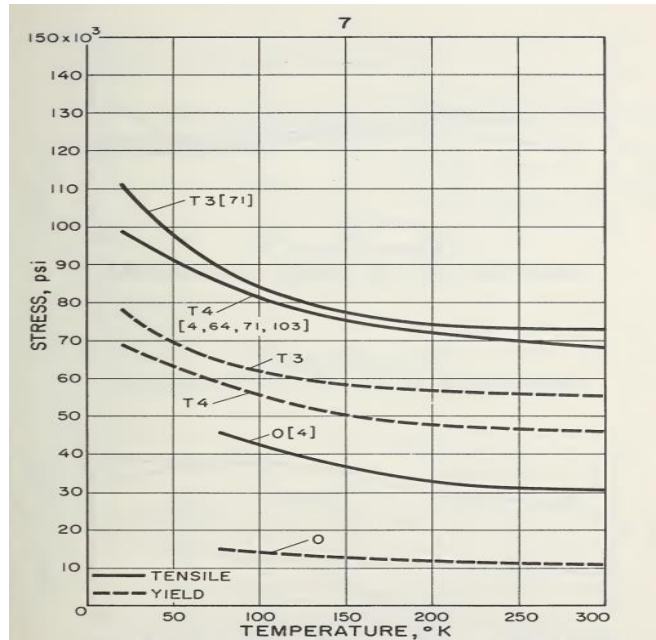


Figure 12: Strength of 2024 Aluminum [4]

A decision matrix was used to select the most suitable material. As described earlier in the design, each material has a scale of 1 to 5, where 5 holds the most weight or value, and a multiplier will vary from 1 to 2 for each criterion. The final scores for each material will be added by column and the component with the highest score will be selected.

Table 1: Material Selection Matrix

Criteria	2024-T4 Aluminum Alloy	2219-T87 Aluminum Alloy	6061-T6 Aluminum Alloy	7075-T73 Aluminum Alloy	Multiplier
Density (ρ)	4	2	5	3	1.5
Young's Modulus (E)	3	4	1	2	2
Tensile Stress (σ_t)	2	3	1	4	1.5
Elongation (ϵ)	4	3	5	1	1
Cost	3	5	4	2	1
Total	22	23.5	20	17.5	

Based on the decision matrix, 2219-T87 Aluminum alloy would be the best material for building the lander's chassis and landing legs. This material has been widely used in the field of aerospace. The mechanical properties of 2219-T87 Aluminum alloy are shown below:

Table 2: Mechanical Properties of 2219-T87 Aluminum Alloy [42]

Density [kg/m ³]	Ultimate Tensile Strength [MPa]	Modulus of Elasticity [GPa]	Poisson's Ratio
2840	476	73.1	0.33
Melting Point [°C]	Specific Heat Capacity [kJ/(kg· °C)]	Thermal Conductivity [W/(m·K)]	Elongation at Break
543 – 643	0.864	121	10%

2219-T87 Aluminum alloy has a relatively high stiffness and strength, and the density of this material is 2840 kg/m³, which is much smaller than steel and titanium alloys. Besides, this material is also relatively cheap - the cost of 2219-T87 Aluminum alloy is only 4 dollars per kilogram. Therefore, using this material to construct the chassis, it could not only guarantee the high stiffness and strength of the structure, but also reduce the mass budget of the mission. Another important thing needs to be mentioned is that although only one material was selected for building the chassis and the main body, the rest parts of the lander could be made of other materials such as steel alloys or composites.

3.3.3 Chassis Structure

In order to carry all necessary payloads, the main body of the lander must be reasonably designed so all available spaces could be utilized efficiently. Thus, an octagonal chamber with nine separated cells was designed, and this internal layout would maximize the space utilization. To further reduce the weight and make placement easier, all internal plates were designed in hollow structure. Figure 13 below shows the geometry and dimensions of the chassis:

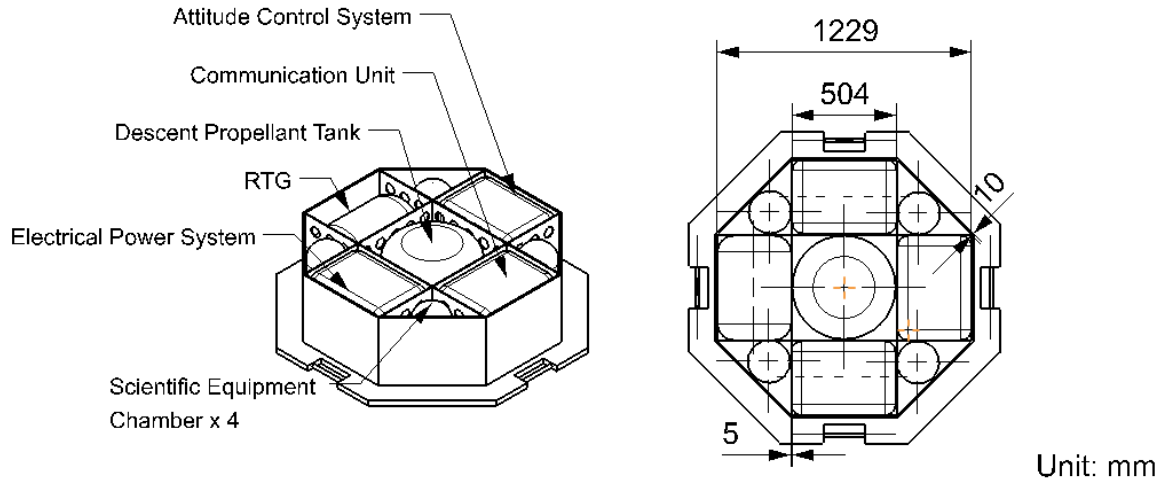


Figure 13: Chassis Octagonal Design

The primary cell at the center of the chassis was designed to place the propellant tank that connects with the descent engine, and the four adjacent cells were used to place the RTG, Power, Communication, and Control systems. The four triangular-shaped cells were designed to place scientific equipment and store ice sample from Europa.

3.3.4 Landing Legs

The lander has four landing legs that were designed for bearing the huge landing impact without causing any serious and permanent damage to the scientific payloads. To increase the reliability of the mechanical deployable and locking systems on each landing leg, four-bar linkage structure was used in the design. Figure 14 below shows the geometry and dimensions of a single landing leg assembly.

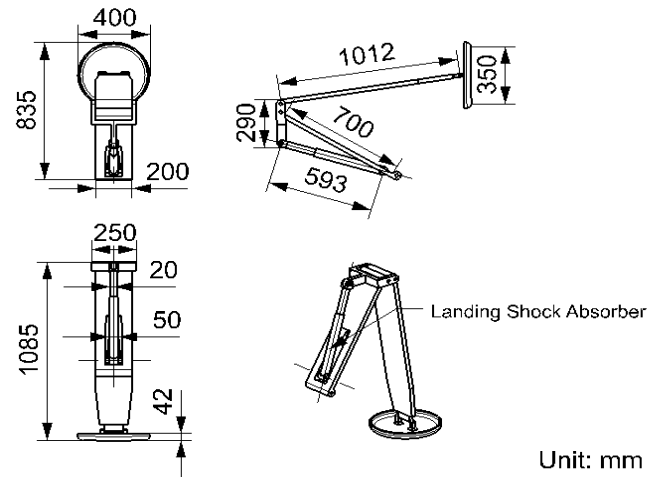


Figure 14: Landing Leg Design

As shown in the figure above, a shock absorber was installed on each landing leg to absorb the impact energy. The landing shock absorber consists of a cylinder and a piston rod, filled with energy-absorbing material and structure inside. The section view of a shock absorber can be seen in Figure 15.

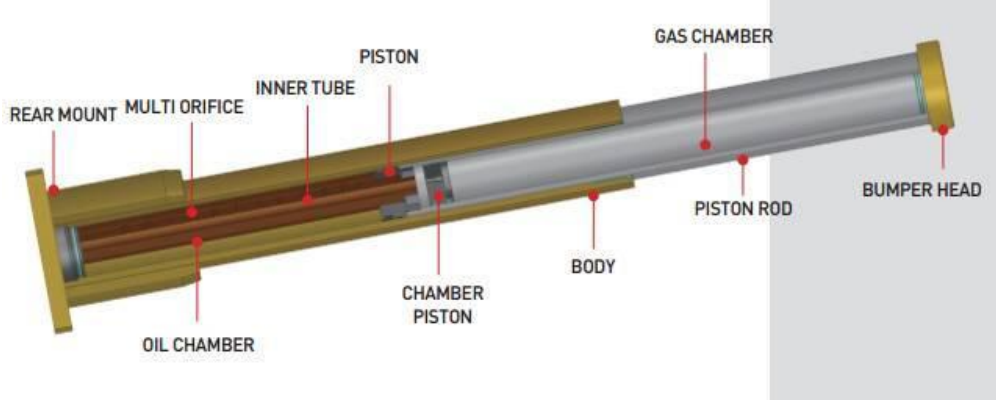


Figure 15: Section View of a Shock Absorber [27]

3.3.5 Final Assembly

For the final design, the lander's chassis is modeled as an octagon block connected to each of the four landing gear assemblies and other components. Figure 16 and Figure 17 show the detailed CAD model of the lander including all major components.

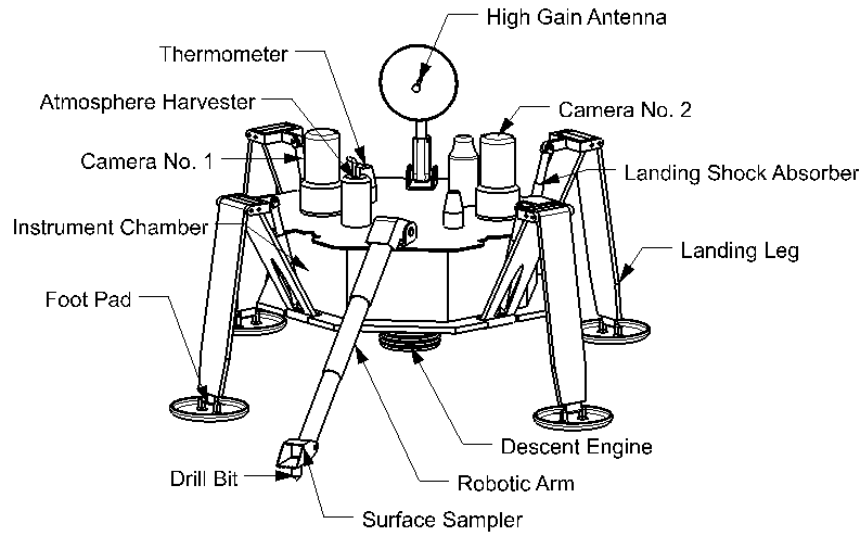


Figure 16: Lander Configuration

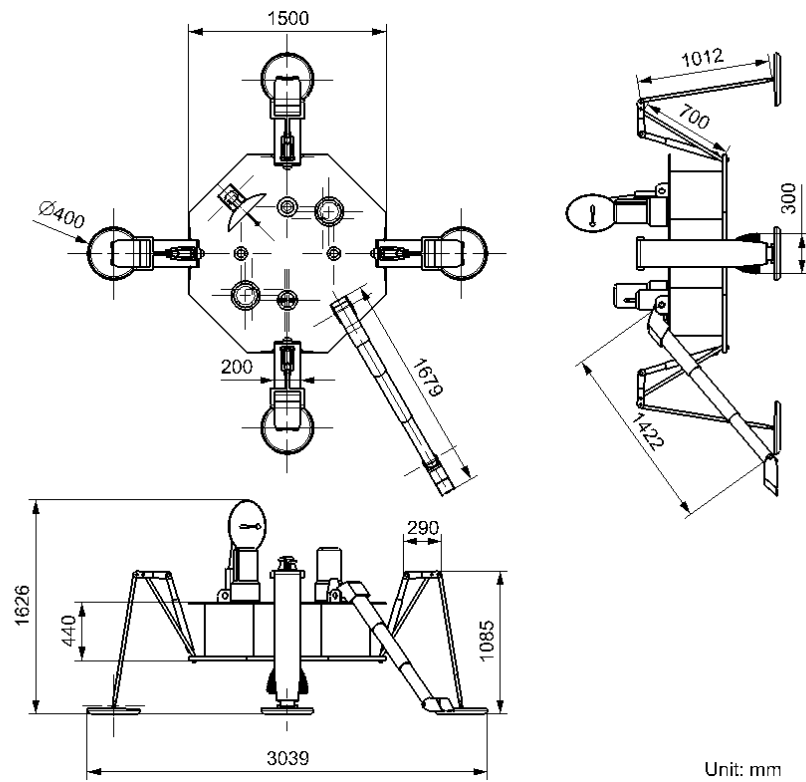


Figure 17: Lander 2-D Sketch

Additionally, because of the foldable design, the lander could be folded into a compact shape, making it easier to fit into a rocket and maximizing the space utilization. Figure 18 and Figure 19 show the geometry and dimensions of the folded lander.

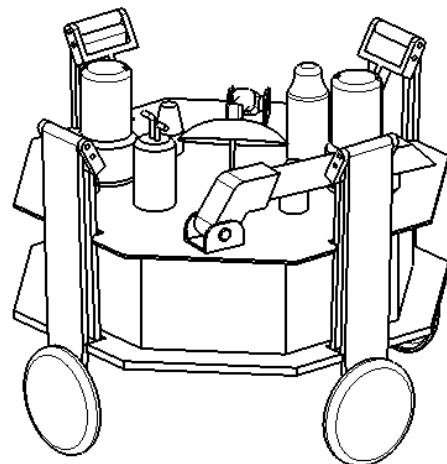


Figure 18: Lander Configuration (folded)

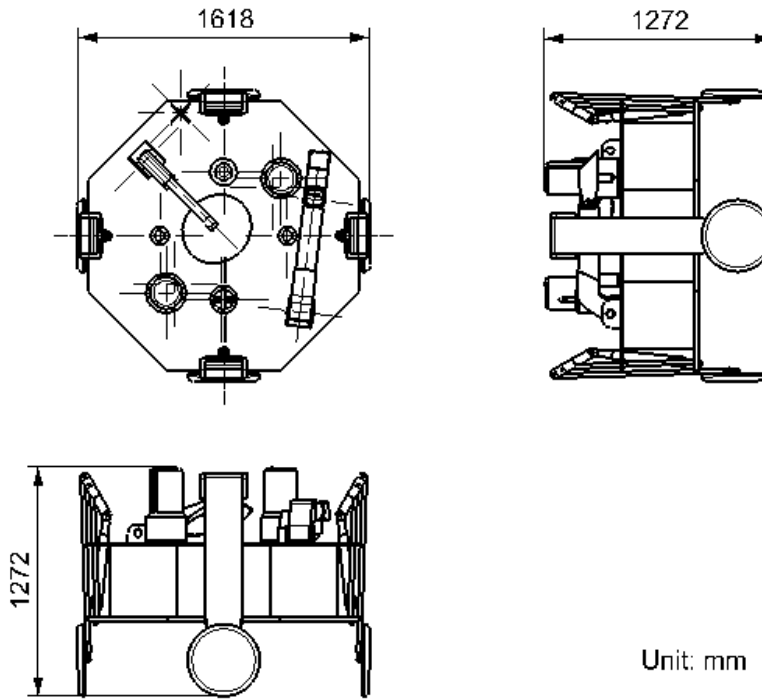


Figure 19: Lander 2-D Sketch (folded)

3.3.6 Finite Element Analysis

To develop a Europa lander that will fulfill all of its mission requirements, one important area of that engineering effort is the landing leg. Since most of a vehicle's mission happens on the Europa's surface, the landing leg must at minimum hold the vehicle's static loads without failure. By using finite element analysis, the designer will analyze the loading characteristics of a simple vehicle landing leg design.

In this analysis, the loading characteristics at the touchdown will be investigated. The touchdown scenario, based on this problem's constraints and design experience will be defined as 3 g's of force (approximately 630 N) in the vertical direction (z-axis) acting on each landing leg. Since each of the landing gear assemblies are identical and equally spaced on the vehicle, Finite Element Analysis will only be performed on one landing gear assembly. For simplicity, all loadings are assumed to occur on Europa ($g = 1.314 \text{ m/s}^2$) and all loadings are assumed to be static in this model.

For simpler analysis, the landing gear assembly geometry was idealized. All edge blends were deleted and the assembly was placed flat on the x-y plane. Using the NX NASTRAN solver, the simulation results are shown below:

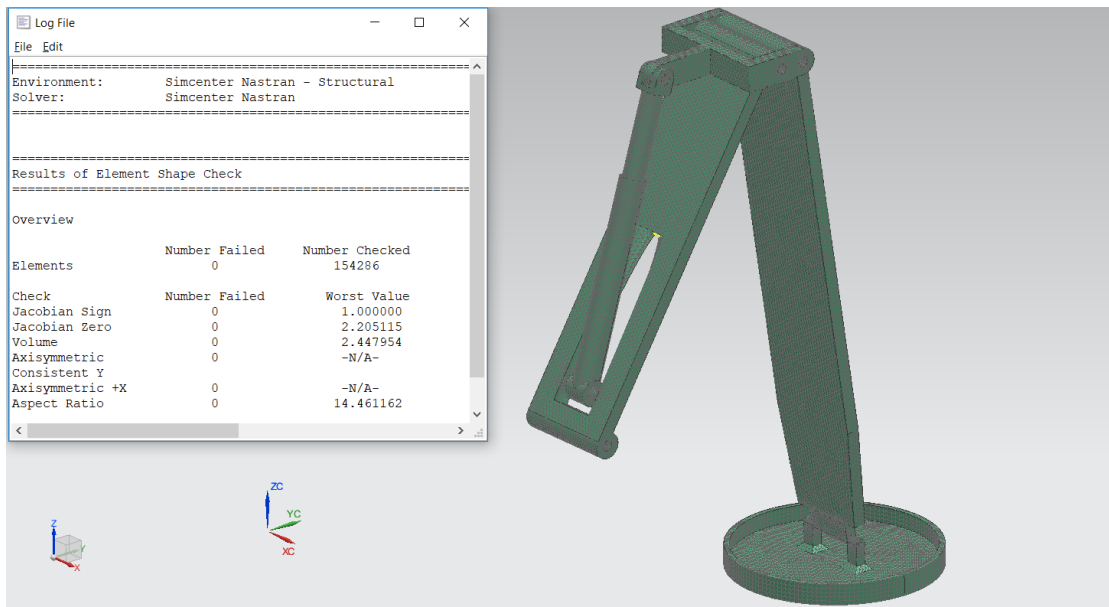


Figure 20: Mesh Type and Total Number

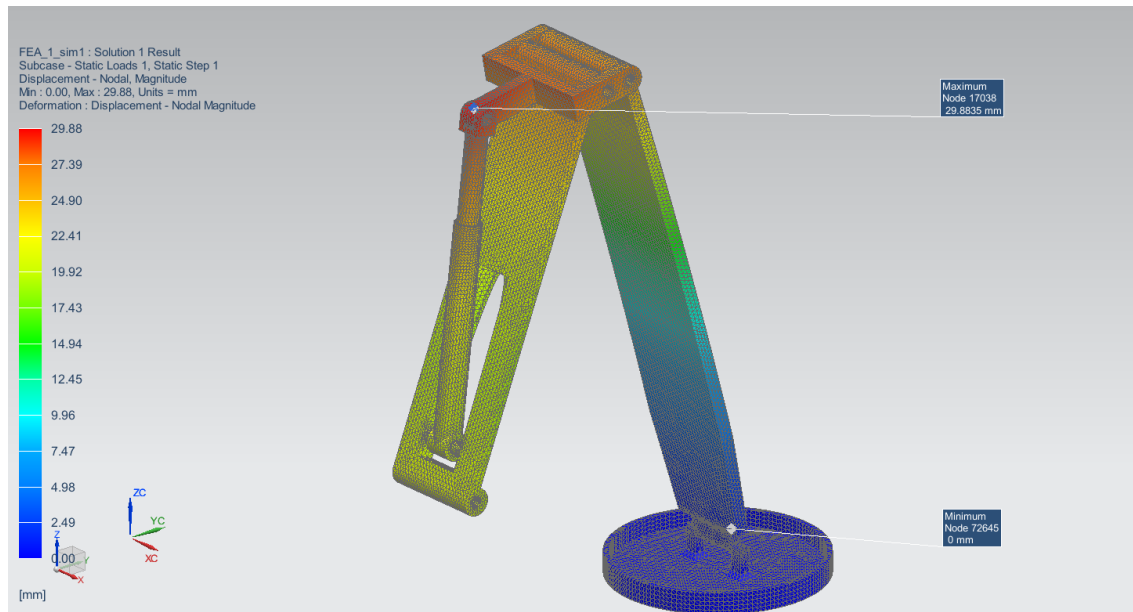


Figure 21: Maximum Displacement

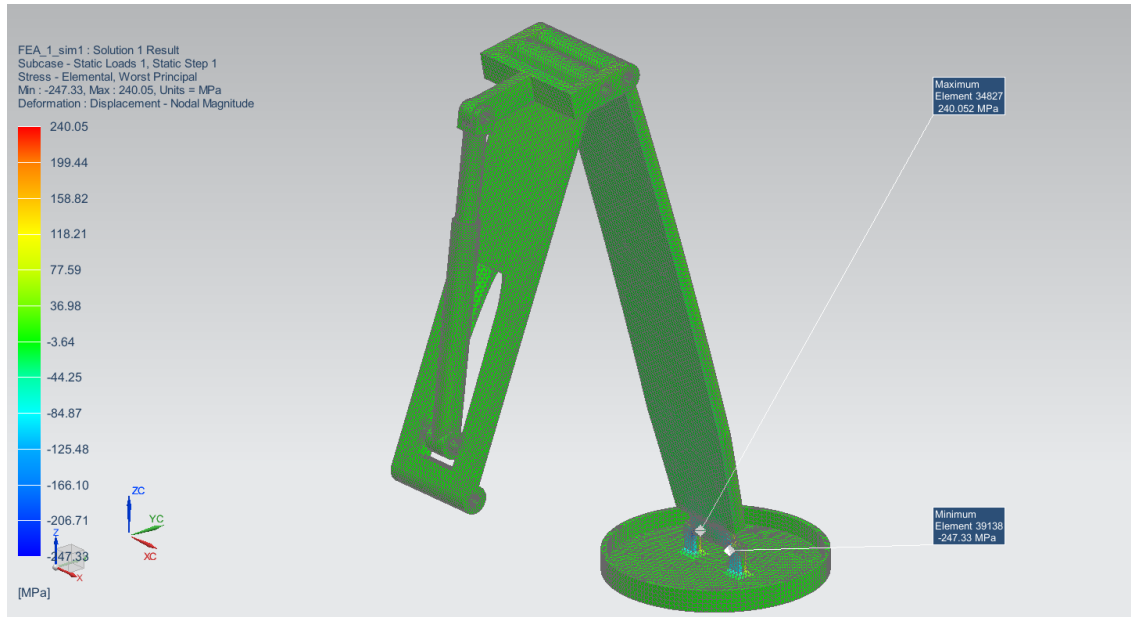


Figure 22: Maximum Principal Stress

Table 3: Mesh Characteristics

Mesh Type	Global Element Size (mm)	No. Elements	Maximum Displacement (mm)	Maximum Stress (MPa)
CTETRA (10)	8.5	154286	29.88	240.05

3.3.7 Future Work

- More factors will be considered for material selection.
- Providing detailed explanation about the size, weight, and cost of each component.
- Determining the deployable/locking mechanism of the landing leg with a detailed CAD model.
- More finite element analysis will be performed to simulate the worst touchdown situation.
- Finite element analysis with all components loaded.

3.4 Mechanisms/Deployables

This section will analyze and discuss the mechanisms and deployables on the Minos Probe. In the Preliminary Design Report, found in Appendix E, the designs for the landing mechanisms/deployables, scientific deployables, and communication deployables were decided upon. This report will analyze and discuss these designs to ensure their effectiveness for the mission.

3.4.1 Landing Mechanisms/Deployables

The Minos Probe will utilize a very flight-proven design of crushable legs and retro rockets for its landing deployable. The system works such that during the descent to the surface of Europa, the retro rockets will fire to reduce the probe's velocity. At the appropriate height the 4 legs will extend and at a height of 2 meters the retro rockets will shut down and the probe will free fall to the surface, landing on the legs. The mechanics of the rockets were discussed by the propulsion engineer in Section 3.2 and the structural integrity of the legs were discussed by the structural engineer in Section 3.3. This section will analyze the 4-bar linkage to be used in extending the crushable legs.

A 4-bar linkage is an age-old method used in variety of machining applications. It consists of four bars/links connected in a loop by four joints. This allows the linkage to rotate freely about one axis, thus letting it extend or contract. If the lengths of the individual links are known, the required angle at which the linkage should be extended to reach a given height can be calculated using methods taught in MANE 4180 Mechanisms. Given a lack of time and expertise in this area, the analysis of the four bar linkage was only partially done. The relevant dimensions of the legs are presented, and if given more time and knowledge, the mathematics would be carried out to determine the appropriate angle needed and the subsequent torque required.

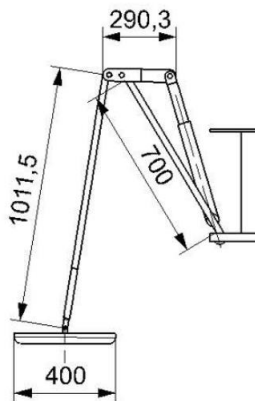


Figure 23: Crushable Legs Dimensions (dimensions in mm)

Once the Minos Probe is safely on the surface of Europa and the legs are in the appropriate position, the joints of the linkage will be locked. The exact method of locking the joints has not been decided on at this moment, but what the intent is to lock as few joints as possible while restricting movement to the legs. This will effectively lock the legs in place will also avoiding

over constraining the legs and applying unnecessary stress on the system. Given more time and knowledge, analysis as taught in MANE 4180 Mechanisms would be done to determine the optimal number of joints to lock. The Minos Probe will remain in this configuration for the remainder of its life.

3.4.2 Scientific Payload

As determined in the Preliminary Design Report, the Minos Probe will carry an ice claw, Surface Dust Analyzer (SUDA), Sample Analysis at Mars (SAM), and a Mastcam-Z. Due to a lack of time and expertise, the design and construction of these instruments will be contracted out to various third party firms. This report will briefly outline the operating parameters of these instruments as defined by the manufacturers.

Ice Claw

The ice claw is a brand new design by NASA's Jet Propulsion Lab. It functions by using a saw blade to carve up the top few inches of surface ice on Europa and then scoop it up in a shovel like mechanism [11]. The claw will be attached to a robotic arm, allowing it to extend out to ensure it collects uncontaminated samples, and then bring those samples back to the probe to be analyzed by the SAM. Given the fact that this is an extremely new design, there is not a lot of data available on the parameters of the claw. Given information found about similar mechanisms on other lander/rover missions, it can be estimated that the mass of the claw will be somewhere around 2-5 kg, while its power use will be around 5-10 watts.

Surface Dust Analyzer (SUDA)

The SUDA is an instrument to be used on the Europa Clipper mission set to launch in 2020. The purpose of the SUDA is to collect and analyze dust and other particles in the atmosphere of Europa. The Minos Probe is intended to pass through a geyser plume while on its descent to the surface. This will allow the SUDA to take sample of ice and water particles ejected by the geyser in the hopes of sampling some from the ocean below the ice crust. This could be essential in determining the potential for life on Europa. The SUDA is a relatively small instrument at only 4 kg [12]. There is no information on the SUDA's power usage as it is a very new design, however it can be estimated to be around 5-10 watts.

Sample Analysis at Mars (SAM)

The SAM is an instrument used on the Mars Curiosity rover. It is designed to take surface samples and heat them up to about 1000 degrees Celsius and vaporize them. The SAM then analyzes the gaseous subcomponents of the samples to determine key information on the formation of Europa. The SAM can determine if methane found was due to geological or biological means helping to identify the potential for life on Europa. The SAM weighs in at a hefty 40 kilograms, but our team is confident that with the hard work and expertise of engineers at NASA, the SAM could be reduced to 20 kilograms. On Curiosity the SAM operates at 40 watts, once again our team is

hopeful to reduce this number, but with the SAM still needing to heat its oven to 1000 degrees Celsius, it is uncertain if this can be achieved [13].

Mastcam-Z

The Mastcam-Z is multispectral stereoscopic imager found on the Mars 2020 Rover. It is an updated version of the highly successfully Mastcam found on the Mars Curiosity Rover. The goal of the Mastcam-Z is to take high definition color images of the surface of Europa. These would be the first images taken from the surface of Europa and would be extremely useful in the study of Europa and its geological and atmospheric processes. The Mastcam-Z is designed to be 4.5 kilograms with a 10% margin, and operate at 17.4 watts [14].

Table 4 summarizes the information discussed in this sub-section.

Table 4: Scientific Payload Mass and Power Usage

Instrument	Mass	Power Usage
Ice Claw	~2-5 kg	~5-10 watts
SUDA	4 kg	~5-10 watts
SAM	20 kg	40 watts (maybe less)
Mastcam-Z	4.5 kg	17.4 watts

All of the instruments described in the sub-section have been designed and tested to withstand the harsh environments of deep space. It is assumed that the manufacturers of each instrument would take the required steps to make each instrument space grade for this mission. As a result, no extra heating or radiation protection, beyond what the manufacturer has instructed, will be needed to operate these instruments.

3.4.3 Communication Deployables

The communication system will utilize two types of deployment devices for its two different antennas. The two ultra-high frequency (UHF) antennas will use a simple spring loaded hinge while the high gain antenna will use a two-axis gimbal. The high gain antenna will be rather small with a diameter of only 28 centimeters, thus the umbrella design discussed in the Preliminary Design Report will not be used. Instead, the antennas small size will allow it to be stowed on its gimbal without needing to fold up.

The UHF antenna will require some analysis to ensure that the spring loaded hinge will function properly. Once again due to a lack of time and expertise on the subject, the fundamental equations and physics will be discussed in this report, but the actual mathematics will not be carried out. In order to find accurate values for this information, extensive testing would need to be performed likely over the course of months.

The core problem with the UHF antenna is determining the preload required on the spring loaded hinge to overcome the latching mechanism at the end of the antenna's rotation. The fundamental equation for this problem is the energy equation listed below, where E is energy, I is the moment

of inertia, ω is the angular velocity, K is the linear stiffness of the torsional spring, and θ is the angular acceleration. The key is to find the angular acceleration in order to find the load that would be applied.

$$E = \frac{1}{2}I\omega^2 + \frac{1}{2}K\theta^2 \quad \text{Eq. 4.1}$$

Where,

$$I = I^{B/B^*} + md^2 \quad \text{Eq. 4.2}$$

$$I^{B/B^*} = mR^2 \quad \text{Eq. 4.3}$$

If given enough time and information, the force required to overcome latching mechanism would be found by calculating the angular acceleration and then confirmed through repeated testing. Given the lack of information and time for testing, the angular acceleration cannot be calculated at this moment. Given information known about the mass and dimensions of the antenna, it can be hypothesized that the preload required on the hinge would likely need to be enough to overcome around 10 inch pounds at the latching mechanism.

The two UHF antennas will also use two pin pullers each to initiate deployment. During launch and travel, the pin pullers will hold the UHF antennas in the horizontal stowed position. At the appropriate time before descent, the pin pullers will fire electronically, releasing the antennas and allowing the spring loaded hinge to deploy them to the vertical position. Each antenna will feature two pin pullers that will operate independently of each other for redundancy. Only one pin puller will need to fire successfully in order to deploy each antenna. The pin puller system will likely use around 10 watts of power.

The two UHF antennas will be mounted on two of the corners of the spacecraft on top of the wall. This will keep the antennas out of the way of the other instrumentation, save space, and allow the antennas to have an unobstructed connection with the RO. The corners are the strongest part of the structure and will provide added support to the system when the antenna is deployed.

The high gain antenna will use a two-axis gimbal design with two independent single-axis actuators. One actuator will be attached to the body of the spacecraft and the other will be carried by the first and attached to the antenna (shown in Figure 24). This will allow the high gain antenna to follow the Rhadamanthus-Orbiter and maintain communication during its entire window of opportunity.

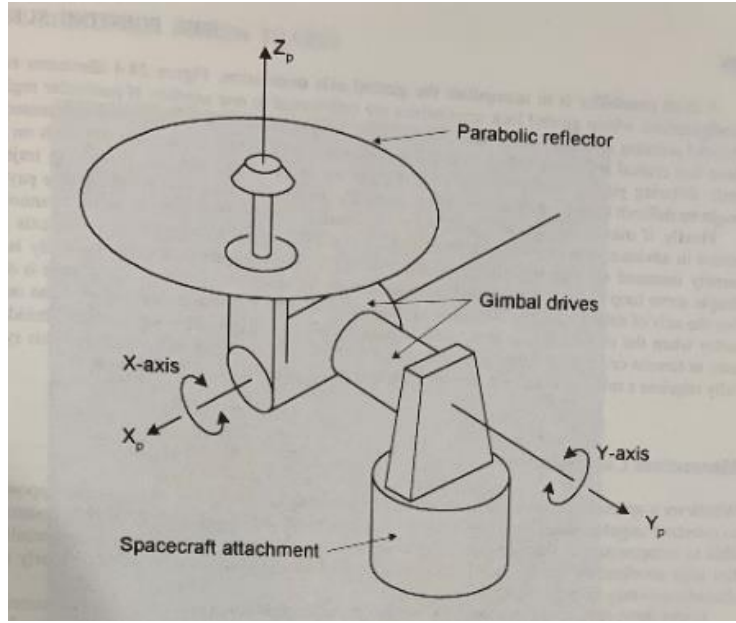


Figure 24: Two-Axis Gimbal [15]

The Minos Probe will use an identical design to the high gain antenna gimbal used on the Mars Exploration Rover (MER). The design features a two-axis gimbal as just described, as well as two potentiometers to determine position of the actuators, and a pin-puller locking mechanism. Figure 25 depicts this design.

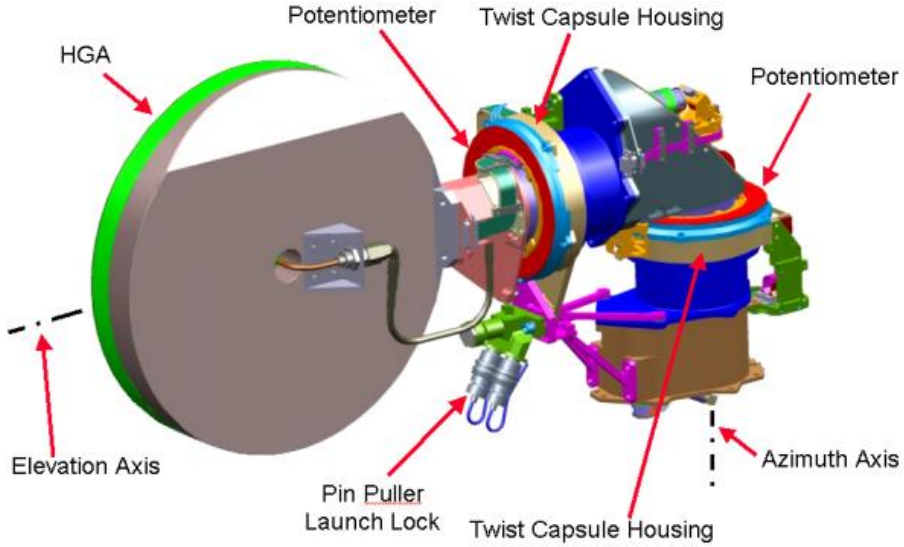


Figure 25: High-Gain Gimbal Design [16]

This design proved very effective on the MER mission and provided a few significant advantages. The first being the potentiometers which determine the position of each actuator and relay that information to the communication system. This will allow for engineers on Earth to ensure that the gimbal is working properly and high gain antenna is following the RO. The second is the pin

puller locking system. This will be useful during launch as it will help prevent the gimbal from moving due to launch loads and potentially damaging the high gain antenna. The pin pullers, as depicted in Figure 26, will fire electronically when the Minos Probe is safely on the surface of Europa allowing the high-gain antenna to begin rotating on its gimbal.

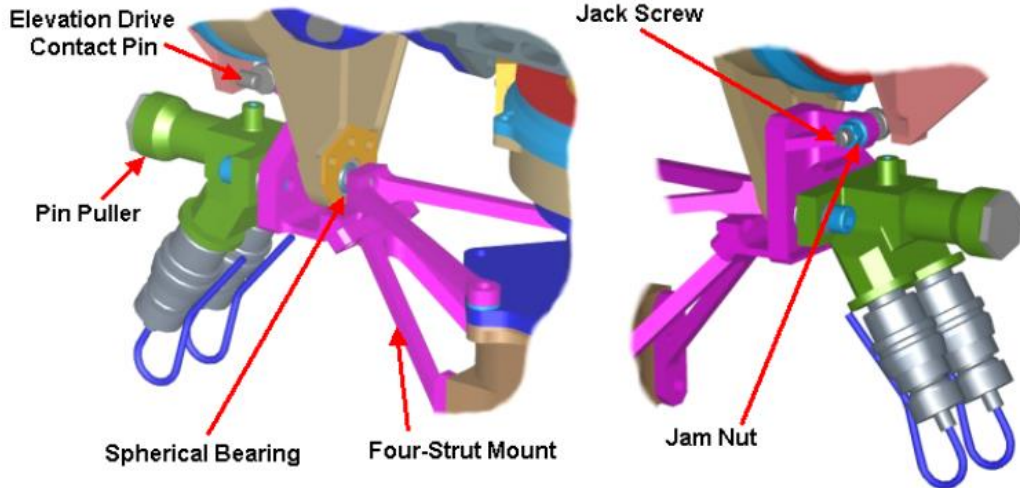


Figure 26: Gimbal Pin-Puller Configuration [16]

3.4.4 Future Work

Future work for the mechanisms/deployables section will include:

- Detailed mathematical analysis of the legs.
- Detailed mathematical analysis of the UHF antenna.
- Extensive testing to determine an accurate pre-load for the torsion springs on the UHF antenna.
- Extensive testing on all components and systems.
- Accurate mass, cost, and torque budgeting analysis.

3.5 Command and Data

To fulfill mission requirements, the probe must be able to fulfill the variety of its mission requirements without much guidance from Earth. To automate the many processes necessary of completing the mission, the command unit will rely on a large series of preprogrammed tasks along with necessary contingencies in case of part failure. Due to the conceptual nature of this report, the specific code will not be included, as it is a significant undertaking, and will require a team months of work. This report will entail the specific processes of each function the probe will endure, as to create a framework for the operation of the MP.

3.5.1 Hardware

For the command unit, the MP will use a RAD750 CPU, a deep space radiation hardened computer. The RAD750 has a long tested flight heritage, and is considered state of the art. The command and data system will also utilize a number of sensors to gather data. These sensors will include; a ranging sensor to gauge altitude, an accelerometer to measure acceleration, a RSI 15-215 reaction wheel to determine orientation, a thermometer to measure temperature, and a barometer for pressure. Altogether the mass of this subsystem will be approximately 8 kilograms.

3.5.2 In Transit to Europa

During the four to five year trip to Europa, the probe will have to continually power up to maintain system functionality. To do this, the command unit will have preprogrammed times approximately once a month to turn on and ensure mechanical systems work, and send the report back to Earth.

3.5.3 Landing

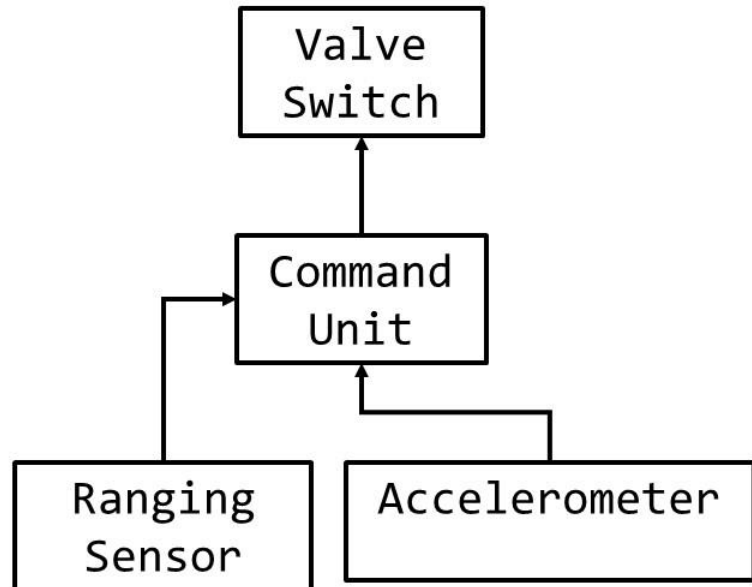


Figure 27: Landing Command Scheme

In order to safely land the probe, it is necessary to have a continual feedback loop between the landing sensors and the thrusters. The landing sensors, the accelerometer and ranging sensor, will be used to track the acceleration and altitude, respectively. The data from these two sensors will

be compared with the planned landing trajectory, and error will be calculated. To reduce the error, the main engine thrusters will be throttled by the propellant valve. This feedback loop will be happening multiple times a second throughout the descent, to ensure a low amount of error and safe landing.

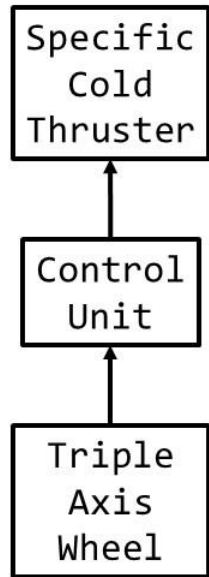


Figure 28: Cold Thrusters Command Scheme

Although it is unexpected due to low atmosphere and low center of gravity, during the landing the probe may lose its orientation. To combat this, cold thrusters have been placed all along the sides of the probe. When the reaction wheel reads that the probe has lost its correct orientation, the control unit will fire the appropriate thruster to return the probe to the right position. This process will also be happening constantly throughout the landing in a feedback loop.

3.5.4 Initial Deployments

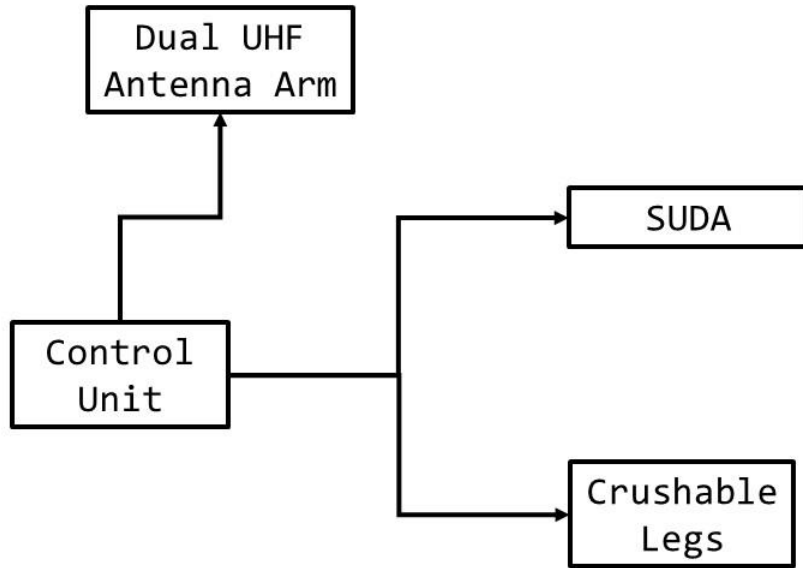


Figure 29: Initial Deployables Command Scheme

During landing, the command unit will give prompts to other mechanical systems to deploy. The crushable legs will deploy first, at a height of around 15 km, due to this location utilizing the least energy. Also at this instant, the SUDA will turn on and start taking atmospheric readings throughout the landing. The purpose of the SUDA is to analyze dust particles of low atmosphere planets. It was developed specifically for the upcoming Europa Clipper mission during flybys, making the use of this instrument during the descent a mission priority.

3.5.5 Sample Collection

To take samples, a number of different instruments will be used. To minimize power output, it was decided that the best course of action was to intermittently take samples, and as soon as the samples had created the sufficient data for the sample, they will be communicated at the closest communication window. This will ensure an efficient use of power and data usage, and will safeguard the chance of the probe failing before the next sample.

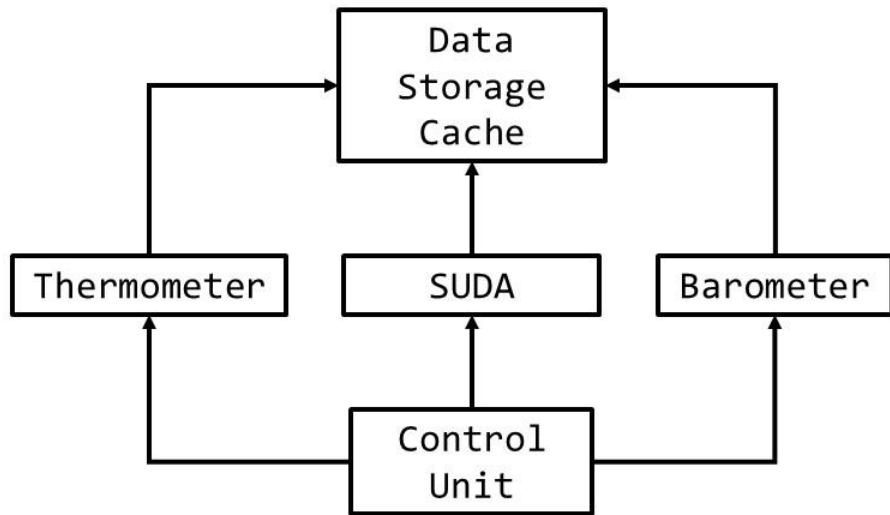


Figure 30: Atmospheric Readings Command Scheme

The figure above represents the instrumentation required to take the atmospheric readings on Europa. Although the SUDA will also be utilized on the landing, it will also be regularly used to analyze dust particles of the atmosphere. Working in conjunction with the SUDA will be simple instruments such as a barometer and thermometer to take pressure and temperature. Of all the scientific instruments onboard the MP, these three take up the least amount of power. Due to this, samples can be gathered much more regularly. The command unit will also record the temperature and pressure every hour to try to form basic weather trends, while the SUDA will be used once a communication window. Due to the heavy power consumption of this process, and the longevity of the mission, it was decided that this sampling process should only occur once every hundred hours.

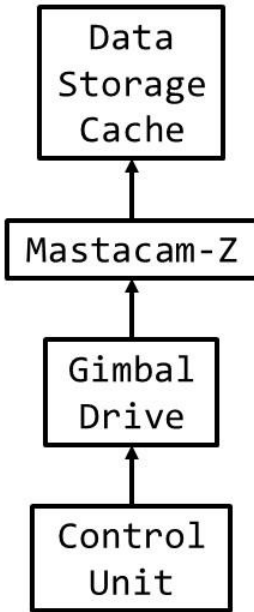


Figure 31: Mastcam-Z Command Scheme

The Mastcam-Z is the onboard camera for the mission. It was developed specifically for deep space use and will be able to withstand the environment. The Mastcam-Z will be mounted on top of the probe on a gimbal drive, allowing it to swivel around to survey the area around it. The command unit will specify that the Mastcam-Z be swiveled fifteen degrees about its axis every Europa day. The camera will then be utilized to capture pictures of the environment at that orientation during light hours and dark hours. Since the length of a day of Europa is approximated 3.5 Earth days, the picture capture will happen only every twice in an 84-hour window. This will limit energy consumption, and still gather the necessary data. In case of a point of interest is located by the ground team on Earth, the RAD750's rewritable EEPROM memory can be reprogrammed to orient the Mastcam-Z in the desired direction and further investigate.

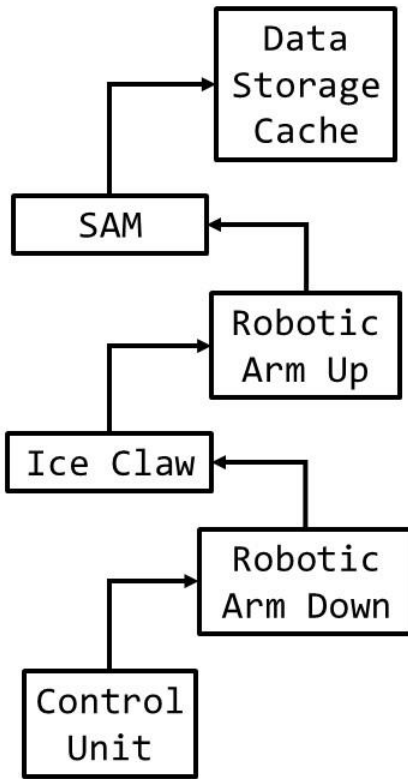


Figure 32: Ice Analysis Command Scheme

To analyze the ice content of Europa, the MP will utilize a number of processes to obtain the samples, then test the contents and record the data. Since the SAM is the most power consuming of all the instrumentation, it will be used the least. It will also become increasing difficult to sample ice farther away due to the stationary nature of the probe. When it is time to collect an ice sample, the stowed robotic arm will deploy and reach the ground, which at the point the ice claw connected to the end will scrape the ground. Once this process happens, the arm will lift back up into its stowed position with the sample. The SAM was developed by NASA for the mars rover, and although it contains many different instruments, it allows a decently hands off approach once the sample is submitted is placed into the end. After this process is complete, the data will be stored and prepare for the next occasion it can transmit.

3.5.6 Window of Communication

After significant orbital trajectory calculations permission, the command unit will be preprogrammed to know when the orbiter will be in a position to transmit data. Updates can constantly be made using markers such as transmit signal strength, and location updates from Earth.

3.5.7 Communication

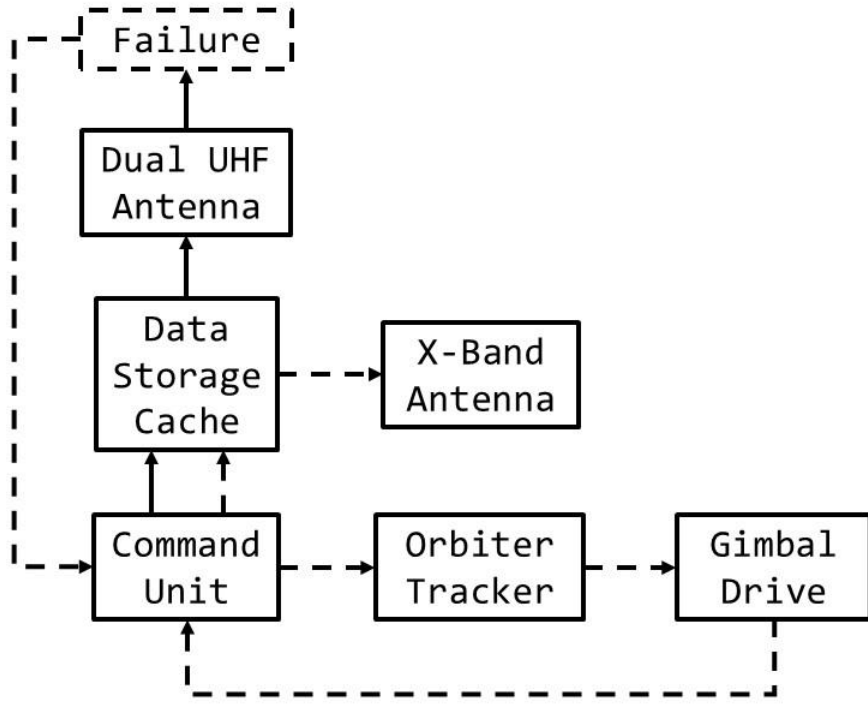


Figure 33: Communication Command Scheme

When the window of communication opens, the MP will have to transmit the data it's been storing in its cache. For primary communications, the data will just be sent out through the UHF antenna once a window of communication has been established. In case of failure, the probe will enact its secondary communication plan. The MP will establish the position of the orbiter using its tracking system, and instruct the gimbal to move in correct orientation. Once a proper orientation has been confirmed, the X-band antenna will transmit the data that the UHF antenna cannot.

3.5.8 Failure Mitigation

The command unit must be ready for how to prioritize sampling and probe life in case of mechanical failure. In future work, the team that builds and tests the probe will have extensive knowledge on what parts fail first, and how to create an order of operations to code into the command unit. Europa's climate is very harsh, and by having a preprogrammed way of prioritizing the necessary components, the mission will last longer.

3.5.9 Power Consumption

Due to the limited power of the RTG, power must be used as efficiently as possible. The command unit will only conduct tests at certain intervals and not take multiple tests at the same time. Furthermore, the command unit will completely shut off instrumentation when not in use, saving more power.

3.5.10 Future Work

Future work will entail the massive amount of coding to safeguard the probe. Once all of the processes have been worked out in a mid-level processing language such as C++, the code will have to be coded into an assembly language, to ensure speed and maximal efficiency. The team that codes the assembly language must work in conjunction with another team constantly testing the mechanical systems. Doing this will save more time, as failures are likely occurring consistently. Do the importance of part functionality in this mission, it is likely half of the programming team will have to be committed to purely testing the code.

3.6 Communications

3.6.1 Communications System Overview

The MP will be communicating solely with the RO and because of this the need for high power communications equipment is eliminated. The probe will have two independent communications systems onboard, utilizing the ultra-high frequency (UHF) and X-Bands. Due to the robust and mission proven UHF transceiver system and the relatively short distances that data will be being transmitted, the UHF system will be the primary communications system used and the X-band will be secondary. The UHF system will use two omni-directional antennas, mounted in orientation 90 degrees apart for maximum coverage. The X-Band system will use a directional high gain antenna (HGA) mounted on gimbals that will track the orbiter as it passes. Because of the additional mechanisms required for the use of the HGA, as well as the higher power requirements, the X-Band system was chosen to be the secondary communications system to help mitigate possible hardware failures and minimize power consumption.

3.6.2 Communications Window

The most important factor when deciding what communications system would serve as the primary was the time window the orbiter and probe would be able to transmit data to each other. Using Satellite Tool Kit (STK) and the Mars Rover missions as a guide, a scenario was generated. The probe was assumed to have landed in the northern hemisphere of Europa, near its pole. The RO was in an orbit that passed nearly overhead of the probe in an orbit having a semi major axis of 2000 kilometers and an eccentricity of 0.1. This yielded a communications time window of 47 minutes with a range varying from 612 kilometers to 1627 kilometers. The probe and orbiter were set to have directional, tracking antennas with a 2-degree beam width. The window of communication would be the same for UHF or X-Band systems.

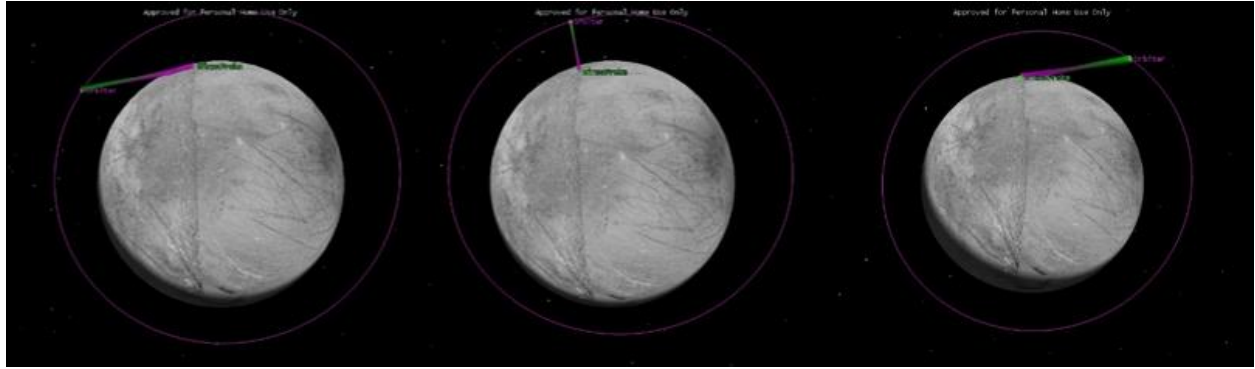


Figure 34: STK simulated orbit and communications between the RO and MP.

The simulated orbit seen in Figure 34, even considering its inaccuracies, yielded a relatively large time window that the probe will be in communications with the orbiter that even if it is reduced by half, is still adequate to justify the use of the UHF as the primary communications system. However, if the orbit of the RO is different enough to the point where window of communications is reduced making the use of the X-Band a better option, the role of the UHF and X-Band systems can be switched, understanding the additional risks associated with the X-Band system.

3.6.3 UHF System

The primary communications system will be using the mission proven C/TT-505 Cincinnati Electronics UHF Transceiver, operating at 400 megahertz. This transceiver is an ideal choice because of its small size, power requirements, robustness and flight heritage. The C/TT-505 has dimensions of 5.1 x 6.8 x 3.7 centimeters and has a mass of 1.9 kilograms. The associated omnidirectional antennas are a simple monopole type antenna measuring 16.9 centimeters in length and 1.9 centimeters in diameter and mass of 0.1 kilograms. The UHF system uses an input power of 6 to 43 watts and an output power of 12 watts. With a total mass of roughly 2.9 kilograms, the UHF system's small footprint and mass lend to minimizing the overall mass budget allowing for more mass to be allocated to the more mass hungry subsystems. The C/TT-505 can transmit and receive data at rates up to 256 kilobits per second (Kbps) [17]. The transceiver is rated to function in a temperature range of -45 degrees Celsius to 72 degrees Celsius [18]. Figure 35 shows a picture of the C/TT-505.



Figure 35: C/TT-505 Transceiver being used on the Minos Probe [21]

The omni antenna that will be used on the probe is linearly polarized with a resulting antenna gain pattern that is not symmetrical as shown in Figure 36.

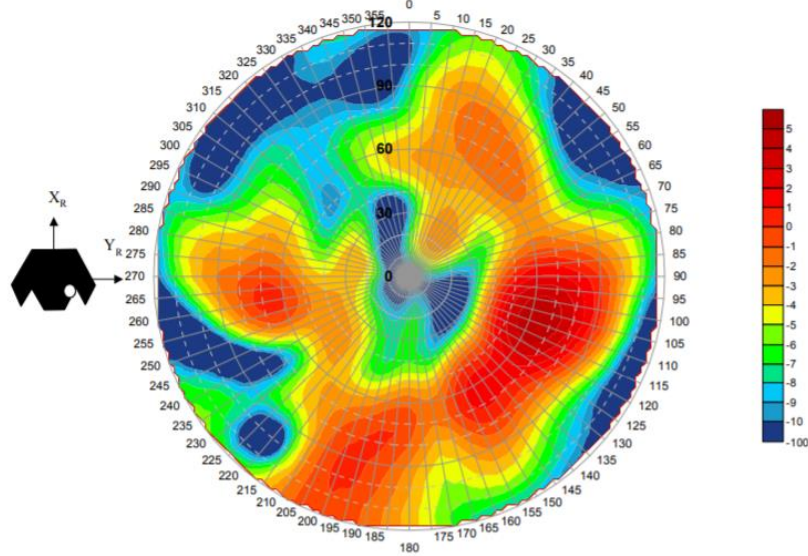


Figure 36: UHG antenna pattern [17]

Due to the asymmetrical pattern of the antenna, data transmission rates can be affected by the altitude of the orbiter, the orbiter's relative position to the probe, and the orientation of the antennas on the probe itself [17]. Mission planning should design the RO's orbit such that it passes through the areas of high gain, ensuring maximum data transfer rates. In ideal conditions, transmitting at 256 Kbps and in contact with the orbiter for the full 47 minutes, the UHF system can transmit up to 747 megabits of data.

3.6.4 X-Band System

The X-Band communications system is made up of multiple components including a small deep space transponder (SDST), solid state power amplifier (SSPA), a diplexer and high gain antenna. The SDST has dimensions of 18.1 x 11.4 x 16.6 centimeters and a mass of 2.7 kilograms. The SSPA has dimensions of 4.4 x 17.2 x 13.4 centimeters and has a mass of 1.3 kilograms. The diplexer allows for transmitting and receiving on a common antenna and has dimensions of 27.2 x 5.6 x 7.9 centimeters and has a mass of .48 kilograms. The X-Band system uses 71.8 watts of input power and can output 16.8 watts of transmission power. The HGA being used is 28 centimeters in diameter and has a mass of 1.1 kilograms [17]. The total system mass, including cabling and connections is 5.02 kilograms. Figure 37 shows the SDST being used on the Minos Probe.



Figure 37: SDST being used on the Minos Probe [17]

The HGA being used is a 0.28 meter diameter printed dipole array with a beam width of 4.2 degrees transmitting and 5 degrees receiving. The gain is 20.5 dB receiving and 24.8 transmitting [17]. The HGA will have to be mounted on a two axis gimbal to accurately track the RO as it passes overhead. Figure 3.5 shows the HGA being used on the Minos Probe.



Figure 38: High gain antenna mounted to 2-axis gimbal being used on the Minos Probe.

With the higher frequency band as well as the high gain antenna, X-band systems are traditionally designed to transmit data very long distances. X-band being used on the Mars Reconnaissance Orbiter can transmit 500 Kbps at 250 million miles and 3-4 megabits at 60 million miles [19]. Data transmission speeds at distances less than 2000 kilometers will be far greater still.

The Friis Transmission Formula [20] can be used to determine the receiving power an antenna receives which in our case can be used to compare the power of the UHF and X-Band systems. The equation

$$P_R = \frac{P_T G_T G_R \lambda^2}{(4\pi R)^2} \quad \text{Eq. 6.1}$$

where P_R is receiving power in watts, P_T is transmitting power in watts, G_T is gain of the transmitting antenna in dB, G_R is gain of the receiving antenna in dB, λ is the wavelength of the frequency being used in meters, and R is the distance between the transmitting and receiving antennas in meters. Assuming the orbiter and probe antennas have the same gain, and are at their maximum distance apart while still being able to communicate, the 400 megahertz UHF system on the orbiter will receive 4.0369×10^{-7} watts. An 8 gigahertz X-Band system on the orbiter will receive much less, 2.873×10^{-8} watts. As shown, the higher frequency results in a lower power received, something known as path loss [20]. For this reason, higher frequency communication systems require directional antennas with high gain.

3.6.5 Future Communication Work

Given more time and resources, there is still much to determine and analyze within the communications subsystem. Antenna theory is extremely complicated resulting in very limited analysis performed. For this reason, existing communications systems that have a proven flight heritage were chosen due to the similarities of the missions. A control system also needs to be determined for use in the X-Band system to track the RO and control the gimbal. Exact data transfer rates, as the orbiter passes through the UHF antenna pattern, and exact transfer rates for close proximity X-Band would also be determined. A more detailed orbital analysis would be

performed once the final orbit of the RO was determined to calculate the exact time window of communications. Placement of all communications components and antennas for optimal performance and minimal interference would also be determined.

3.7 Thermal Control

3.7.1 Preliminary Design

The thermal control system (TCS) needs to keep all parts and instruments of other subsystems within acceptable temperature ranges for all modes of operation in all thermal environments required for the mission. The TCS will also be responsible for limiting damage to electronics from charged particles present in Jupiter's magnetosphere. In the PDR, it was shown that this will be accomplished by heating with radioisotope heater units (RHU), transferring internal heat with thermal straps, radiating external heat with a structural panel radiator, and protecting from charged particles with a titanium vault. Table 5 shows the components of the probe and their acceptable temperature limits.

Table 5: Acceptable Temperature Ranges

Component	Acceptable Temperature Range
Propellant	-11 to 21 °C
Control System	-50 to 150 °C
Chassis	less than 543 °C
Batteries	-30 to 40 °C
UHF Antenna	-45 to 72 °C

3.7.2 Heating

To determine the required number of heaters required by the probe, the environment in which the probe experiences the most extreme cold was analyzed. This environment is on the surface of Europa, where temperatures are minus 160 degrees Celsius. [21] The RTG supplies the probe with 2000 watts of heat. If the entire exterior of the probe had an ideal emissivity of 1, the equation

$$\varepsilon = \frac{Q}{A\sigma(T_{hot}^4 - T_{cold}^4)} \quad \text{Eq. 7.1}$$

where Q is the amount of heat being transferred, A is the surface area of the exterior of the probe, ε is the emissivity of the outside surface of the probe, σ is the Stefan–Boltzmann constant, T_{hot} is the temperature inside the probe, and T_{cold} is the outside temperature, can be used to find that the interior temperature would be 34 degrees Celsius. This temperature is at least 64 degrees Celsius warmer than the minimum temperature for all components of the probe, therefore no RHUs will

be needed to provide the probe with extra heat. The probe will also not need any MLI, as this will only make the probe warmer and 34 degrees is already too warm for the propellant tanks. Instead, the probe will generate all its heat from the RTG and will be painted with a white paint which has an emissivity of 0.92.

3.7.3 Internal Heat Transfer

In order to find the amount of heat needed to be transferred to each compartment of the probe, a desired temperature was chosen for each compartment based on the components within. These temperatures are listed in Table 6. Based on these desired temperatures, an aluminum thermal strap was sized to transfer heat to each compartment. All straps have the same length of 0.433 meters due to symmetry, and each strap's cross-sectional area is listed in Table 7. Calculations for this sizing using the equation

$$Q = \frac{kA\Delta T}{L} \quad \text{Eq. 7.2}$$

where Q is the amount of heat being transferred through the strap, A is the cross-sectional area of the strap, ΔT is the difference in temperature at the ends of the strap, and L is the length of the strap, can be found in Appendix D. In total, 1064 watts of heat is transferred from the RTG to other components of the probe through thermal straps weighing a total of 105 grams.

Table 6: Desired Temperatures by Compartment

Compartment	Desired Temperature
Propellant Tank	10 °C
Scientific Chambers next to RTG (SC1s)	10 °C
Power	0 °C
Control	0 °C
Communication	0 °C
Scientific Chambers next to Communications (SC2s)	-10 °C

Table 7: Thermal Strap Cross-sectional Areas

Thermal Strap	Cross-sectional Area (mm²)
RTG to Propellant Tank	103
Propellant Tank to Communications	697
RTG to SC1s	114
SC1s to Power and Control	1,058
Power and Control to SC2s	361

3.7.4 Thermal Radiation

The entire exterior of the probe will be painted with NASA/GSFC NS74 white paint which has an emissivity of 0.92. At a temperature of 146 °C, the panels around the RTG radiate 936 watts of heat away from the probe. The other compartments of the probe radiate the other 1064 watts of heat produced by the RTG.

3.7.5 Future Work

- Create a more accurate model and perform finite element analysis.
- Finalize desired temperatures, especially those of the scientific chambers.
- Research more types of paint and finalize choice.
- Analyze different operating modes in different thermal environments, including LEO, transfer, and descent to Europa.
- Perform laboratory testing that simulates these environments.
- Continuously update as other subsystems are updated.

4 Budgets Summary

4.1 Mass Budget

Table 8: Mass Budget

Subsystem	Mass (kg)
Power	60
Propulsion	384
Structures	250
Mechanisms/Deployables	30
Command and Data	5
Communications	10
Thermal Control	5

4.2 Power Budget

Table 9: Power Budget

Subsystem	Power (W)
Deployables	80
Command and Data	14
Communications	115

4.3 Propulsion Budget

Table 10: Propulsion Budget

Item	Mass (kg)
Attitude	5
Main Engine	14
MMH	115
N ₂ O ₄	250

5 Risks

The Minos Probe is a single mode of failure spacecraft such that if any subsystem were to fail, the entire mission would be lost. For this reason, extensive thought and planning was dedicated to risk assessment and mitigation.

5.1 Public Health, Environmental, Social, Cultural, and Economic Risks

As with any space mission, the Minos Probe mission does not come without risks. When building a spacecraft is important to consider that the risks will have public health, environmental, social, cultural, and economic factors.

The main public health risk of the Minos Probe is the RTG. If the spacecraft were to explode during launch, the RTG would rain down on the Earth. This has the potential to pose a serious risk to the health of the surrounding areas due to the RTG's intense radiation. Building the spacecraft also poses a public health risk to those working on it. If engineers and technicians do not follow protocol, there is a serious risk of injury on the job. These risks can be mitigated by extensive testing and inspection prior to launch to reduce the likelihood of launch failure and by enforcing strict protocol and regulation at the workplace.

The RTG also poses a threat to the environment. Should the spacecraft explode during launch, the RTG would rain down on the surrounding area. The RTG's radiation would prove to be a serious environmental hazard and could take years to fully clean up. The Minos Probe also poses an environmental threat to Europa. If the landing is not properly executed, the spacecraft could potentially contaminate the surface of Europa. Whether it be due to the exhaust from the rocket engines or a foreign contaminant on the spacecraft, it could be catastrophic to the mission. A contaminated surface would yield inaccurate results and jeopardize the entire mission.

Social and economic risks of the mission come due to the fact that funding a mission of this magnitude will cost billions of dollars. Because NASA is a US government agency, these funds come predominantly from taxpayer money. If the public does not feel that this mission is worthy, or if the probe fails to return any significant results, the public may not approve of their money being spent in this manner. This has the potential to reduce funding for future NASA missions as well.

The cultural risk in this mission comes from interest of the public in this program. If the mission does not yield significant results, there is the possibility that the public will lose interest in Europa and space in general. Because NASA is a publicly funded agency, their missions live and die with the public's interest.

5.2 Mission Risks

5.3 Power Risks and Mitigations

The electrical power system is an essential component of the spacecraft design and any form of failure within that subsystem may mean the end of the entire mission. The risks associated with the electrical power system include environmental contamination, radiation damage, RTG failure, and secondary battery failure. In the case of environmental contamination, the RTG emits radiation

in the form of alpha and beta particles as a consequence of the decay process of the radioactive material (^{238}Pu) that powers the device. Since one of the key goals of the MP mission is to discover any evidence of the existence of life, any radiation leak coming from the RTG may cause any samples collected to become contaminated. In order to mitigate this risk, the RTG must have adequate shielding through a lead sheet so that radiation is blocked from escaping the device. This also applies to radiation damage, as a high dose of radiation over a period of time can damage other electronics within the spacecraft. Furthermore, in the case of an RTG failure, any structural damage done to the RTG from a launch vehicle crash or a failed landing of the spacecraft may mean the exposure of the radioactive material to the environment and a massive amount of radiation leakage. In order to mitigate an RTG failure, proper safety guidelines must be followed while handling and constructing the device to ensure it is in good condition for launch and proper protocol must be adhered to in regards to mission control and descent onto Europa. Lastly, secondary battery failure may lead to certain components not receiving enough power to perform their desired tasks and cause the mission to stall. To mitigate this risk, redundancy will be incorporated into the design with the addition of two Li-Ion batteries.

5.4 Propulsion Risks and Mitigations

The Propulsion system for the Minos Probe poses a significant amount of risk due to the prevalence of single point failures. Engine failure could potentially occur due to the extreme environmental factors the probe will experience during the mission. Attitude control will also suffer from the same environmental factors as the main engine. A failure in either of these systems would likely result in the loss of the MP.

Steps have been taken in the design to reduce the risk of failure in either of these components. First, thermal properties of propellant were made a priority. UDMH was selected for fuel because of its lower freezing point than Hydrazine and its ability to be stored. Cold gas for the thrusters was also selected for the same reason.

Environmental contamination and health hazards are both deemed critical risks associated with the mission. UDMH is highly toxic and harmful to harmful humans. Additionally, the surface of Europa could become contaminated by exhaust products from the main engine. In order to manage these risks, the utmost safety procedures will be followed in the production and loading of UDMH into the spacecraft. The descent trajectory profile was designed such that main engine shutdown occurs at two meters from the surface. An altitude buffer will help to prevent contamination of the surface. Lastly, the ice claw mechanism will cut into the surface to reduce the likelihood of sample contamination from exhaust gases.

5.5 Structures Risks and Mitigation

The main risks for the structures are component failure and material quality dissatisfaction. Components failure due to the harsh environmental condition on Europa could result catastrophic consequences such as structural distortion and breakage. Material quality dissatisfaction would result fractures occur inside the components under the impact force of landing.

In order to mitigate the structures risks to an acceptable level, ground testing and manufacturing quality control have to be performed to bring everything under control. Since the structural components of the lander cannot be repaired or replaced during the mission, the worst cases must be considered in the design review and ground testing process.

5.6 Mechanisms/Deployables Risks and Mitigations

There are a variety of risks involved in each mechanism/deployable present on the Minos Probe. As with all aspects of the spacecraft, these risks must be addressed in order to ensure a design that will minimize their impact.

The major risk involved in the deployment of the crushable legs is a malfunction in the four bar-linkage. The most likely scenario would be due to damage caused during launch of the spacecraft. If this were to occur, the legs would not be able to successfully deploy and would make landing much more difficult. To combat this, each individual leg will deploy independently of the others. This will prevent an entire system failure should one leg malfunction. Although it will be far more difficult, a landing on three legs would still be possible. Extensive testing and design will be conducted in order to ensure that the four-bar linkages on the legs are space ready for this mission.

The major risk with the scientific payloads is a system failure due to harsh environmental conditions. The extreme cold of deep space and Europa could potentially degrade the scientific instrumentation. Whether it be in a complete system failure, or inaccurate data it would be catastrophic to the mission. To combat this, extensive testing and design would be done by the manufacturers of the instruments to ensure their functionality in these harsh conditions.

The major risk with the communication deployables once again is failure of the components. The likely scenario would be either the failure of the spring or gimbal or the failure of the electronic components. In either case this would most likely be due to launch loads or extremely cold temperature. As with most of the spacecraft, this will be mitigated through extensive testing and design.

5.7 Command and Data Risks and Mitigations

To mitigate failure of the command unit, a number of precautions will be taken. First, the command unit will require adequate thermal insulation, and will utilize a number of passive thermal control techniques to ensure that the temperature is kept at efficient, optimum levels. Secondly, the probe will have a secondary chip inside the probe that will have all of the same functionality of the primary chip, and just be connected in case of primary unit failure. Lastly, the ground team in earth will possibly notice some unexpected code issues due to the improper estimates of the environment of Europa. To combat this, the clock times for functions will be constantly analyzed, and updates will be made through the RAD750 rewritable EEPROM memory.

5.8 Communications Risks and Mitigations

Communications is a mission critical system and failure of the system would kill the mission. Component failure could render the communications system useless. Flight tested equipment that has been used on past missions will be selected to help mitigate a component failure. Additionally, two frequency bands will be used with independent transceivers, each having multiple antennas. This will ensure that anything short of a catastrophic failure to the communications system, the probe will be able to communicate to the orbiter in some fashion.

Europa is known to have an atmosphere and it is possible that frozen water droplets are present which could introduce interference to the communication system. To avoid any risks to the transmission of commands and data due to atmospheric interference, the frequencies selected are UHF and X-band, both of which are not known to be affected by this type of interference.

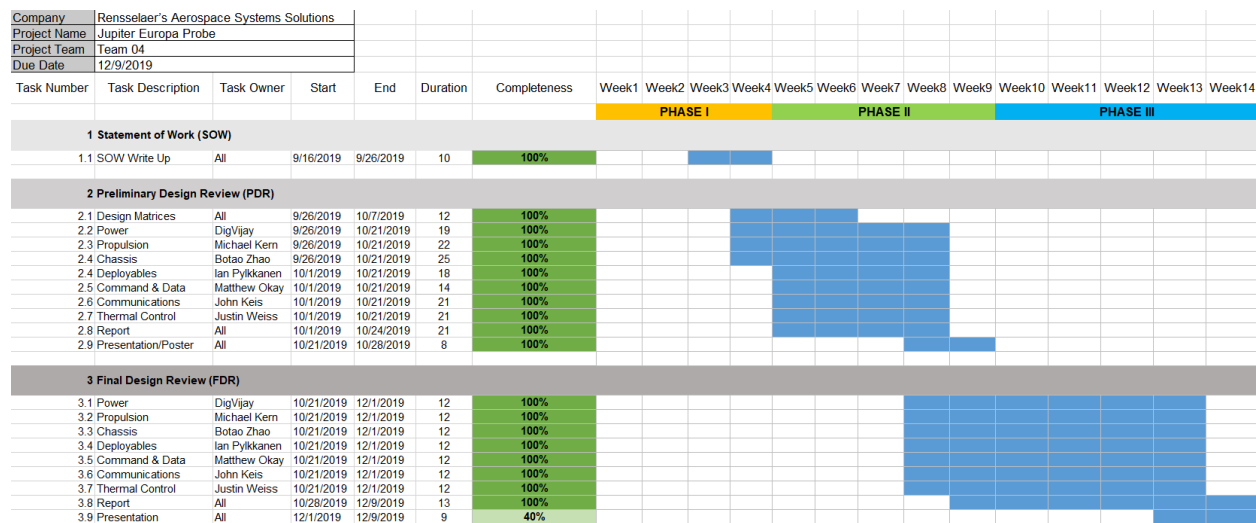
The orbiter's trajectory could also introduce a risk should it be out of range of the communication system. The landing site of the probe could also impose a communications risk if there is an object in-between it and the orbiter during the window of communications time. Proper mission planning and landing site selection will be critical to mitigate these risks.

5.9 Thermal Control Risks and Mitigations

Thermal Control is a critical subsystem of the probe. Failure to properly control the temperature of the probe's components could result in their failure, which could be detrimental to the overall mission. Most risk mitigation will be accomplished by creating an accurate mathematical model for which to analyze the thermal properties of and the heat transfer through the probe. The thermal control system is completely passive, so improper temperature control due to an inaccurate mathematical model won't be corrected by on-board computers. To mitigate the risk of components falling outside their temperature range, the system was designed to allow a margin of error of 10 degrees Celsius for each compartment. In addition to developing an accurate model, risk will also be mitigated by ensuring proper techniques during manufacturing to avoid any defects. This will prevent failures that may be caused by thermal straps detaching from their interfaces and heat not transferring through the structure of the probe as expected.

6 Timeline and Planning

The starting date for the project is September 12. Each team member dedicates to one subsystem of the project. The final design report has been finished so far and the presentation will be held on December 9. The project gantt chart with approximate timeline and schedule is shown below:



7 Conclusion

Over a period of 14 weeks, Team 4 developed a design for a spacecraft to exceed NASA and the ESA's requirements for the Minos Probe.

The probe detailed in this report is capable of surviving several years in space en route to Europa. Thermal management was carefully considered to ensure that all vital systems remain within operating conditions. Upon arriving at Jupiter's icy moon the MP will descend to the surface using a soft-landing by way of rocket propulsion. A radioisotope thermoelectric generator will power the MP for the duration of the mission. The communication system can transfer 700 MB of scientific data per uplink window. A suite of sensors and instruments allow the Minos Probe to collect surface and atmospheric samples. Additionally, a multi-spectral stereoscopic imaging capability was added to increase the breadth of scientific data collected by the probe. Command and data will deliver this information back to Earth, while keeping the MP up and running in the Aluminum alloy light weight design. All together these subsystems provide a functional and promising Europa lander.

This design finds the perfect medium of ambition and reliability given its cutting edge and space proven technology. NASA and ESA have invested an immense amount of time and money in the pursuit of landing on Europa and our team is confident we can deliver this. The design of the Minos Probe provides opportunities to make unprecedented achievements and provide groundbreaking discoveries. NASA and ESA are on the pursuit of finding life in the universe, and the Minos Probe will take them there.

References

- [1] "Multi-mission radioisotope thermoelectric generator," [Online]. Available: https://en.wikipedia.org/wiki/Multi-mission_radioisotope_thermoelectric_generator#/media/File:MMRTG_schematic_english_labels.png. [Accessed 8 December 2019].
- [2] R. L. Cataldo and G. L. Bennett, "U.S. Space Radioisotope Power Systems and Applications: Past, Present and Future," *Radioisotopes - Applications in Physical Sciences*, pp. 13-15, 2011.
- [3] NASA/Jet Propulsion Laboratory-Caltech, "Energy Storage Technologies for Future Planetary Sciences Missions," 2017.
- [4] Research Interfaces, "Battery Technology for Mars missions," 2 May 2018. [Online]. Available: <https://researchinterfaces.com/battery-technology-mars-missions/>. [Accessed 7 December 2019].
- [5] Wikipedia, "Battery management system," 3 December 2019. [Online]. Available: https://en.wikipedia.org/wiki/Battery_management_system. [Accessed 7 December 2019].
- [6] R. Ewell, B. V. Ratnakumar, M. Smart, K. B. Chin, L. Whitcanack, S. R. Narayanan and S. Surampudi, "Battery Control Boards for Li-Ion Batteries on Mars Exploration Rovers," 2004.
- [7] "Space Power and Energy Storage," *NASA Technology Roadmaps*, 2015.
- [8] Crane Aerospace & Electronics, "NASA's Mars Science Lab, Curiosity, Lands on Mars with Interpoint DC-DC Converter," [Online]. Available: <https://www.craneae.com/news/NewsStory.aspx?ID=225>. [Accessed 7 December 2019].
- [9] "Vacco Space Products," [Online]. Available: https://www.vacco.com/images/uploads/pdfs/cold_gas_thrusters.pdf. [Accessed 7 December 2019].
- [10] "In-Space Propulsion Data Sheets," 13 September 2019. [Online]. Available: <https://www.rocket.com/sites/default/files/documents/In-Space%20Data%20Sheets%209.13.19.pdf>. [Accessed 7 December 2019].
- [11] T. Greicius, "NASA Tests Robotic Ice Tools," 30 March 2017. [Online]. Available: <https://nasa.gov/feature/jpl/nasa-tests-robotic-ice-tools>.
- [12] S. Kempf, "SUDA: A Dust Mass Spectrometer for Compositional Surface," European Planetary Science Congress, 2014.

- [13] "SAM," [Online]. Available: <https://mars.nasa.gov/msl/spacecraft/instruments/sam/>.
- [14] "Mastcam-Z," [Online]. Available: <https://mars.nasa.gov/mars2020/mission/instruments/mastcam-z/>. [Accessed 7 December 2019].
- [15] P. L. Conley, *Space Vehicel Mechanisms: Elements of Successful Design*, New York: John Wiley & Sons, Inc., 1998.
- [16] J. Sokol, S. Krishnan and L. Ayari, "High Gain Antenna Gimbal for the 2003-2004 Mars Exploration Rover Program," National Aeronautics and Space Administration, 2019.
- [17] J. Taylor, A. Makovsky, A. Barbieri, R. Tung, P. Estabrook and A. G. Thomas, "Mars Exploration Rover Telecommunications," National Aeronautics and Space Administration, Pasadena, California, 2005.
- [18] W. Kuhn and Y. Tugnawat, "UHF Micro-Transceiver Development Project," 2017.
- [19] "MARS Reconnaissance Orbiter X-Band Communications," NASA, [Online]. Available: <https://mars.nasa.gov/mro/mission/communications/commxband/>. [Accessed 20 November 2019].
- [20] "The Friis Equation," [Online]. Available: <http://www.antenna-theory.com/basics/friis.php>. [Accessed 29 November 2019].
- [21] E. Howell, "Europa: Facts About Jupiter's Icy Moon and Its Ocean," Space.com, 22 March 2018. [Online]. Available: <https://www.space.com/15498-europa-sdcmp.html>. [Accessed 22 October 2019].
- [22] J. Taylor, D. K. Lee and S. Shambayati, "Mars Reconnaissance Orbiter Telecommunications," National Aeronautics and Space Administration, Pasadena, California, 2006.
- [23] D. G. Gilmore, *Spacecraft Thermal Control Handbook*.
- [24] "Thermal Control," NASA, [Online]. Available: <https://sst-soa.arc.nasa.gov/07-thermal>. [Accessed 22 October 2019].
- [25] "Juno Armored Up to Go to Jupiter," NASA, 12 July 2010. [Online]. Available: https://www.nasa.gov/mission_pages/juno/news/juno20100712.html. [Accessed 22 October 2019].
- [26] M. D. Griffin and J. R. French, *Space Vehicle Design*.

- [27] H. H. M. V. P. C. G. H. M. K. C. CLAUSEN1, "THE HUYGENS PROBE SYSTEM DESIGN," ESA Science Directorate, Scientific Project Department, ESTEC, Postbus 299, NL-2200 AG, 2002.
- [28] B. Systems, "RAD750 3UCompactPCI Technical Specificaitons," 2018. [Online].
- [29] "Cassini Mission History," [Online]. Available: <https://solarsystem.nasa.gov/missions/cassini/mission/spacecraft/huygens-probe/>.
- [30] C. D. Brown, Elements of Spacecraft Design, Reston, VA: American Institute of Aeronautics and Astronautics, Inc., 2002.
- [31] F. V. Bennett, "Apollo Lunar Descent and Ascent Trajectories," NASA, 19-21 January 1970. [Online]. Available: <https://www.hq.nasa.gov/alsj/nasa58040.pdf>. [Accessed 20 October 2019].
- [32] H. H. Haglund, "Surveyor III: Mission Report," JPL, 1 September 1967. [Online]. Available: <https://www.hq.nasa.gov/alsj/a12/Surveyor-III-MISSIONRpt1967028267.pdf>. [Accessed 2019 October 18].
- [33] K. C. Wu, J. Antol, J. J. Watson, R. J. Saucillo, D. D. North and D. D. Mazanek, "Lunar Lander Structural Design Studies at NASA Langley," National Aeronautics and Space Administration, Hampton, Virginia, 2006.
- [34] W. Rits, "A Multipurpose Deployable Membrane Reflector - A New Design Concept," November 1996. [Online]. Available: <https://www.esa.int/esapub/bulletin/bullet88/rits88.htm>.
- [35] J. Hsu, "DUAL DRILL DESIGNED FOR EUROPA'S ICE," 15 April 2019. [Online]. Available: <https://www.astrobio.net/news-exclusive/dual-drill-designed-for-europas-ice/>.
- [36] T. Greicus, "Electra Relay Radio on MAVEN Mission to Mars," 28 February 2014. [Online]. Available: <https://www.nasa.gov/jpl/maven/electra-relay-radio-pia17952/#.XbDOq-hKiUl>.
- [37] "STS-34 Galileo processing at KSC's SAEF-2 planetary spacecraft facility," [Online]. Available: <https://science.ksc.nasa.gov/mirrors/images/images/pao/STS34/10063715.jpg>.
- [38] "Space Communications with Mars," [Online]. Available: <http://www.astrosurf.com/luxorion/qsl-mars-communication3.htm>.
- [39] "RADIO FREQUENCIES FOR SPACE COMMUNICATION," [Online]. Available: <http://www.spaceacademy.net.au/spacelink/radiospace.htm>.
- [40] "Properties of Aluminum Alloys at Cryogenic and Elevated Temperatures," [Online]. Available: <https://www.totalmateria.com/page.aspx?ID=CheckArticle&site=ktn&NM=23>.

- [41] "Communications With Earth," [Online]. Available:
<https://mars.nasa.gov/msl/mission/communications/#data>.
- [42] "ASM Aerospace Specification Metals," [Online]. Available:
<http://www.aerospacemetals.com/contact-aerospace-metals.html>.
- [43] "Agency Chart," September 2019. [Online]. Available:
https://www.nasa.gov/sites/default/files/atoms/files/agency_chart_sept_2019.pdf.
[Accessed 21 November 2019].

Appendix A

Deliverables

Table 11: Course Deliverables

Date	Deliverable
21-Oct-19	Preliminary Design Report
28-Oct-19	Preliminary Design Presentation Poster
9-Dec-19	Final Design Report
9-Dec-19	Final Design Presentation Poster

Risk Tables

All risk tables were calculated using NASA's risk assessment matrix where severity is ranked as either negligible, marginal, critical, or catastrophic.

Table 12: Mission Risk Table

Risk	Potential Cause	Severity	Mitigation
Environmental	Launch failure leading to chemical and radiological contamination, Europa landing failure leading to similar contamination of Europa	Catastrophic	Extensive Testing, Proper QA practices followed, Proper Containment
Public Health	Chemical or radiological exposure due to launch failure	Catastrophic	Extensive Testing, Proper QA practices followed, Proper Containment
Social	Cost of mission	Critical	Successful Mission Warrants Justification
Cultural	Damage to national pride and lack of confidence/support for space program in event of mission failure, damaged international relations in event of failed launch when carrying radiological components through atmosphere	Critical	Flight proven launch vehicle, redundancy of systems, comprehensive testing
Economic	Cost of mission, Wasted funding and man hours if mission fails	Critical	Successful Mission Warrants Justification

Table 13: Power System Risk Table

Risk	Potential Cause	Severity	Mitigation
Environmental Contamination	Radiation from RTG	Critical	Adequate Shielding
RTG Failure	Launch Vehicle/Spacecraft Crash or Explosion	Catastrophic	Extensive Ground Testing, Mission Control Design
Secondary Battery Failure	Environmental factors	Critical	Redundancy, Quality Control, Extensive Ground Testing
Radiation Damage	Radiation from RTG	Critical	Adequate Shielding

Table 14: Propulsion System Risk Table

Risk	Potential Cause	Severity	Mitigation
Engine Failure	Environmental factors	Catastrophic	Extensive research, Thermodynamic analysis of components at wide range of temperature bands
Attitude Control Failure	Actuator failure due to environmental factors	Catastrophic	System Redundancy, robust actuators
Environmental Contamination	Toxic products of combustion	Critical	Descent engine shutdown at an altitude of 2m, Drill into ice to collect samples

Table 15: Chassis Risk Table

Risk	Potential Cause	Severity	Mitigation
Landing Gears Release/Engage System Failure	Components Failure, Environmental Factors	Catastrophic	Manufacturing Quality Control, Extensive Ground Testing
Structural Failure	Engineering/Design Failures, Environmental Factors	Catastrophic	Extensive Ground Testing

Table 16: Mechanisms/Deployables System Risk Table

Risk	Potential Cause	Severity	Mitigation
Crushable Legs Failure Under Landing Loads	Component Failure, Environmental Factors	Marginal	Quality Design, Redundancy Manufacturing Quality Control, Extensive Ground Testing
Scientific Equipment Failure	Component, Failure, Environmental Factors	Catastrophic	Quality Design, Quality Control, Extensive Ground Testing
Antenna Deployment Failure	Component Failure, Structural Damage During Launch	Critical	Redundancy, Quality Control, Extensive Ground Testing

Table 17: Command and Data System Risk Table

Risk	Potential Cause	Severity	Mitigation
Hardware Freeze	Extreme Cold Temperatures	Catastrophic	Adequate Thermal Insulation
CPU Chip Failure	Manufacturing error, lifespan	Catastrophic	Secondary Processing Unit
Software Error	Coding error, inadequate estimation's of environment	Critical	Consistent software updates and analysis by team on earth

Table 18: Communications System Risk Table

Risk	Potential Cause	Severity	Mitigation
Component failure	Gimbal failure, HGA deployment failure, Electronics failure of transceiver	Catastrophic	Use flight heritage equipment, extensive ground testing, redundancy
Communications Interference	Atmospheric conditions, obstruction by planetary object	Critical	Ensure RO trajectory is planned properly
Safety of Assembly and Test Technicians	Unsafe working conditions, care not taken while working on energized equipment	Critical	Adhere to electrical safety guidelines, Proper oversight while testing
Environmental , Cultural, Political, Social	N/a	Negligible	N/a

Table 19: Thermal System Risk Table

Risk	Potential Cause	Severity	Mitigation
Environmental Contamination	Radiation from RHU	Critical	Shielding on RHU
Failure to Regulate Temperature Properly	Inaccurate mathematical model	Critical	Quality Control, Extensive Ground Modeling and Testing
Failure to Properly Transfer Heat	Poor connections to thermal straps and/or at structural joints	Critical	Quality Control, Extensive Ground Testing

Appendix B

Table 20: MER X-band and UHF Mass and Input Power Summary [17]

Assembly	Input Power, W	RF Power out, W	Mass, kg	Quantity	Mass Total, kg	Dimensions, cm
X-Band						
SDST each			2.682	1	2.682	$18.1 \times 11.4 \times 16.6$
Receiver (R) only	11.0					
R+exciter, two-way (coherent)	13.3					
R+exciter, one-way (aux osc)	13.8					
SSPA	58	16.8	1.300	2	2.600	$4.4 \times 17.2 \times 13.4$
Hybrid			0.017	1	0.017	2.5×1.0
WTS			0.378	1	0.378	$4.1 \times 9.65 \times 10.9$
CTS			0.062	3	0.187	$5.3 \times 3.0 \times 4.0$
Coax			0.057	4	0.228	
Diplexer			0.483	1	0.483	$27.7 \times 5.6 \times 7.9$
Attenuator			0.004	1	0.004	0.79×2.18
HGA			1.100	1	1.100	28.0 dia.
CLGA			0.431	1	0.431	10.0×2.3
BLGA			0.235	1	0.431	10.3×3.5
RLGA			0.775	1	0.431	60.2×3.1
PLGA			0.020	1	0.020	1.5×1.5
MGA			0.499	1	0.499	23.4×13.4 at rim
Terminations, dummy loads, etc.			0.006	4	0.026	
X-band totals	71.8 max	16.8	5.367		6.835	
UHF						
UHF transceiver	6 rx only 43 rx/tx	12 *	1.900	1	1.900	$5.1 \times 6.8 \times 3.7$
Diplexer			0.400	1	0.400	$2.9 \times 3.7 \times 1.3$
CTS			0.083	1	0.083	$5.3 \times 3.0 \times 4.0$
RUHF			0.100	1	0.100	$16.9 \times 1.9 \times 1.9$
DUHF			0.100	1	0.100	$16.9 \times 1.9 \times 1.9$
Coax			0.300	1	0.300	

* UHF RF power out is measured at diplexer output.

Table 21: MRO Telecom Mass and Power Summary [22]

Assembly	Subtotal, kg	Total mass, kg	Spacecraft power input, W	RF power output, W	Note
X-band transponder		6.4	16		Orbit average power
SDSTs (2)	5.8				
x4 frequency multiplier+bracket	0.1				
Other microwave components	0.5				
Traveling-wave tube amplifiers		12.1			
X-band TWTA (2)	1.9		172	102	100 W nominal
Ka-band TWTA	0.8		81	34	35 W nominal
X-band electronic power converters	3.0				
Ka-band electronic power converter	1.5				
Diplexers and brackets	1.8				
Waveguide transfer switches	1.5				
Other microwave components	1.4				
Miscellaneous TWTA hardware	0.2				
X-band and Ka-band antennas		22.6			
HGA prime reflector	19.1				
Antenna feed assembly	1.6				
LGAs and polarizers	0.8				
Miscellaneous antenna hardware	1.1				
HGA gimbals and drive motors		45.0	14		Orbit average power
Waveguides and coax		8.3			
USOs (2)		1.7	5		Orbit average power
UHF subsystem		11.5			
Electra transceivers (2) (each transciever has an integral solid-state RF power amplifier)	10.1		71	5	On, full duplex (17.4 W standby)
UHF antenna and radome	1.4				
String switch (S)	0.1				
Telecom total		<u>107.7</u>	<u>359</u>		

Table 22: STK Communications Simulation

Approved for Personal Home Use Only

Facility-MinosProbe-Sensor-X-Band-To-Satellite-Orbiter-Sensor-Sensor3: Inview Azimuth, Elevation, & Range

X-Band-To-Sensor3 - AER reported in the object's default AER frame

	Time (UTCG)	Azimuth (deg)	Elevation (deg)	Range (km)
20 Nov 2019 17:15:03.608	257.726	0.000	1414.059482	
20 Nov 2019 17:16:03.000	258.008	2.075	1361.532896	
20 Nov 2019 17:17:03.000	258.315	4.261	1308.739110	
20 Nov 2019 17:18:03.000	258.645	6.546	1256.309199	
20 Nov 2019 17:19:03.000	259.005	8.944	1204.347424	
20 Nov 2019 17:20:03.000	259.398	11.467	1152.972174	
20 Nov 2019 17:21:03.000	259.830	14.132	1102.318682	
20 Nov 2019 17:22:03.000	260.311	16.955	1052.542249	
20 Nov 2019 17:23:03.000	260.851	19.956	1003.822033	
20 Nov 2019 17:24:03.000	261.463	23.157	956.365415	
20 Nov 2019 17:25:03.000	262.165	26.582	910.412870	
20 Nov 2019 17:26:03.000	262.983	30.254	866.243165	
20 Nov 2019 17:27:03.000	263.952	34.200	824.178427	
20 Nov 2019 17:28:03.000	265.122	38.441	784.588327	
20 Nov 2019 17:29:03.000	266.570	42.997	747.892062	
20 Nov 2019 17:30:03.000	268.413	47.874	714.556252	
20 Nov 2019 17:31:03.000	270.848	53.062	685.086272	
20 Nov 2019 17:32:03.000	274.217	58.521	660.008316	
20 Nov 2019 17:33:03.000	279.170	64.154	639.840273	
20 Nov 2019 17:34:03.000	287.052	69.763	625.051682	
20 Nov 2019 17:35:03.000	300.808	74.904	616.016938	
20 Nov 2019 17:36:03.000	325.703	78.526	612.970250	
20 Nov 2019 17:37:03.000	0.230	78.854	615.973467	
20 Nov 2019 17:38:03.000	26.933	75.748	624.906166	
20 Nov 2019 17:39:03.000	41.855	71.011	639.481284	
20 Nov 2019 17:40:03.000	50.308	65.810	659.281022	
20 Nov 2019 17:41:03.000	55.557	60.614	683.804486	
20 Nov 2019 17:42:03.000	59.094	55.613	712.513358	
20 Nov 2019 17:43:03.000	61.633	50.884	744.870617	
20 Nov 2019 17:44:03.000	63.546	46.454	780.367343	
20 Nov 2019 17:45:03.000	65.042	42.324	818.538505	
20 Nov 2019 17:46:03.000	66.249	38.479	858.969888	
20 Nov 2019 17:47:03.000	67.246	34.900	901.298924	
20 Nov 2019 17:48:03.000	68.087	31.563	945.211845	
20 Nov 2019 17:49:03.000	68.809	28.445	990.438979	
20 Nov 2019 17:50:03.000	69.438	25.524	1036.749345	
20 Nov 2019 17:51:03.000	69.993	22.779	1083.945294	
20 Nov 2019 17:52:03.000	70.488	20.190	1131.857541	
20 Nov 2019 17:53:03.000	70.934	17.742	1180.340766	
20 Nov 2019 17:54:03.000	71.339	15.419	1229.269809	
20 Nov 2019 17:55:03.000	71.711	13.208	1278.536449	
20 Nov 2019 17:56:03.000	72.054	11.097	1328.046693	
20 Nov 2019 17:57:03.000	72.373	9.076	1377.718516	
20 Nov 2019 17:58:03.000	72.671	7.136	1427.479981	
20 Nov 2019 17:59:03.000	72.951	5.269	1477.267677	
20 Nov 2019 18:00:03.000	73.215	3.467	1527.025427	
20 Nov 2019 18:01:03.000	73.465	1.726	1576.703208	
20 Nov 2019 18:02:03.000	73.704	0.038	1626.256254	
20 Nov 2019 18:02:04.363	73.709	0.000	1627.380091	
Global Statistics				
Min Elevation	20 Nov 2019 18:02:04.363	73.709	0.000	1627.380091
Max Elevation	20 Nov 2019 17:36:37.949	345.696	79.204	613.987556
Mean Elevation			31.840	
Min Range	20 Nov 2019 17:36:03.216	325.817	78.534	612.970229
Max Range	20 Nov 2019 18:02:04.363	73.709	0.000	1627.380091
Mean Range			1007.838497	

Appendix C

Analysis Code 3.1

```
%Define Constants
mu      = 3201;
r       = 1561;
g       = 1.315;
alt     = 100;
altTD   = 0:100;

v1    = sqrt(mu/(r+alt));
h2    = sqrt(2*mu).*sqrt(((r+alt).*(r+altTD))./((r+alt)+(r+altTD)));
v2a  = h2./(r+alt);
v2b  = h2./(r+altTD);
v3   = sqrt(mu./(r+altTD));
vf   = sqrt(2.*g.* (altTD*1000))/1000;

deltaV = (v1-v2a)+(v2b-v3) + v3 + vf;

hold on
plot (deltaV,altTD, 'LineWidth', 2);
plot([1.3 2], [15 15], '--black');
pbaspect([1 1 1])
xlabel('\Delta V Required (Km/s)');
ylabel('TDA (Km)');
title('Terminal Descent Altitude (TDA) vs \Delta V');
```

Analysis Code 3.2

```
hold on
pos = [-1 -1 2 2];

%Outer Orbit
rectangle('Position',pos,'Curvature',[1 1],'LineStyle','--')

%Europa
rectangle('Position',pos/4,'Curvature',[1 1],'FaceColor','Black')

%Semi Circle
th1 = linspace( pi/2, -pi/2, 100);
R1 = 1; %or whatever radius you want
x1 = R1*cos(th1);
y1 = R1*sin(th1);
plot(x1,y1,'black','LineWidth',2);

%Ellipse
th2 = linspace (0, -pi, 100);
e = 0.5;
R2 = 0.703*(1-e^2)./(1+e*cos(th2));
x2 = R2.*sin(th2);
y2 = R2.*cos(th2)+0.053;
plot(x2,y2,'k','LineWidth',2);

%Dashed Ellipse
th3 = linspace (0,2*pi, 100);
e = 0.5;
R3 = 0.703*(1-e^2)./(1+e*cos(th3));
x3 = R3.*sin(th3);
y3 = R3.*cos(th3)+0.053;
plot(x3,y3,'k','LineStyle','--');

%Inner Orbit
rectangle('Position',pos/2.5,'Curvature',[1 1],'LineStyle','--')

axis equal
set(gca,'visible','off')
pbaspect([1 1 1])
```

Analysis Code 3.3

```
hold on
pos = [-1 -1 2 2];

%Europa
rectangle('Position',pos,'Curvature',[1 1],'FaceColor','Black')

%Terminal Descent
th2 = linspace (0, pi, 100);
e = 0.85;
R2 = 0.46*(1-e^2)./(1+e*cos(th2));
x2 = R2.*sin(th2);
y2 = R2.*cos(th2)+1.53;
plot(x2,y2,'k','LineWidth',2);

%Hollman Transfer
th3 = linspace (0,-pi/2, 100);
e = 0.5;
R3 = 2.812*(1-e^2)./(1+e*cos(th3));
x3 = R3.*sin(th3);
y3 = R3.*cos(th3)+0.195;
plot(x3,y3,'k','LineWidth',2);

%Inner Orbit
rectangle('Position',pos*1.6,'Curvature',[1 1],'LineStyle','--')

axis equal
set(gca,'visible','off')
pbaspect([1 1 1])
```

Appendix D

Finding temperature of RTG compartment:

$$Q_{RTG} - Q_{radiated} = 0$$

$$Q_{rad,RTG} = Q_{RTG} - Q_{rad,prop} - 2Q_{rad,SC1} - Q_{rad,power} - Q_{rad,control} - Q_{rad,com} - 2Q_{rad,SC2}$$

$$Q_{rad,RTG} = Q_{RTG} - Q_{rad,prop} - 2Q_{rad,SC1} - 3Q_{rad,com} - 2Q_{rad,SC2}$$

$$Q_{rad,RTG} = Q_{RTG} - A_{prop}\epsilon\sigma(T_{prop}^4 - T_c^4) - 2A_{SC}\epsilon\sigma(T_{SC1}^4 - T_c^4) - 3A_{com}\epsilon\sigma(T_{com}^4 - T_c^4) - 2A_{SC}\epsilon\sigma(T_{SC2}^4 - T_c^4)$$

$$Q_{rad,RTG} = 2000W - 166W - 2(116W) - 3(165W) - 2(85.6W)$$

$$Q_{rad,RTG} = 2000W - 1064W$$

$$Q_{rad,RTG} = 936W$$

$$T_{RTG}^4 = T_c^4 + \frac{Q_{rad,RTG}}{A_{RTG}\epsilon\sigma} = (113K)^4 + \frac{936W}{(0.587m^2)(0.92)\left(5.67 * 10^{-8} \frac{W}{m^2 K^4}\right)}$$

$$T_{RTG} = 419K = 146^\circ C$$

Length of thermal straps are taken to be twice the thickness of the walls between compartments. Due to symmetry, all lengths are the same.

$$L = 2(0.005 m) = 0.01 m$$

Thermal straps from Power and Control to SC2s:

$$Q_{rad,SC2} = Q_{power,SC2} = \frac{kA_{power,SC2}(T_{power} - T_{SC2})}{L}$$

$$A_{power,SC2} = \frac{(Q_{rad,SC2})(L)}{k(T_{power} - T_{SC2})} = \frac{(85.6 W)(0.01 m)}{\left(237 \frac{W}{mK}\right)(10 K)} = 361 mm^2$$

Thermal straps from SC1s to Power and Control:

$$Q_{rad,power} + Q_{power,SC2} = Q_{SC1,power} = \frac{kA_{SC1,power}(T_{SC1} - T_{power})}{L}$$

$$A_{SC1,power} = \frac{(Q_{rad,power} + Q_{rad,SC2})(L)}{k(T_{SC1} - T_{power})} = \frac{(165 W + 85.6 W)(0.01 m)}{\left(237 \frac{W}{mK}\right)(10 K)} = 1058 mm^2$$

Thermal straps from RTG to SC1s:

$$A_{RTG,SC1} = \frac{(Q_{rad,SC1} + Q_{rad,power} + Q_{rad,SC2})(L)}{k(T_{RTG} - T_{SC1})} = \frac{(116 W + 165 W + 85.6 W)(0.01 m)}{\left(237 \frac{W}{mK}\right)(136 K)} \\ = 114 \text{ mm}^2$$

Thermal strap from Propellant to Communication:

$$A_{prop,com} = \frac{(Q_{rad,com})(L)}{k(T_{prop} - T_{com})} = \frac{(165 W)(0.01 m)}{\left(237 \frac{W}{mK}\right)(10 K)} = 697 \text{ mm}^2$$

Thermal strap from RTG to Propellant:

$$A_{RTG,prop} = \frac{(Q_{rad,prop} + Q_{rad,com})(L)}{k(T_{RTG} - T_{prop})} = \frac{(166 W + 165 W)(0.01 m)}{\left(237 \frac{W}{mK}\right)(136 K)} = 103 \text{ mm}^2$$

Total mass of thermal straps:

$$m = \rho_{aluminum} L (2A_{power,SC2} + 2A_{SC1,power} + 2A_{RTG,SC1} + A_{prop,com} + A_{RTG,prop}) \\ m = \left(2710 \frac{kg}{m^3}\right)(0.01 m)(3.86 * 10^{-3} \text{ m}^2) = 0.105 \text{ kg}$$

Appendix E

Europa Surface and Atmospheric Sample Probe

“Minos Probe”

Team 4

Preliminary Design Report



Under the Direction of Professor K.S. Anderson

MANE 4850 Space Vehicle Design Capstone

October 21, 2019

Rensselaer Polytechnic Institute

Table of Contents

Acknowledgements	78
Contributions	78
Executive Summary	79
List of Terms, Acronyms, and Abbreviations	80
List of Tables	82
List of Figures	83
1 Introduction and Background	84
1.1 Past Missions	84
1.2 Mission Purpose	84
2 Scope	84
2.1 Customer Requirements	84
2.2 Objectives	84
2.3 Considerations	85
2.3.1 2Technical Issues	85
2.3.2 Environmental Constraints	85
2.3.3 Political Constraints	85
2.3.4 Cost Constraints	86
3 Design	86
3.1 Power	86
3.1.1 Power Source Selection	86
3.1.2 RTG Radioisotope Selection	89
3.1.3 RTG Model Selection	89
3.1.4 Power Storage Selection	91
3.1.5 Power System Future Work	92
3.2 Propulsion	92
3.2.1 Landing Category Selection	92
3.2.2 Landing Approach Selection	93
3.2.3 System and Propellant Selection	94
3.3 Chassis	96
3.3.1 Chassis Design Specifications	96
3.3.2 Chassis Materials	97

3.3.3	Chassis Structure	98
3.3.4	Chassis Future Structural Work	100
3.4	Mechanisms/Deployables	100
3.4.1	Landing Mechanisms/Deployables	100
3.4.1.1	Landing Mechanisms/Deployables Selection	100
3.4.2	Scientific Mechanisms/Deployables:	102
3.4.2.1	Scientific Mechanisms/Deployables Selection	102
3.4.3	Communication Deployables	105
3.4.3.1	Communication Deployables Selection	105
3.5	Command and Data	109
3.5.1	Command and Data Requirements	109
3.5.2	Command and Data Selection	109
3.6	Communications	110
3.6.1	Communications Selection Requirements	110
3.6.2	Communications Selection Criteria	111
3.6.3	Future Communication Work	113
3.7	Thermal Control	113
3.7.1	Heating	113
3.7.2	Internal Heat Transfer	114
3.7.3	Thermal Radiation	115
3.7.4	Charged Particle Protection	116
3.7.5	TCS Description	116
3.7.6	Future Work	117
4	Risks	118
4.1	Power Risks and Mitigations	118
4.2	Propulsion Risks and Mitigations	118
4.3	Chassis Risks and Mitigation	119
4.4	Mechanisms/Deployables Risks and Mitigations	119
4.5	Command and Data Risks and Mitigations	119
4.6	Communications Risks and Mitigations	119
4.7	Thermal Control Risks and Mitigations	120
5	Timeline and Planning	121

6 Conclusion	122
References	123
Appendices	126
Deliverables	126
Risk Tables	126

Acknowledgements

As a team, we would like to thank Dr. Kurt Anderson. As a professor and associate dean in the Mechanical, Aerospace and Nuclear Engineering department at Rensselaer Polytechnic Institute, his insight and teachings from his many years of experience in the space industry have been invaluable.

Contributions

Team 4 Contributions		
	Section	Contributor
-	Report Structure and Formatting	Ian Pylkanen, John Keis
-	Executive Summary	Ian Pylkanen, John Keis
1	Introduction and Background	Ian Pylkanen, John Keis
2	Scope	Matthew Okay
3.1	Power Systems	DigVijay Ghule
3.2	Propulsion	Michael Kern
3.3	Chassis	Botao Zhao
3.4	Mechanisms/Deployables	Ian Pylkanen
3.5	Command and Data	Matthew Okay
3.6	Communications	John Keis
3.7	Thermal Control	Justin Weiss
0	Risks	All members
0	Timeline and Planning	Botao Zhao
7	Conclusion	Ian Pylkanen

Executive Summary

This report outlines the preliminary design of the Minos Probe (MP) and will detail both current and anticipated progress of the design process. The Minos Probe is a probe intended to land on Jupiter's moon Europa and take samples of the surface ice and atmosphere. The Minos Probe will travel to Europa on-board the Rhadamanthus-Orbiter (RO). Once RO reaches Europa, the Minos Probe will be jettisoned and perform a powered descent onto the surface of Europa performing a soft landing. Once on the surface of Europa, the Minos Probe will collect valuable data on the composition of Europa's surface and atmosphere. The data will be transmitted back to RO and subsequently on to earth. The Minos Probe will not leave the surface of Europa.

This report will touch on past missions that will allow for a better understanding of the overall purpose of the current planned mission. Customer requirements will be stated to provide a guide of the project objectives, considerations, and requirements. The preliminary design of the Minos Probe will be detailed in its seven sub-systems: power, propulsion, chassis, deployables, command and data, communications, and thermal control. Decision matrices, trade studies, and benchmarking will be completed for each sub-system and detailed in each respective section. A risk analysis will then be addressed for all sub-systems, as well as the Minos Probe as a whole. A timeline for future development will be provided followed by a conclusion of the report.

It is important to note that this report is covering only the preliminary design process. Some areas of the report require additional research and collaboration with an orbiter team making them incomplete to an extent. Additionally, the designs proposed in this report are subject to change as more research is conducted and final decisions are made.

List of Terms, Acronyms, and Abbreviations

BAE - British Aerospace

CPU - Central Processing Unit

EEPROM - Electrically Erasable Programmable Read-Only Memory

EPS - Electrical Power System

ESA - European Space Agency

GPHS-RTG - General-Purpose Heat Source Radioisotope Thermoelectric Generator

JPL - Jet Propulsion Lab

K - Kelvin

Ka-Band - 27-40 GHz

Ku-Band - 12-18 GHz

MB - Mega Bites

MHW-RTG - Multihundred-Watt Radioisotope Thermoelectric Generator

MLI - Multilayer Insulation

MMH - Monomethylhydrazine

MMRTG - Multi-Mission Radioisotope Thermoelectric Generator

MP - Minos Probe

MSL - Mars Science Laboratory

NASA- National Aeronautics and Space Administration

REASON - Radar for Europa Assessment and Sounding: Ocean to Near-Surface

RHU - Radioisotope Heating Units

RO- Rhadamanthus-Orbiter

RTG - Radioisotope Thermal Generator

SAM - Sample Analysis at Mars

S-Band - 2-4 GHz

SHF - Super High Frequency

SNAP-19 - Systems Nuclear Auxiliary POWER 19

SUDA - Surface Dust Analyzer

TCS - Thermal Control System

UHF - Ultra-High Frequency (300 MHz to 3 GHz)

X-Band - 8 – 12 GHz

List of Tables

Table 1: Power Source Decision Matrix	88
Table 2: RTG Isotope Selection Matrix.....	89
Table 3: RTG Selection Matrix.....	90
Table 4: Power Storage Selection Matrix	92
Table 5: Landing Method Decision Matrix	92
Table 6: Landing Mechanism Decision Matrix	93
Table 7: Rocket Fuel Decision Matrix.....	94
Table 8: Chassis Material Selection Matrix.....	97
Table 9:Chassis Structure Decision Matrix	98
Table 10: Landing Mechanism/Deployables Selection Matrix	102
Table 11: Scientific Mechanism/Deployables Selection Matrix	105
Table 12: Communication Deployables Selection Matrix.....	108
Table 13: Communication Band Selection Matrix	111
Table 14: Communication Antenna Selection Matrix	112
Table 15: Heating Selection Matrix.....	114
Table 16: Heat Transfer Selection Matrix	115
Table 17: Radiator Selection Matrix.....	116
Table 18: Course Deliverables.....	126
Table 19: Power System Risk Table.....	126
Table 20: Propulsion System Risk Table.....	126
Table 21: Chassis Risk Table.....	127
Table 22: Mechanisms/Deployables System Risk Table.....	127
Table 23: Command and Data System Risk Table	128
Table 24: Communications System Risk Table.....	128
Table 25: Thermal System Risk Table.....	129
Table 26: MER X-band and UHF Mass and Input Power Summary	130
Table 27: MRO Telecom Mass and Power Summary	131

List of Figures

Figure 1: Operating Regimes of Spacecraft Power Sources	87
Figure 2: Diagram of an MMRTG	91
Figure 3: Properties of Propellants [3]	94
Figure 4: Bipropellant System [3]	95
Figure 5: Cold Gas System [3]	95
Figure 6: Chassis Hexagonal Design	96
Figure 7: Lander Configuration	99
Figure 8: Lander 2-D Sketch	99
Figure 9: Latching Hinge Design [8]	106
Figure 10: Galileo High Gain Antenna Umbrella Design [9]	107
Figure 11: Wrap-Rib Antenna Design [10]	107
Figure 12: Two-Axis Gimbal Design [8]	108
Figure 13: RAD750 CPU Processing Table [14]	110

1 Introduction and Background

1.1 Past Missions

Key missions in the past, present, and future are briefly described in the bullet points that follow.

- 1973, 1974: Pioneer 10 and 11 become the first orbiters to image Europa during their flybys of Jupiter.
- 1979: Voyager 1 and 2 take higher resolution images of Europa during their flybys of Jupiter. Icy surface observed. Speculation of ocean underneath.
- 1995-2003: Galileo takes the most detailed images of Europa.
- 2007: New Horizons images Europa on its way to Pluto.
- 2013: NASA's Hubble Telescope observes what is theorized to be plumes of water spouting from geysers on Europa's surface.
- Europa Clipper is a future mission to orbit Jupiter and take detailed images and data of Europa's surface.

1.2 Mission Purpose

As human kind we greatly value life and know how vast it can be in all of its forms. We are a curious species by nature and have an inherent gene for exploration. For centuries we have wondered what is beyond earth and is it possible that life could exist elsewhere. This mission is an exploratory mission designed to further study Jupiter's moon, Europa. The hope is to analyze the composition of Europa's atmosphere and surface to discover if it contains any of the elements we know are associated with the presence of life. This mission would be the first to land and analyze physical samples Europa. This mission will provide some of these answers and provide a framework for future missions to the surface of Europa.

2 Scope

2.1 Customer Requirements

The National Aeronautics and Space Administration (NASA) and the European Space Agency (ESA) have outlined a need for further investigation of Europa. The customer requires that a probe be delivered to the surface of the moon and conduct atmospheric analysis. This requires a need to (1) deliver the scientific payload to Europa/Jupiter orbit, (2) successfully deploy the probe and land on the surface and, (3) take atmospheric measurements that can then be transmitted to the orbiter and then to earth.

2.2 Objectives

This report details the design and development of the probe, which will be capable of safely landing on the surface and conducting analysis to be transmitted to the orbiter. This project consists of a design phase, followed by a development phase. The design was divided into seven subsystems; thermal control, mechanisms/deployables, propulsion, chassis, power systems, communications and command and data.

2.3 Considerations

2.3.1 Technical Issues

An unmanned landing in Europa's atmospheric conditions is unprecedented, and thus will require a state of the art propulsive system.

Due to high amounts of radiation, communication windows to the orbiter will be limited. A significant delay between the Minos Probe and Earth will need to be accounted for. This could potentially cause a problem with the probe to go unnoticed on earth until it is too late to try and reprogram.

Surface temperatures on Europa are exceptionally cold, averaging around 110 Kelvin. To combat this, a strong thermal control system must be utilized, with minimal room for failure, making the design of a high functioning thermal control system a top priority. Additionally, at low temperatures optical distortion can occur, and can make imaging a more difficult task.

2.3.2 Time Constraints

NASA has not defined any specific time requirements at this time. Depending on the trajectory taken, it could take the RO and Minos Probe several years to reach Europa. The Minos Probe is currently being designed to have a life span of around one year on the surface of Europa. The only time requirements at the moment are due to the launch window. Deep space travel requires departing the earth at a time when Jupiter and Earth are at their closest.

2.3.3 Environmental Constraints

The environmental constraints occur in two different environments, one on earth and one on Europa. On earth, the environmental constraints are mostly concerned with the launch of the spacecraft. Due to the probe's design, there will be a large amount of radioactive material aboard, between the Radioisotope Thermal Generator (RTG) power source and the Radioisotope Heating Units (RHU). A launch failure can result in mandated quarantine zone due to large amount of radiation that can be released upon a crash. Furthermore, even if the radioactive units are protected, a crash with leaked propellant can cause environmental damage.

On Europa, the largest environmental constraints come from data collection. During landing, if the thrusters are not turned off at an adequate position, there is a possibility of propellant contamination. It is also possible that the scientific instrumentation can become contaminated from substances on earth, and skew the data in an untruthful way.

2.3.4 Political Constraints

A mission of this magnitude can have a large array of political consequences. Due to highly radioactive materials, there can be skepticism from political constituents on the risk-reward practicality of the mission. There can be further skepticism in this regard for the high cost of the mission, that will have to come from taxpayers, and may not be considered worth the price. The last majorly political issue will regard if the mission discovers possibilities of life, and how this may affect the fundamental human understanding of the universe.

2.3.5 Cost Constraints

The cost constraints of this mission will involve the specific agencies funding the mission. This may vary due to different government policies, and geopolitical climates in the countries funding the mission.

3 Design

As a general statement in regards to the decision matrices used in the selection criteria for each of the MP subsystems, a criteria and weighting scale system will be described that will be used for all used for all design selections by all group members. Component choices will be listed in columns and criteria will be listed in rows. A ranking scale will be used for each criterion of each component using a scale of 1 to 5, where 5 holds the most weight or value. Additionally, a weighting system will be used to add or take away value for a specific criterion. This weight will vary from 1 to 2 and will act as a multiplier to the score of each components criteria score. The weight factor will be the final column to clearly show the weight each group member put on a specific criterion. The final scores for the component choices will be added by column and the component with the highest score will be selected.

3.1 Power

The electrical power system (EPS) is an essential component of a spacecraft system and a key aspect to any space mission's success. The EPS is responsible for providing power to other subsystems of the spacecraft in order to facilitate their necessary functions throughout the vehicle's desired lifespan. Furthermore, the EPS encompasses several different aspects including power generation, storage, distribution, and regulation/control. In order to select the power source and storage for the MP mission, preliminary research and analysis was conducted in the form of trade studies and decision matrices.

3.1.1 Power Source Selection

In regards to the power source of the MP, several options were considered including solar arrays, a radioisotope thermoelectric generator (RTG), primary batteries, fuel cells, and a nuclear reactor. The criteria for the selection of the power source include mass, cost, power capacity, duration, volume, and mission risk. In order to narrow down the selection process, the nominal duration for each of the power sources was highly examined since the minimum lifespan of the MP is predicted to be a year. According to Figure below, RTGs, solar arrays, and nuclear reactors all have operating regimes that are within the domain of the lifespan of the mission, while primary batteries and fuel cells fall short of the intended duration.

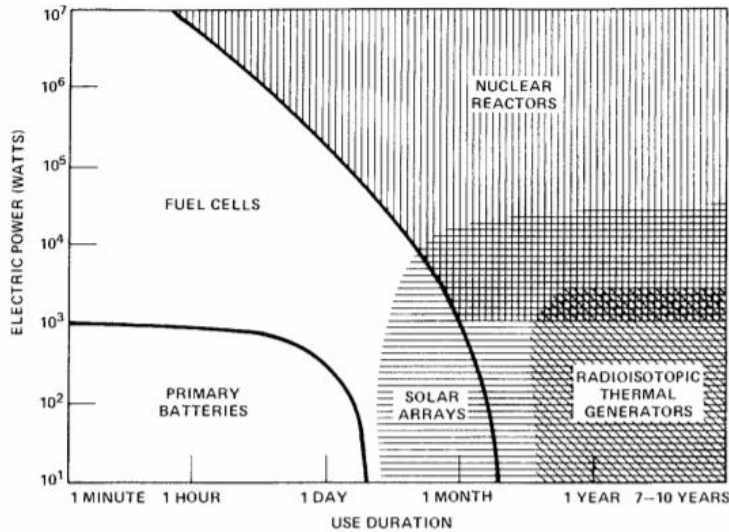


Figure 1: Operating Regimes of Spacecraft Power Sources

Firstly, solar arrays have historically been the primary source of power for unmanned spacecraft that operate inside the asteroid belt. Solar arrays rely on an assembly of photovoltaic cells in order to convert solar radiation into electricity. Some applications of this technology include the International Space Station, the Hubble Space Telescope, and the Juno space probe. Furthermore, solar arrays have become an industry standard due to their extensive heritage, proven reliability, relatively long lifetime, and comparatively low cost. They also pose minimal risk to the environment and human life. However, some drawbacks for solar arrays include the need for larger surface area for high-powered spacecraft leading to more complex deployment methods, a dependence on the availability of sunlight, performance deterioration over its lifetime due to radiation damage, and susceptibility to temperature fluctuations. In the case of the mission to Europa, solar arrays pose a severe risk to the mission due to the fact that the MP will operate beyond the asteroid belt causing solar radiation to be too weak to produce sufficient power to the spacecraft.

Secondly, RTGs are another popular power source option for planetary type space missions. RTGs rely on an array of thermocouples to convert the heat released by the decay of a radioactive material into electricity through the thermoelectric effect. Some applications of this technology include Galileo, New Horizons, and the Curiosity rover. The benefits of RTGs are that they are completely independent of sunlight, have a long operational lifespan, are compact, and do not experience performance deterioration from solar radiation or temperature fluctuations. The disadvantages of RTGs include not being able to be turned off, being relatively heavy, require shielding and cooling, and pose a moderate risk to humans and the environment due to the radioactive materials. In terms of the MP mission, the RTG is a leading contender for the selection of a power source since the lack of solar intensity on Europa would not be a factor and the heat radiation from the device would help to combat the extreme cold temperatures on the surface of the moon.

Thirdly, primary batteries are a common power source option for space missions that have a duration of a few days or less. Primary batteries are batteries that are designed to be used once and

are not rechargeable. They are simple, low cost, low mass, and have minimal risks to the environment and human life. However, since the MP mission is projected to be a year or longer, primary batteries will not be a good power source option.

Fourthly, fuel cells are an uncommon power source option that converts chemical energy of a fuel and an oxidizer into electricity through redox reactions. The most common type of fuel cell consists of hydrogen and oxygen as the reactants and water as the byproduct of the reaction. This system poses a minimal risk to the environment and human life, however the maximum duration of this power source is only on the order of months which will not be sufficient for the MP mission.

Lastly, nuclear reactors are a rare power source option that converts heat from nuclear fission into electricity. They are able to generate high power outputs for long durations while also being independent from environmental factors. However, this technology has seen minimal use in previous space missions due to the fact that nuclear reactors are extremely heavy, highly costly due to the amount of shielding and cooling required to protect the spacecraft, and provide severe risk to the environment and human life because of the radiation produced from the reaction.

Table 1: Power Source Decision Matrix

Criteria	Solar Arrays	RTG	Primary Batteries	Fuel Cells	Nuclear	Multiplier
Mass	4	2	5	3	1	1.25
Cost	4	2	5	2	1	1
Power Capacity	3	3	1	3	5	1.75
Duration	4	5	1	2	5	2
Volume	3	2	5	2	1	1.5
Mission Risk	2	5	1	3	4	2
Total	30.75	32.75	24.5	24	30.5	

According to Table , the RTG would be the best power source option for the MP mission to Europa. The most important criteria considered in the selection process included mission risk, duration, and power capacity. Although the nuclear reactor also performed well in these areas, it did not do well in all the other categories. On the other hand, the RTG was a more well-rounded power source option while also outperforming the other contenders in the most important categories. The lifespan of an RTG can have a minimum of around 10-20 years with no specific maximum depending on the radioisotope used. Also, RTGs can generate a power density of about 2-5 W/kg with a maximum power output of 50-300 W and a maximum heat output of 500-2000 W. This would allow the MP to thoroughly explore the surface of Europa in regards to time, provide steady power to all other subsystems, and also combat the extreme cold temperatures by redirecting heat from the thermoelectric modules to the rest of the spacecraft. However, with this decision comes a dramatic increase in mass, cost, and volume of the spacecraft which must be accounted for in the structure of the design.

3.1.2 RTG Radioisotope Selection

Furthermore, the radioisotopes that were considered to power the RTG include plutonium-238 (^{238}Pu), strontium-90 (^{90}Sr), polonium-210 (^{210}Po), and americium-241 (^{241}Am). The criteria for the decision matrix included shielding, power density, half-life, and cost. The radioisotope used in an RTG has a significant impact on the overall lifespan of the mission, the amount of power supplied to the spacecraft per unit mass, and the complexity and structure of the RTG design. Historically, ^{238}Pu has been the most common radioisotope used in past space missions, coming in the form of plutonium(IV) oxide (PuO_2).

Table 2: RTG Isotope Selection Matrix

Criteria	^{238}Pu	^{90}Sr	^{210}Po	^{241}Am	Multiplier
Shielding	5	1	5	3	1.75
Power Density	3	3	5	2	1.25
Half-Life	4	3	1	5	2
Cost	2	5	3	4	1
Total	22.5	16.5	20	21.75	

Based on Table 2, the best radioisotope to power the RTG is ^{238}Pu . The most important criteria considered included the half-life and shielding. ^{238}Pu has a long half-life of 87.7 years, a reasonable power density of 0.57 W/g, and only radiates an alpha particle and a relatively low-energy beta particle during the decay process. This leads to ^{238}Pu having the lowest shielding requirements and only needing less than 2.5 mm of lead shielding to block the radiation, or in many cases, no shielding at all since the casing already provides an adequate amount of shielding. On the other hand, ^{90}Sr requires a large amount of shielding due to the fact that it gives off high-energy gamma radiation as it decays. This is not desirable because long-term radiation exposure in a spacecraft can damage unprotected electronics. Other candidates such as ^{210}Po had comparable low shielding requirements to ^{238}Pu and an exceptional power density of 140 W/g, however, it has the shortest half-life of only 0.378 years which would not be sufficient for the duration of the MP mission. Also, ^{241}Am was another promising candidate for the radioisotope selection due to its significantly longer half-life of 432 years compared to ^{238}Pu , which could hypothetically power an RTG for centuries. However, ^{241}Am only has a power density of 0.114 W/g which is less than $\frac{1}{4}$ that of ^{238}Pu and further it produces high-energy gamma radiation which would then require more shielding. Although, ^{238}Pu is the best choice for the radioisotope it does come at a monetary cost since it is one of the more expensive radioisotopes at around \$3000/W.

3.1.3 RTG Model Selection

Also, the RTG models that were considered for the MP mission include the multi-mission radioisotope thermoelectric generator (MMRTG), the general-purpose heat source radioisotope thermoelectric generator (GPHS-RTG), the multihundred-watt radioisotope thermoelectric generator (MHW-RTG), and the modified Systems Nuclear Auxiliary POWER 19 (SNAP-19). The MMRTG is the most current model of the RTG developed by Aerojet Rocketdyne and Teledyne Energy Systems for NASA space missions such as the Mars Science Laboratory (MSL)/Curiosity rover. The MMRTG is based on telluride thermoelectric technology used in the

SNAP-19 RTG program which had shown that it could be used both in space and on a planetary surface and is powered by eight ^{238}Pu dioxide GPHS modules, providing about 2 kW of thermal power. The design goals for the MMRTG include having a flexible modular design in order to meet the power requirements of a wide range of space missions, ensuring a high degree of safety, optimizing power levels over the lifetime of the mission, and minimizing the weight of the device. The GPHS-RTG is specific design that was used on the Ulysses (1990), Galileo (1989), Cassini-Huygens (1997), and New Horizons (2006) space missions. The design excelled in power generation with its use of 572 silicon-germanium unicouples. The MHW-RTG were developed for the Voyager (1 & 2) spacecrafats and was able to generate 157 W of electric power at beginning of life (BOL) with 312 unicouples. Lastly, the SNAP-19 was specially modified to perform on the surface of Mars with the launch of Viking landers 1 and 2 (1975) and generated 42.7 W of electrical power, however this technology significantly outdated compared to the MMRTG. The criteria for the decision matrix includes mass, cost, power output, heat output, volume, and mission risk.

Table 3: RTG Selection Matrix

Criteria	MMRTG	GPHS-RTG	MHW-RTG	SNAP-19	Multiplier
Mass	4	2	4	5	1.25
Cost	4	1	3	5	1
Power Output	4	5	4	1	1.75
Heat Output	4	5	4	1	1.75
Volume	3	1	4	5	1.5
Mission Risk	5	1	4	1	2
Total	37.5	24.5	36	24.25	

According to Table 3, the best choice for the RTG model used on the MP mission is the state-of-the-art MMRTG. The most important criteria considered was mission risk, power output, heat output, and volume. The MMRTG is a well-balanced design that incorporates PbTe/TAGS thermoelectric couples that produce 110 W of electric power and 2000 W of thermal power at BOL. Also, with a mass of 45 kg, the MMRTG provides 2.4 W/kg of electric power at BOL. Furthermore, the dimensions of the MMRTG are 64 cm in diameter (fin-tip to fin-tip) by 66 cm tall. Although the GPHS-RTG produced triple the amount of electrical power and double the amount of thermal power than the MMRTG, it had a significantly higher mass, cost, and volume which was not ideal for the MP mission to Europa.

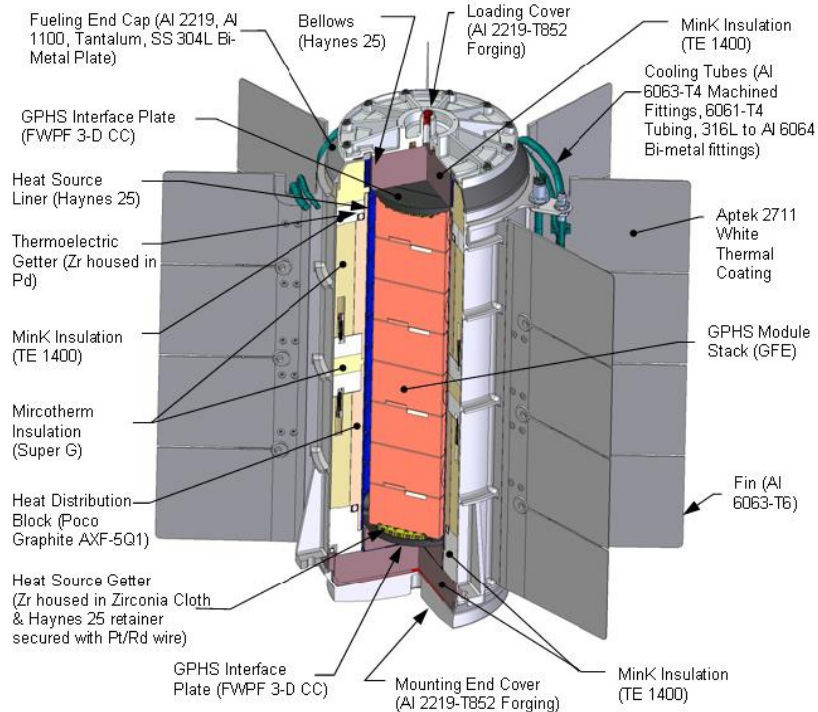


Figure 2: Diagram of an MMRTG

3.1.4 Power Storage Selection

In regards to the power storage of the MP, the secondary batteries that were considered included lithium-ion (Li-Ion), nickel cadmium (NiCd), and nickel hydrogen (NiH₂). Secondary batteries are batteries that can be recharged from another energy source, such as solar arrays or an RTG, and can deliver power to the spacecraft subsystems during periods where the power needs exceed the power capacity of the source. Silver zinc (AgZn) was not considered due to its extremely limited lifespan of 30-90 days which did not meet the mission requirements. NiCd and NiH₂ have been the industry standard for many years for spacecraft applications and has had its most common use for low earth orbit (LEO) spacecraft designs. However, these secondary batteries are limited by their large masses, low energy densities, and low cell voltages. NiCd has an energy density of 20-30 (W*h)/kg and a cell voltage of 1.25 V, while NiH₂ has an energy density of 60-70 (W*h)/kg and a cell voltage of 1.30 V. On the other hand, Li-Ion batteries have a very high energy density of 250-650 (W*h)/kg and a higher cell voltage of 2.5-3.4 V. Li-Ion batteries have been used for many planetary space missions over recent years such as the MSL/Curiosity rover and is planned to be used on the future Mars 2020 rover. The criteria for the decision matrix include mass, cost, storage capacity, duration, volume, and mission risk.

Table 4: Power Storage Selection Matrix

Criterion	Lithium-Ion	NiCd	NiH2	Multiplier
Mass	5	2	3	1.5
Cost	3	4	3	1
Storage Capacity	5	2	4	2
Duration	4	3	3	1.75
Volume	5	1	3	1.25
Mission Risk	5	3	3	2
Total	43.75	23.5	30.5	

Based on Table 4, the Lithium-Ion batteries was selected to deal with power storage on the MP. The Li-Ion batteries were above all the best solution for power storage in the case of the MP mission due to its reliability, low mass, and superior performance. The MP spacecraft will likely include two Li-Ion batteries in order to incorporate redundancy into the design and to fulfill the overall power requirements of the spacecraft equipment.

3.1.5 Power System Future Work

Future work on the power system will include the following:

- Compute the exact power requirements of the spacecraft
- Design final configuration for RTG and Li-Ion batteries within the MP spacecraft
- Define final power schedule for spacecraft subsystems

For the Final Design Report, the initial assumptions will need to be refined and a detailed and numerical analysis must be developed in order to have a more accurate representation of the actual power requirements of the MP.

3.2 Propulsion

3.2.1 Landing Category Selection

The Minos Probe propulsion system is responsible for safely transiting the probe from the Orbiter onto the surface of Europa. In broad terms, the three main categories of landing were compared as shown in Table 5.

Table 5: Landing Method Decision Matrix

Criteria	Impactor	Hard Landing	Soft Landing	Multiplier
Mass Required	4	2	1	1
Instrument Survivability	1	3	5	1.5
Total	5.5	6.5	8.5	

An impactor is a free fall descent onto the surface. A vertical descent velocity of greater than 2 m/s is considered a hard landing. Given the sensitive scientific instruments involved in the mission, survivability was made a priority. As a result, a soft landing was selected to execute a controlled deorbit and descent profile [1]. A touchdown velocity of < 2 m/s on the surface of Europa is planned. Research on efficient planetary landing schemes showed that an effective approach would be divided up into three distinct phases: fuel-optimum braking phase, landing approach transition phase, and terminal descent phase.

3.2.2 Landing Approach Selection

Table 6: Landing Mechanism Decision Matrix

Criteria	Airbags	Rocket	Sky Crane	Multiplier
Mass Required	4	2	1	1.5
Complexity	4	3	1	1.5
Landing Site Flexibility	2	4	5	1
Instrument Survivability	2	5	5	2
Total	18	21.5	18	

Next, to be considered was the type of soft landing to be utilized. This analysis was performed from a propulsion standpoint, while the same landing systems were considered by the mechanisms/deployables team from a feasibility standpoint. Airbags have been effectively used on missions to Mars, particularly with the Pathfinder, Spirit, and Opportunity landings. A heat shield and parachute slow the descent through the atmosphere. At a low altitude, large airbags inflate around the probe and it proceeds to disengage from the parachute and bounce along the surface before coming to a rest. While this method benefitted from low mass and less complexity, it would still require rocket powered deceleration, offered poor landing site control, and exposed the probe to potential damage.

A rocket descent is the most standard approach of landing. Rocket power is fully responsible for reducing the probe's velocity to under 2 m/s. While requiring more mass and guidance software, is arguably lower risk than airbags and has less structural mass than a "sky crane"

A "sky crane" is a novel idea that involves lowering the probe from a hovering platform via cables. This was notably used on the recent Curiosity rover mission. This approach can place the probe on the surface with almost zero vertical velocity and no contamination to the surface from propellant that may affect any potential samples. The biggest drawback is the very high structural mass component associated with the self-contained platform unit.

After comparing each of the three methods in Table 6, a completely rocket powered descent was selected as the best option. The next consideration is which propellant would be the best suited for the mission.

3.2.3 System and Propellant Selection

Table 7: Rocket Fuel Decision Matrix

Criteria	Hydrazine	N ₂ O ₄ – N ₂ H ₄	LOx – LH ₂	LF – LH ₂	LOx-RP1	Multiplier
Mass of Propellant and Structure	2	4	5	5	4	2
Stability	5	5	2	2	3	1.5
Thermal Properties	2	2	1	1	2	1.5
Toxicity	2	2	5	1	3	1
Total	16.5	20.5	19.5	15.5	18.5	

For the purpose of the preliminary design report analysis, a few assumptions were used. First, an orbit altitude of 100 km was used for propellant mass determination. The system was considered ideal so the ideal rocket equation could be used. Secondly, the probe's mass was estimated to be between 500-750kg. Lastly, the total change in velocity that must be counteracted by the propulsion system was approximated by 2 km/s. This value came from an analysis of a circular orbital velocity at 100 km above Europa, and historical data of the Apollo Command Module. [2]

Propellant	Symbol	Mole weight	Freezing point, °K	Boiling point, °K	Density at 20°C	Vapor pressure	
						kPa	°C
Chlorine trifluoride	ClF ₃	92.46	191	284.9	1.825	143	43.3
Fluorine	F ₂	38	53.7	84.8	1.51	34	-197
Hydrazine	N ₂ H ₄	32.05	274.7	386.4	1.008	1.4	20
Hydrogen	H ₂	2.02	13.7	20.4	0.071	7.0	-259
MMH	CH ₃ N ₂ H ₃	46.08	220.9	359.9	0.8765	4.8	20
Nitric Acid	HNO ₃	63.02	231.9	358.4	1.513	6.41	20
Nitrogen tetroxide	N ₂ O ₄	92.02	261.9	294.3	1.447	103	20
Oxygen	O ₂	32	54.4	90.0	1.14	50.7	-189
RP-1	CH _{1.9-2.0}	175	228.7	455-533	0.806	0.14	20
UDMH	(CH ₃) ₂ N ₂ H ₂	60.10	215.9	337	0.793	16.4	20

Figure 3: Properties of Propellants [3]

Based on an analysis of four bi-propellants and a hydrazine monopropellant, a hydrazine – dinitrogen tetroxide was most optimal. Hydrazine however has a few variants that give it thermal properties that are more desirable for space travel. Monomethylhydrazine (MMH) has a marginally lower specific impulse than hydrazine but has a freezing point that is approximately fifty degrees Kelvin lower. This tradeoff makes MMH much better suited to survive the frigid conditions the probe will encounter in space and on Europa. In a direct comparison, bi-propellant MMH dinitrogen-tetroxide system is the superior choice for a powered descent onto the surface of Europa. [3]

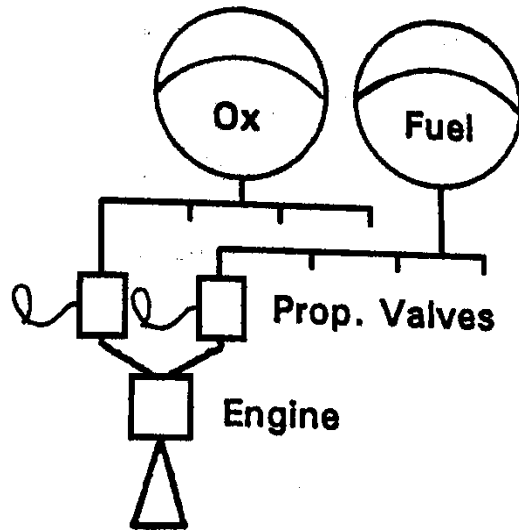


Figure 4: Bipropellant System [3]

To supplement the main rocket, cold gas thrusters will be used to provide attitude control throughout descent. A cold gas system is ideal for this application because of its relatively low structural mass, reliable and simple design, and are scaled appropriately for a spacecraft in the Minos Probe's weight class.

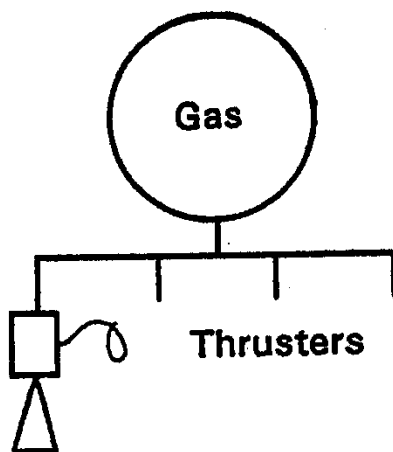


Figure 5: Cold Gas System [3]

3.3.4 Propulsion System Future Work

Future work of the propulsion system will include:

- Schematic detailing bi-propellant system
- Determination of propellant mass required
- Numerical analysis of constrained fuel-optimal landing approach
- Development of tank specifications based on propellant storage needs
- Details for cold-gas attitude control system

3.3 Chassis

3.3.1 Chassis Design Specifications

The chassis of the lander is one of the most critical parts in the overall design. The design of the chassis will not only be associated with the lander's performance, but also the layout and the operating modes of the payloads. To develop a working lander that will fulfill all of its mission requirements, the lander must be able to carry all required scientific instruments, survive landing on the surface of Europa and sample the surface-ice and atmosphere.

In order to carry all necessary payloads, the main body of the lander must be reasonably designed so all available spaces could be utilized efficiently. Thus, as shown in Figure 6 below, a hexagonal chamber with multiple separated cells was designed, and this internal layout would maximize the space utilization.

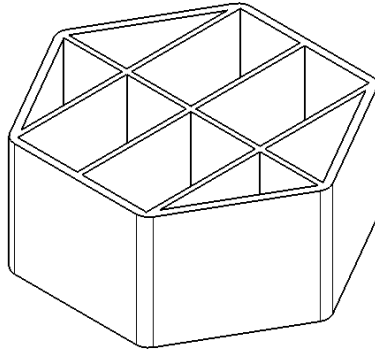


Figure 6: Chassis Hexagonal Design

During the landing, the lander will be dropped from the orbiter and then going into free fall. A descent engine mounted in the bottom of the chassis will be used to provide reverse thrust to slow down the free fall velocity. The three engines will keep working until the speed of the lander is reduced to near 0 at the altitude about 2 meters above the desired landing zone, then the three engines will be shut down to let the lander fall on the surface of Europa. In order to withstand the force of high-G movement and impact, the materials and structures of the lander's chassis must be highly robust so the lander could survive after the impact. Once the lander was successfully landed on the surface of Europa, the scientific instruments will start collecting detailed data of the atmosphere, and two robotic arms will start to sample the surface-ice.

Weight is also an important factor need to be considered in this mission. After consulting with an orbiter team, the maximum weight limit for the lander will be restricted to 2000kg at launch and the folded size will be 2m×2m×1m.

3.3.2 Chassis Materials

For the material selection, five main factors were considered: density, Young's Modulus (stiffness), Tensile Stress (strength), elongation, and cost. In this case, five possible materials were selected for constructing the chassis and the main body of the lander. They are 2024-T4 Aluminum Alloy, 2219-T87 Aluminum Alloy, 6061-T6 Aluminum Alloy, 7075-T73 Aluminum Alloy, and R56410 Titanium Alloy. Only Aluminum and Titanium Alloys were considered because the two materials have relatively low densities and would not get brittle in an extremely low temperature environment.

A decision matrix would be used to select the most suitable material. As described earlier in the design, each material has a scale of 1 to 5, where 5 holds the most weight or value, and a multiplier will vary from 1 to 2 for each criterion. The final scores for each material will be added by column and the component with the highest score will be selected.

Table 8: Chassis Material Selection Matrix

Criteria	2024-T4 Aluminum Alloy	2219-T87 Aluminum Alloy	6061-T6 Aluminum Alloy	7075-T73 Aluminum Alloy	R56410 Titanium Alloy	Multiplier
Density (ρ)	4	2	5	3	1	1.5
Young's Modulus (E)	3	4	1	2	5	2
Tensile Stress (σ_t)	2	3	1	4	5	1.5
Elongation (ϵ)	4	3	5	1	2	1
Cost	3	5	4	2	1	1
Total	22	23.5	20	17.5	22	

Based on the decision matrix, 2219-T87 Aluminum alloy would be the best material for building the lander's chassis because it has relatively high stiffness and strength with the lowest cost. An important thing needs to be mentioned is that although only one material was selected for building the chassis and the main body, the rest parts of the lander could be made of other materials such

as Titanium alloys or composites. The details of this part would be explained in the Final Design Report.

3.3.3 Chassis Structure

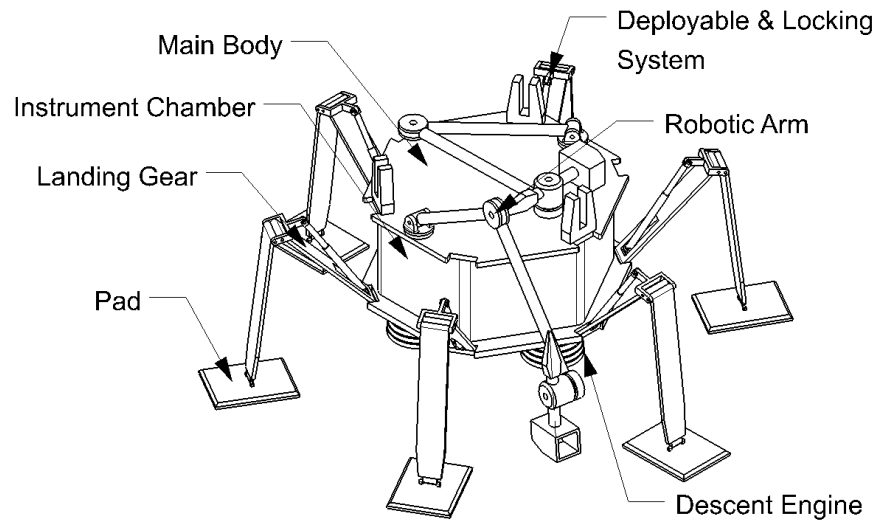
There are two main types of lander structure: truss structure and plate structure. For the truss structure, the main load-bearing frame is constructed by beams and joints, and its advantages are light-weight, small size, and low cost. Plate structure, on the other hand, is constructed by multiple plates, and its load-bearing frame would be honeycomb shaped which could allow the structure to bear enormous forces without failure.

Another decision matrix would be used to determine the most practical structure. Since there are only 2 possible structures for the lander, each criterion was ranked from 1 to 2 with a multiplier also varied from 1 to 2. The matrix is shown below:

Table 9:Chassis Structure Decision Matrix

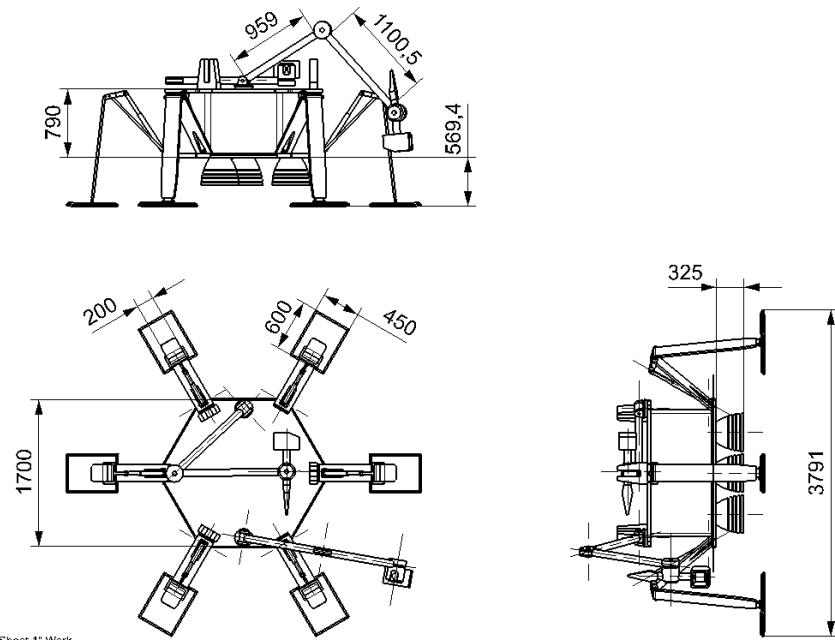
Criteria	Truss Structure	Plate Structure	Multiplier
Bearing Capacity	1	2	2
Manufacturing	1	2	1.5
Weight	2	1	2
Assembly	1	2	1
Cost	2	1	1
Total	10.5	12	

According to the final scores, plate structure would be the best choice for this mission. Comparing with a truss structure, a plate structure could carry heavier payloads and the structure itself would be easier to manufacture and assembly. The CAD model of the lander is shown in Figure 7 and Figure 8.



Sheet "Sheet 1" Work

Figure 7: Lander Configuration



Sheet "Sheet 1" Work

Figure 8: Lander 2-D Sketch

3.3.4 Chassis Future Structural Work

- The internal layout for each component would be determined.
- The size, weight, and cost of each component will be finalized.
- The locking system of the landing gear would be further discussed and analyzed.
- Appropriate dimensions would be included in the CAD drawing with more details.
- Finite element analysis (FEA) would be used for predicting how the lander reacts in the real situation.

3.4 Mechanisms/Deployables

Section 3.4. will outline the mechanisms and deployables to be used on the Minos Probe. The mechanism and deployables represent an essential sub system to the Minos Probe. A failure by any one of them could jeopardize the entire mission. The mechanisms and deployables to be analyzed are as follows: landing mechanism/deployables, scientific deployables, and communication deployables.

3.4.1 Landing Mechanisms/Deployables

When landing the Minos Probe on the surface of Europa, it is essential to make sure that safety of the lander is held with the utmost importance. There are many factors at play when determining the best mechanism to deploy during a landing including, the velocity in which the lander will touch down, the terrain of the surface, the atmospheric conditions, mass, and fuel consumption. All of these factors were be taken into account when deciding on the most effective mechanism to deploy during landing.

3.4.1.1 Landing Mechanisms/Deployables Selection

Four types of deployable mechanisms were considered when deciding on the proper landing technique for the Minos Probe: parachute with retro rockets, airbags, crushable legs with retro rockets, and a sky crane. Each mechanism will be analyzed for its advantages and disadvantages followed by a decision matrix used to make the final decision.

Parachute and Retro-Rockets:

A parachute and retro-rocket design is one of the oldest landing mechanism designs. Used on the Mars landers Viking 1 and 2 in 1976, it is a proven and reliable design. The design works such that when the lander enters the atmosphere after its initial descent a supersonic parachute will deploy. As the atmosphere gets thicker during descent, the parachute will inflate producing a drag force. Eventually, at a specified altitude, the parachute will release and the retro-rockets will fire, lowering the lander the rest of the way to the surface. The rockets usually turn off very near the surface with the lander's velocity almost zero. This will cause the lander to free fall a few feet to the surface. The advantages of this design are its simplicity and reliability. The design merely consists of a supersonic space grade parachute, and a specified number of retro-rockets, which are used in almost all landing stages. The design has also had repeated success on the surface of mars as previously mentioned. However, there is one major reason that the parachute and retro-rocket design would not work when landing on Europa. Europa's atmosphere is so thin that it would have almost no effect on the parachute. There is not enough air for the parachute to inflate, and

thus not only would it not supply any drag, it could possibly get in the way as it lays limp. For this reason, a parachute and retro-rocket design was eliminated.

Airbags:

Airbags are a proven method utilized on multiple Mars rover landings, including the Mars Spirit, Opportunity, and Pathfinder rovers. The idea behind airbags would be to protect the lander upon impact allowing for a higher velocity landing. In previous missions, including the Mars rover missions mentioned, the air bags were coupled with a parachute and retro-rockets to slow the rate of descent. The parachute and retro-rockets would eventually be cut loose and the rover with inflated airbags would fall into a free fall. The airbags often caused the rover to bounce up to five stories high and roll for 1 kilometer. The major benefits to airbags include reliability and fuel consumption. Airbags have been proven effective on a multitude of rover landings on Mars and the moon. Airbags would also decrease fuel consumption on the descent as the impact velocity would be higher. However, there are significant drawbacks to airbags that ultimately render them ineffective for the Minos Probe. As previously stated, with Europa's thin atmosphere, a parachute would be essentially useless. The airbags would likely still be able to operate solely with the help of retro-rockets, but larger rockets would likely need to be designed. The major concern for airbags is due to the terrain of Europa. The treacherous surface could potentially host deep crevasses or large ice spikes that would pose a serious threat to a bouncing lander. Not enough is known about the surface of Europa to justify taking such a risk. As a result, the airbag approach was eliminated.

Crushable Legs and Retro-Rockets:

The crushable legs and retro-rockets design is another old design. Initially used on the lunar module, it is a great design for landing on celestial bodies with little to no atmosphere. The design is very simple where after the initial descent phase at a specified altitude, the retro-rockets on the lander fire. The rockets continuously adjust thrust, slowly decreasing the velocity of the lander until it is just above the surface. At some point during descent the legs would unfold and stretch downward. Just above the surface, the engines shut down causing the lander to free fall the last few feet. Upon impact the legs absorb the energy and disperse it through a design that allows for some "give". This design has some distinct advantages; it is a simple proven design that does not require a parachute or airbags which were previously rendered ineffective. The one major drawback of the design is its fuel consumption. Because the lander gets no help from a parachute, and must come to a full stop at the surface, the retro-rockets are responsible for providing the entirety of the delta V required. As a result, a significant amount of fuel is required to ensure a successful landing. Coupled with the conclusion made in section 3.2, it was decided that the Minos Probe will utilize a crushable legs and retro-rockets design upon landing.

Sky Crane:

The final design considered is a rather new design. Utilized on the Mars Curiosity Rover, a sky crane is a mechanism in which the lander hangs down from a "sky crane" containing retro-rockets. The rockets fire slowly decreasing the descent velocity and placing the lander on the surface. Once the lander is safely on the surface, the sky crane detaches from the lander and flies away to a crash site. While this is a fascinating new technology, it is unnecessary for the Minos Probe. The sky

crane is design for extremely large landers/rovers that are too large for airbags, and cannot afford to have dust from the surface kick up due to the rockets. Neither of these cases are essential to the Minos Probe. The sky crane has also only been used in one instance, and thus reliability is a concern. The added mass and risk that would come with installing a sky crane to the Minos Probe is not something worth inducing, therefore, the sky crane was eliminated.

Table 10 shows the selection matrix used to make the decision to use crushable legs and retro-rockets on the Minos Probe. The criteria used in the selection matrix was the same as what was described in section 3.

Table 10: Landing Mechanism/Deployables Selection Matrix

Criteria	Parachute and Retro-Rockets	Airbags	Crushable Legs and Retro-Rockets	Sky Crane	Multiplier
Space Readiness	5	5	5	3	1.5
Effectiveness on Europa	1	2	5	5	1.75
Fuel Required	4	3	1	1	1.25
Cost	N/A	N/A	N/A	N/A	1
Total	14.25	14.75	17.5	14.5	

After coming to a decision on the crushable legs and retro-rocket design, the next step is to conduct analyses to determine the specifics of the design. For the final design report, detailed analysis on every aspect of the design will be provided. Work will be done in conjunction with propulsion, structures, and power to determine mass, materials, structural design, fuel, and various other aspects. Accurate cost and mass estimates will also be provided for the design in the final design report.

3.4.2 Scientific Mechanisms/Deployables:

As previously stated, Minos Probe's mission is to land on Europa's surface and collect both atmospheric and surface samples. To do so, the appropriate scientific equipment will need to be on-board the lander. NASA and ESA have a storied legacy of being as ambitious as possible, while maintain a high probability of mission success. As a result, additional science equipment will be added to the lander to collect a variety of data. While additional mass will have to be added to the budget, the data collected will prove to be worth price. The selection process of the instrumentation to on Minos Probe is detailed in the following sub-section.

3.4.2.1 Scientific Mechanisms/Deployables Selection

When deciding on the best science equipment to use on Minos Probe, a multitude of different equipment performing different tasks were analyzed. Due to a lack of expertise in the development of scientific equipment, this portion of the probe will be contracted out to various companies. The designs considered were based heavily on legacy equipment used on various Mars rovers and other spacecraft. The equipment considered are, a JPL designed ice drill, a JPL designed ice claw, the

Europa Clipper SUDA, the Mars Curiosity Rover SAM, the Mars 2020 Rover Mastcam-Z, and the Europa Clipper REASON.

Ice Drill/Claw:

As stated in the Mission Purpose, Europa is of great interest to NASA and ESA due to the presence of liquid water and ice and the potential for life. Drilling into the ice to collect samples would determine whether there is or has ever been the presence of life on Europa. Because of this, the ice drill/claw is considered to be the most important piece of equipment on Minos Probe. According to NASA, in order to collect pristine uncontaminated samples, ice would need to be collected from at least 8 inches below the surface. Recent design and testing by NASA's Jet Propulsion Lab (JPL) at California Institute of Technology have yielded promising, results on a potential drill design [4]. JPL's drill would be a nuclear powered drill using plutonium to melt the ice as the drill works its way through. Once the drill has gone deep enough (likely 1-2 meters) the melted ice would be pumped up to the lander to be analyzed for potential biological components. While JPL's drill would provide ground breaking information on the potential for life elsewhere in our solar system, it does not come without significant risks and drawbacks. The shear monetary and mass cost of bringing along plutonium would almost certainly exceed the budget. The political consequences of launching plutonium would also likely result in some serious resistance and backlash from the United States and other nations around the world. Considering these facts, an alternative to ice drilling has been considered.

The alternative to drilling would be to use an ice claw to scrape ice off the surface for sampling. The scraped samples would then be loaded into the lander for analysis. This design is attractive as it would avoid the use of nuclear power. The claw would run off the lander's main power supply and would have no need for a melting mechanism, greatly reducing the potential political fallout. However, this design also has its drawbacks. The claw would not be able to penetrate nearly as deep as an ice drill. Requirements will be made to have the claw be able to dig at least 8 inches deep as to meet NASA's recommendation for pristine samples.

SUDA:

The Surface Dust Analyzer (SUDA) is a time-of-flight mass spectrometer present on NASA's soon to be launched Europa Clipper mission [5]. SUDA measures the composition of small solid particles that have been ejected from Europa's surface. Included in the ejection are water and ice particles from Europa's large geysers. SUDA was analyze the chemical composition of the particles it collects as well as search for biological traces. In order to most effectively utilize SUDA, the best course of action would be for the Minos Probe to fly through a plume from a geyser while making its descent to the surface. By doing so SUDA would analyze particles from Europa's surface as well as from the ocean water deep below. SUDA could potentially be used alongside an ice drill, or in replacement of one due to its ability to sample ice particles without the need of plutonium. It weighs in at only 4 kilograms, make it very affordable to add to the Minos Probe, while providing the potential for ground breaking information.

SAM:

The Sample Analysis at Mars is the main surface analyzer on board the Mars Curiosity Rover. SAM analyzes the chemical composition of rock and dirt samples collected by the rover [6]. SAM works by loading the samples into an oven and vaporizing them. The released gases are then separated and identified. A laser spectrometer is then used to determine if methane found is produced by geological or biological processes. On Curiosity SAM weighs in at a hefty 40 kilograms, however through extensive research and testing by NASA and ESA, the SAM can be reduced to 20 kilograms.

While NASA has given the requirement of sampling the surface ice and atmosphere, our team prides itself in going above and beyond the call of duty. Given the gravity of this mission and the potential to provide ground breaking information on Europa and the potential for life in our solar system, a proposal has been made to add additional technology to analyze Europa even further. The equipment considered is detailed in the following paragraphs.

Mastcam-Z:

The Mastcam-Z is a multispectral stereoscopic imager found on the Mars 2020 Rover. It is based heavily on the successful Mastcam found on the Curiosity Rover, but with some minor improvements. The Mastcam-Z would take extremely detailed color images of the surface of Europa and serve two major functions on the Minos Probe: “characterizing the overall landscape geomorphology, processes, and the nature of the geological record (mineralogy, texture, structure, and stratigraphy) at the rover field site” [7] and “assess current atmospheric and astronomical conditions, events, and surface-atmosphere interactions and processes” [7]. On the Mars 2020 Rover, Mastcam-Z also serves as a navigation tool, but this would not be necessary for the Minos Probe as it will not move. The Mastcam-Z would be a great addition to the Minos Probe for the reasons just stated in addition to its ability to provide the first imaging of Europa from the surface. NASA’s current estimate has the Mastcam-Z at 4.5 kilograms given a 10% margin. This makes its quite affordable and very attractive.

REASON:

The Radar for Europa Assessment and Sounding: Ocean to Near-Surface (REASON) is an ice penetrating radar that will be on board NASA’s Europa Clipper mission set to launch in the early 2020s. The radar will be used to analyze the characteristics of the surface of Europa, including examining roughness to determine a suitable landing spot and looking for pockets of water within the ice shell that could potentially host important chemicals for life. REASON will also use dual frequency radar to determine how thick the surface ice is and where the ocean begins. REASON currently weighs in at 32.2 kilograms and uses 55 watts of power.

As seen in Table 11, it has been decided to include an ice claw, the SUDA, the SAM, the and Mastcam-Z on the Minos Probe. The criteria used in the selection matrix was such the same as described at the beginning of section 3. The ice drill and ice claw were then compared head to head to decide which one would be included on the Minos Probe. The three highest scores of the remaining four equipment will be included in the Minos Probe.

Table 11: Scientific Mechanism/Deployables Selection Matrix

Criteria	Ice Drill	Ice Claw	SUDA	SAM	Mastcam-Z	REASON	Multiplier
Mass	2	5	4	1	4	1	1.5
Space Readiness	1	1	2	5	5	2	1.75
Science Impact	5	3	5	4	3	3	1.5
Cost	N/A	N/A	N/A	N/A	N/A	N/A	1
Total	12.25	13.75	17	16.25	19.25	9.5	

3.4.3 Communication Deployables

In this sub-section, the mechanisms used to deploy and gimbal the ultra-high frequency (UHF) Omni and Low Gain communication antennas will be analyzed. The specific criteria used to determine the antennas used can be found in section 3.6. The deployment of the antennas on the Minos Probe is essential to the success of the mission. Without a way to successfully communicate to the probe, it will not be able to land on Europa's surface nor will it be able to transmit data if it were to somehow land. Because of this, only use the most reliable and effective methods of deployment will be used.

3.4.3.1 Communication Deployables Selection

There are two antennas on the Minos Probe, and each will need a different deployable design. The first will require a hinge design to snap the UHF Omni antenna from a horizontal to a vertical position. The second antenna (low gain) will be on gimbal that will allow it to rotate in two degrees of rotational freedom. In order to determine the best possible designs for deploying both antennas, a few different proven methods were considered and compared.

UHF Omni

The UHF Omni antenna is a single rod antenna that will require a hinge to snap it from the horizontal to the vertical position. Initially, the antenna will be stowed along the top surface of the Minos Probe, and when appropriate will rotate 90 degrees to the upright position. To do so there is one age-old proven method to use; a spring loaded hinge design. In this design, the hinge will be loaded with multiple torsion loaded springs. While in the stowed position, the antenna will be held down by dual pin pullers at the tip of the antenna. The pin pullers will be fired electronically when appropriate and the springs will cause the hinge to rotate and the antenna to snap into place. Once the antenna has rotated 90 degrees, a latch system will activate holding the antenna in place. Figure 9 shows an image of a typical spring loaded hinge with a latch.

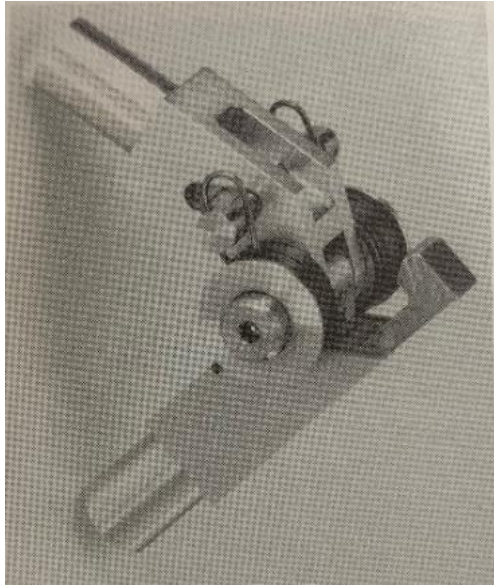


Figure 9: Latching Hinge Design [8]

For the final design report, further analysis on the hinge and antenna design will be conducted to determine if a damping mechanism is needed. If so, a crush block, or some other deformable material, would be the most likely to be used.

The spring loaded hinge designed is an extremely trusted and widely used design for deploying antennas on spacecraft. For this reason, the only other design considered was using an actuator to drive the rotation of the hinge rather than springs. This design is often used when the deployable needs to be re-stowed. This is not the case for the UHF Omni antenna and therefore, the added cost and risk of implementing an actuator is not worth it.

Low Gain

The low gain antenna will require mechanism for deployment as well as a gimbal. Initially the low gain antenna will be stowed by one of three methods: umbrella, wrap-rib, or springback. The umbrella design functions almost exactly like an umbrella. The antenna is initially folded up on itself as shown in Figure 10. At the appropriate time, the antenna will be deployed by an actuator that opens all the ribs simultaneously.



Figure 10: Galileo High Gain Antenna Umbrella Design [9]

In the wrap-rib design the antenna is initially folded up in a circular pattern. At the appropriate time, the ribs will unfold deploying the antenna as shown in the Figure 11. The wrap-rib design is typically used for large stand-alone antennas and is likely not the best option for the Minos Probe.

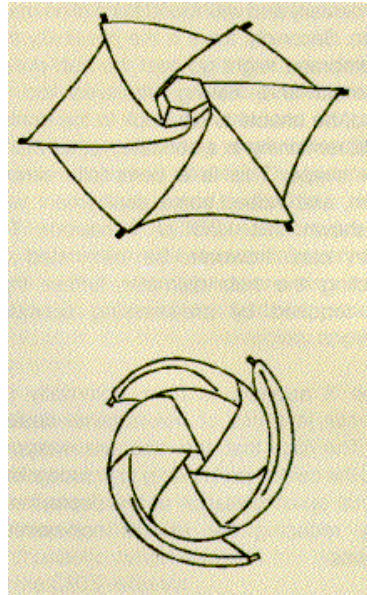


Figure 11: Wrap-Rib Antenna Design [10]

The final deployment design considered is a springback design. This is a relatively new design in which strain memory structures are used to send the antenna from its initial folded up state to its deployed state. This design however is intended for larger antennas and has not been frequently proven in space.

Given the small size of the low gain antenna on board the Minos Probe and the reliability of the design, the umbrella design will be the most effective method of deployment for the low gain antenna. Table 12 shows the criteria used to decide the appropriate design for the communication deployable mechanism. The same method for criteria and multiplier was used as in the previous sub-sections. For the final design report, collaboration with the power system will be done to determine specifics of the actuator necessary to deploy the antenna, and further analysis will be performed.

Table 12: Communication Deployables Selection Matrix

Criteria	Umbrella	Wrap-Rib	Springback	Multiplier
Space Readiness	5	5	2	1.5
Size Appropriate	5	3	2	1
Total	12.5	10.5	5	

The low gain antenna will also be on a gimbal in order to have a wider range of communication with the RO. Almost always a two-axis gimbal is used in situations such as these. Considering there is no need for a three-axis gimbal, none will be analyzed for this design. A standard two-axis gimbal similar to what will be used in this case is shown in Figure 12.

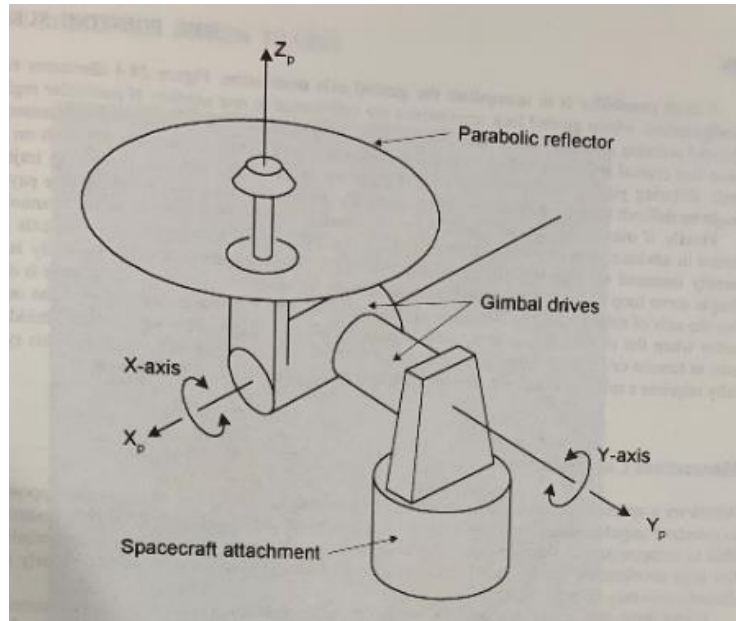


Figure 12: Two-Axis Gimbal Design [8]

The two-axis gimbal design will be coupled with a torque-multiplied actuator to drive rotation. There are two common designs for motors for this actuator: a torque motor and a stepper motor. Torque motors are typically used in scenarios with a long life, high rate of rotation, and tight control is necessary, such as an “antenna-positioning mechanism used in applications where the antenna is constantly acquiring new targets” [8]. This fits the case of the low gain antenna perfectly, as it will need to constantly follow the RO spacecraft to maintain communication. Because of this, the torque motor will be used on the Minos Probe low gain antenna.

3.5 Command and Data

3.5.1 Command and Data Requirements

The command and data system is responsible for storing the scientific measurements and integration of electrical components. This requires the command and data system to be the most risk averse subsystem of the probe, due to the probes inability to function without it working correctly. To ensure survivability of the mission, the embedded processor must be able to withstand large temperature fluctuations and radiation, making the computing power limited. The control unit will also be necessary in maintaining a thermal equilibrium by using feedback from local sensors and relaying electrical power to the necessary heating units. Additionally, the control unit must also coordinate between the correct deployable instrumentation to gather scientific data. The telemetry must then be stored in a reliable manner until a proper window for communication opens. After failures in mission pasts, alternative options of storing and transmitting data must be accounted [11].

The embedded control unit will spend the period of travel to Europa in perpetual sleep, but must power on intermittently to ensure systems functionality. Furthermore, an error detection device must be utilized to distinguish single bit errors on deployable measurements, and report with the concurrent data. In addition, the unit must be able to be reprogrammed with an electrically erasable programmable read-only (EEPROM), to account for possible issues in software implementation. A system with two parallel control and data units should be utilized to safeguard the mission. [12]

3.5.2 Command and Data Selection

Due to the mission requirements for command and data, the best choice to use is a BAE RAD750 CPU. The RAD750 has a respectable and tested flight heritage, and has been an industry standard for deep space missions since its first use in the Mars Reconnaissance Orbiter in 2005, and is slated for use in the upcoming Mars 2020 mission. [13] The RAD750 will be able to store 128 MB of data before communication and function with a speed of 134 MHz. [14] The CPU’s EEPROM will also allow for mission control on earth to change directives and fix and possible bugs upon landing.

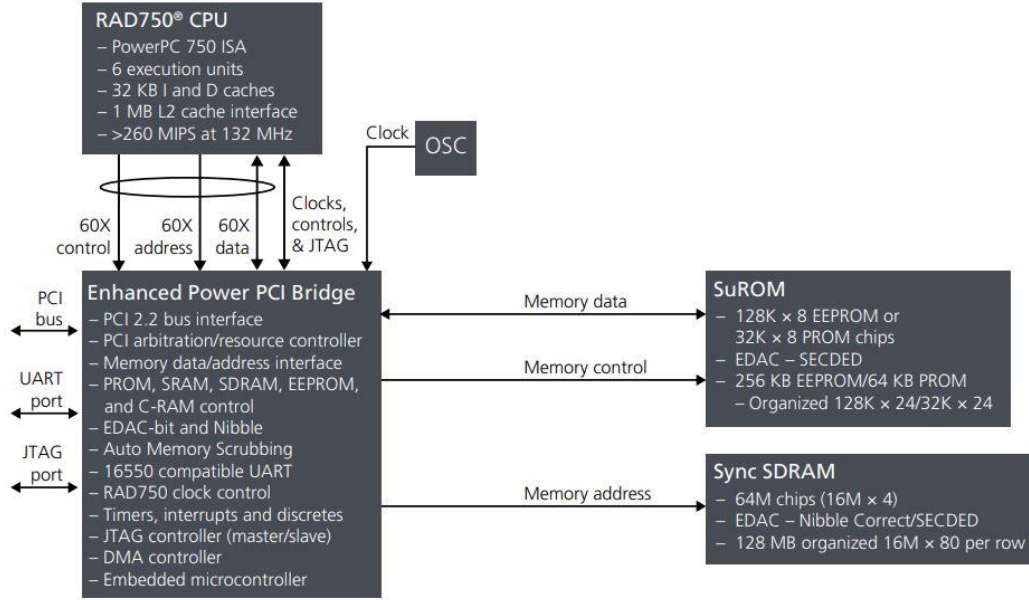


Figure 13: RAD750 CPU Processing Table [14]

3.6 Communications

3.6.1 Communications Selection Requirements

The communications system is responsible for receiving and transmitting data both to the orbiter and possibly as a backup, to Earth. The proper functioning of this system is essential to the mission as it will be responsible for communicating commands to the probe from either the RO or Earth, as well as sending data from sample analysis done by the probe to the RO or Earth. Considerations to be made are power consumption, data transmission rates, band frequency, range, cost, antenna accuracy, size and associated risks. This system needs to be redundant in some form to ensure failure of a communications component will not render the mission a failure.

The RO will either be orbiting Europa or Jupiter while the MP will be stationary on Europa, which is orbiting Jupiter. This makes limited windows of time where the MP can communicate with either the RO or Earth. For this reason, data transmission rates are desired to be high. An antenna with a wide field of view, or an antenna on a gimbal would be desirable to increase the amount of time communications are possible. A frequency should be chosen as to not interfere with the frequency of the electronics used to control the MP itself, and one that is resistant to atmospheric effects. The communications package should be able to reliably send and receive data the distances required to the RO in orbit and to Earth, should that form of redundancy be chosen. Power and cost are ideally minimized, but importance to mission can affect these criteria. The more complex the system, the more risks that are associated, which need to be minimized. Due to the inherent complexity of the mission, a communication system should be chosen that has existing flight heritage, minimizing the chance of unforeseen failures.

3.6.2 Communications Selection Criteria

The band, or frequency range, that a communication system uses is a major part of its transmitting capabilities. The bands commonly used in space communication are S-Band, X-Band, Ku-Band, and Ka-Band. The lower frequency bands that are part of the ultra-high frequency (UHF) and lower super high frequency (SHF), S and X, offer lower data rates however they aren't as affected by atmospheric absorptions such as rain fade, whereas that the higher frequency Ku and Ka bands are. Europa is known to have an atmosphere which needs to be taken into consideration. Juno is currently orbiting Jupiter and uses both X and Ka bands which could introduce interference between the RO and MP.

The MP's communication will follow the same model current Mars rovers where data will be relayed to the orbiter and then back to earth, and vice versa. The best approach for redundancy is for the communications package of the MP is to have dual bands both communicating with the RO. The amount of power and accuracy required to have meaningful communication directly with earth from the surface of Europa rendered that option very undesirable and therefore was not considered when constructing the decision matrix for the communication bands.

Table 13: Communication Band Selection Matrix

Criteria	Lower UHF	S-Band	X-Band	Ku-Band	Ka-Band	Multiplier
Cost	*	*	*	*	*	1
Power Consumption	5	4	3	2	2	1.25
Transmission Rate	3	3	4	5	5	1.5
Atmospheric Tolerance	5	5	4	2	1	1.5
Total	18.25	17	15.75	13.75	11.5	

Table 13 indicates that a lower UHF system would be the best frequency choice for the MP and X-band will be chosen as a redundant band due to the legacy systems available. Cost criteria needs to be further researched and will be addressed in the final design report. Due to its flight heritage, the CMC Cincinnati Electronics UHF transceiver will be used for the primary communications with RO. This system uses between 6 and 43 watts with a nominal power consumption of 12 watts. It will transmit and receive up to 256 kbps. The system, including multiple antennas has a mass of 2.9 kilograms. The X-band communications equipment will be that used on the MER's as most aspects of their mission are similar, and the equipment has a proven flight heritage. This system uses 71.8 watts at its maximum and generates a significant amount of heat which can be used to

keep the electronics bundle warm. The system has a mass between 5.3 and 6.8 kilograms, depending on antenna and redundancy configuration, which will be determined in the final design report.

Antenna selection can be broken down into omni-directional antennas for UHF, and high gain and low gain antennas used for X-band. Low gain antennas are generally smaller and have a larger field of view, however the data rates it is capable of receiving and transmitting are relatively low compared to a high gain antenna. A high gain antenna has field of view that is much smaller than a low gain antenna and will need an accurate gimbal system to achieve the same length communication window.

Table 14: Communication Antenna Selection Matrix

Criteria	UHF Omni	Low Gain	High Gain	Multiplie r
Transmission Rate	3	4	5	1.75
Transmission Window	5	3	1	1.5
Directional Control	5	4	2	1.5
Size	3	4	5	1.25
Range	2	4	5	1
Total	26	26.5	24.5	

With antenna selection, the most important factor to consider is to get as much data transferred to the RO in the small window of time that is available for transmission. Because the transfer of data is occurring at relatively short distances, range is not greatly weighted. Data transfer rate and the available window of time that data can be transferred are most important. Table 14 shows that an Omni-directional antenna will be used for the UHF system and a low gain antenna will be used for the X-band system. However, because the communications system is essential to the mission two UHF antennas and both a low gain and high gain antenna will be used in the communications system. The mass of multiple antennas was included in the estimate for the overall mass of the communications systems and is relatively low, allowing for the additional antennas to be considered. Additionally, with the addition of a gimballed high gain antenna in the X-band system, the window of communication time outweighs the small sacrifice in mass.

3.6.3 Future Communication Work

For the final design report, the team will be “pairing” with an orbiter team that best aligns with each other’s mission objectives. This will determine if the orbiter will be in an orbit around Europa or Jupiter. These two different orbits will play a large role on the decision of what will be the primary communications system. This is due to the speed of the orbiter and time the orbiter will be in sight of the probe, the X-band with the use of the high gain antenna may be the best option for the higher data rates. It may be determined that because the window of communication is so small, a K-band radio would be most desirable because it has potential to reach transfer rates of 400 megabits-per-second. This would require further research on proven systems as well as a new mass analysis.

3.7 Thermal Control

The purpose of the thermal control system (TCS) is to keep all parts and instruments of other subsystems within acceptable temperature ranges for all modes of operation in all thermal environments required for the mission. The TCS will also be responsible for limiting damage to electronics from charged particles present in Jupiter’s magnetosphere. This will be accomplished by taking four major parts into consideration; heating, internal heat transfer, thermal radiation, and charged particle protection.

3.7.1 Heating

Heating the spacecraft is important in order to keep components of the probe warm enough for proper use. The highest that the surface temperature gets on Europa is minus 160 degrees Celsius [15]. This is too cold for many components, including batteries, computers, and deployable mechanisms. Therefore, extra heat will need to be added to the system. Two methods of heating were considered, radioisotope heater units (RHU) and electric heaters. For most space missions, electric heaters are preferred over RHUs because they are cheaper, smaller, lighter, and more easily controlled. However, for deep space missions, where solar panels are ineffective and power is a very scarce commodity, RHUs are often used. Besides not needing any power, RHUs are also beneficial due to their reliability. Electrical heaters require thermostats, circuitry, and sometimes software in order to control them so the correct amount of heat is provided. RHUs, however, will reliably produce heat for many years and up to decades as the radioactive material continues to decay [15].

Six criteria were taken into account when choosing between RHUs and electric heaters. The most important factors were reliability, or risk to the mission, effectiveness, defined as the amount of heat produced per mass, and power usage. Reliability was of upmost importance because a malfunction in the heating system causing a component to fall outside acceptable temperature ranges could be detrimental to the entire mission. Effectiveness was defined on a per mass basis because saving mass anywhere that is possible is helpful to the design of all subsystems. Power usage is important because there will be a very limited amount of power available and if power is generated through a thermoelectric generator, it becomes inefficient to convert from heat, to electricity, back to heat. The other three criteria were price, controllability, and environmental risk. Price was taken to be less important because we do not yet have a monetary budget and for a mission of this importance and complexity, the customer will most likely be willing to pay more

for an increase in probability of mission success. Controllability was considered less important because as long as an accurate model exists and correct calculations are made, controllability is not necessary and adds complexity and chance of failure. Environmental risk was considered less important because a risk to the environment would only be present in the unlikely event of a launch failure or crash landing.

Table 15: Heating Selection Matrix

Criteria	RHU	Electric	Multiplier
Price	3	5	1
Reliability	5	2	1.5
Effectiveness	3	5	1.5
Power Usage	5	1	1.5
Controllability	4	5	1
Environmental Risk	3	5	1
Total	29.5	27	

3.7.2 Internal Heat Transfer

The internal heat transfer system will be responsible for facilitating the transfer of heat from heat sources to heat sinks within the spacecraft. Heat sources include RHUs needed for the TCS, thermoelectric generators, and any electronic components that may produce excess heat. Heat sinks include electronics and components that must be kept warmer than they keep themselves and any radiators, if needed for the TCS. Three methods of internal heat transfer were considered: thermal straps, heat pipes, and fluid loops. Thermal straps are thin, flexible straps made of materials with high thermal conductivity, such as aluminum, copper, or graphite [16]. Heat pipes consist of a vapor chamber and a wick containing liquid. When heat is applied to one end of the pipe, the liquid in the wick evaporates. This increases the vapor pressure at the warm end and pushes the vapor to the cool end, where it condenses and is absorbed by the wick. This phase change facilitates the transfer of heat from the warm end to the cool end. Fluid loops consist of a pump, a heat exchanger, and a heat source. Cold fluid is pumped to the heat exchanger, where thermal energy is transferred from the component to be cooled to the fluid. This fluid is then pumped to a heat source where the thermal energy is removed from the fluid. The heat that is removed from the fluid can then be transferred to a component that needs more thermal energy, or

it can be radiated into space. The cooled fluid is then pumped back to the heat exchanger and the cycle continues [15].

Six criteria were considered in selecting a method of heat transfer. The most important criteria were reliability, or risk to mission, power usage, and mass. Reliability is important because a failure resulting in a reduction in the amount of heat transferred can cause components to become too hot or too cold, jeopardizing their performance and the mission. Power usage and mass are important because there are tight budgets for both of these resources. The next most important criterion was effectiveness. This was not considered as important as the top three since it is not yet known how much thermal energy will need to be transferred, and whether or not the less effective methods will be effective enough. Price and controllability were the two least important criteria for the same reasons as described in the selection of the heating system. There is not yet a well-defined monetary budget and controllability and complexity that is not necessarily needed if an accurate model exists.

Table 16: Heat Transfer Selection Matrix

Criteria	Thermal Straps	Heat Pipes	Fluid loops	Multiplier
Price	5	4	3	1
Effectiveness	3	4	5	1.25
Reliability	5	3	1	1.5
Controllability	3	3	5	1
Power Usage	5	5	1	1.5
Mass	5	4	2	1.5
Total	34.25	30	20.25	

3.7.3 Thermal Radiation

In the case of buildup of excess heat in the probe, a radiator may be needed in order to expel the extra thermal energy. On the surface of Europa, it is likely that this will not be necessary due to the extreme cold. However, since RHUs can't be turned off and the probe will need to be designed to survive in the extreme cold of Europa, there may be a buildup of heat as the probe travels from Earth to its destination. If a radiator is needed, there are three options to consider: a structural panel, a body-mounted radiator, and a deployable radiator. Structural panels are often used to radiate heat since they add very little complexity to the spacecraft. Face sheets can be placed on both sides of a structural panel in order to adjust their thermal properties to facilitate the correct

amount of thermal radiation. Body-mounted radiators can be used when structural panels won't provide enough radiation or there are no structural panels that would work well. If the probe cannot provide enough space to radiate heat from its structure, a deployable radiator may be required. Deployable radiators increase the available surface area from which heat can be radiated [15].

There were five criteria taken into account for deciding on a proper radiator. Reliability, power usage and mass were determined to be the most important factors for the same reasons given in the selection of an internal heat transfer system. Effectiveness was defined as the amount of heat that could radiated per volume and was considered to be of low importance because it is not anticipated that much heat will need to be radiated. Price was a less important criterion due to the same reason as above, lack of a well-defined monetary budget.

Table 17: Radiator Selection Matrix

Criteria	Structural panel	Body mounted	Deployable	Multiplier
Price	5	4	3	1
Effectiveness	2	4	5	1
Reliability	5	4	2	1.5
Power Usage	5	4	3	1.5
Mass	5	3	1	1.5
Total	29.5	24.5	17	

3.7.4 Charged Particle Protection

Jupiter has the largest and strongest magnetosphere of all the planets in our Solar System. This magnetosphere traps charged particles from solar wind in belts of intense radiation around Jupiter. These particles can wreak havoc on the electrical components of the probe, so a solution must be designed in order to protect these components. A possible solution is to use dense metals, such as titanium or lead, in order to prevent these particles from reaching the delicate components. This solution is inspired by NASA's Juno spacecraft, which had a vault made of one-centimeter-thick titanium that housed the electronics of the spacecraft [17]. More analysis into the protection from charged particles will be included in the final design report, once there is a better idea of the mission's expected life.

3.7.5 TCS Description

The TCS will accomplish its goal of keeping all components of the probe within acceptable temperature limits through three parts: heating, internal heat transfer, and radiation. The heating will be mostly supplied through RHUs, but if the changing environments and operational modes experienced necessitate that some heat sources have the ability to be turned off and on, electric

heaters may also need to be used. This will be analyzed further and finalized in the final design report. Heaters will be attached to batteries, electronics, deployable mechanisms, and fuel tanks and lines. Multilayer insulation (MLI) will also be placed on the outside of structural panels in order to keep as much heat in as possible.

The internal heat transfer will be facilitated as much as possible through the structures of the probe designed by the chassis subsystem. This will save on mass as it will decrease the components used by the TCS for heat transfer. In order to transfer heat through the structures, conduction pads, thermal grease, and metal-loaded epoxy can be used at joints [18]. These methods will be explored further in the final design report. Where heat transfer through the probe's structure will not be sufficient, hardware will need to be used in the form of thermal straps, heat pipes, and/or fluid loops, in that order of precedence. Thermal straps will be used as much as possible due to their simplicity and light weight, but if the required amount of heat transfer becomes too large for the straps to be feasible, heat pipes and fluid loops may need to be used. These heat transfer mechanisms will transfer excess heat from heat sources to heat sinks.

The radiation of excess heat will be accomplished through a passive structural panel. Face sheets will be put on some of the outer structural panels of the probe in order to achieve desirable thermal properties. In the unlikely event that this is unable to provide enough radiation, a body-mounted or deployable radiator may need to be used.

3.7.6 Future Work

Future work to accomplish for the final design report begins with getting values for acceptable temperature ranges for and heat generated by all components of other subsystems during all operation modes. After, pairing with an orbiter team, different thermal environments will be defined and a system will be defined to keep all components within their temperature ranges in all thermal environments during all operational modes. Then analysis will be done to determine the amount of heat to be added to or removed from each subsystem. The arrangement of subsystems in the probe will be altered where possible to facilitate the transfer of heat through the structure of the probe. The number of RHUs and thermal straps required by each subsystem will be determined. Finally, the maximum amount of excess heat that will need to be radiated at some point during the mission will be determined and an appropriate radiator will be sized and chosen.

4 Risks

The Minos Probe is a single mode of failure spacecraft such that if any subsystem were to fail, the entire mission would be lost. For this reason, extensive thought and planning was dedicated to risk assessment and mitigation.

4.1 Power Risks and Mitigations

The electrical power system is an essential component of the spacecraft design and any form of failure within that subsystem may mean the end of the entire mission. The risks associated with the electrical power system include environmental contamination, radiation damage, RTG failure, and secondary battery failure. In the case of environmental contamination, the RTG emits radiation in the form of alpha and beta particles as a consequence of the decay process of the radioactive material (^{238}Pu) that powers the device. Since one of the key goals of the MP mission is to discover any evidence of the existence of life, any radiation leak coming from the RTG may cause any samples collected to become contaminated. In order to mitigate this risk, the RTG must have adequate shielding through a lead sheet so that radiation is blocked from escaping the device. This also applies to radiation damage, as a high dose of radiation over a period of time can damage other electronics within the spacecraft. Furthermore, in the case of an RTG failure, any structural damage done to the RTG from a launch vehicle crash or a failed landing of the spacecraft may mean the exposure of the radioactive material to the environment and a massive amount of radiation leakage. In order to mitigate an RTG failure, proper safety guidelines must be followed while handling and constructing the device to ensure it is in good condition for launch and proper protocol must be adhered to in regards to mission control and descent onto Europa. Lastly, secondary battery failure may lead to certain components not receiving enough power to perform their desired tasks and cause the mission to stall. To mitigate this risk, redundancy will be incorporated into the design with the addition of two Li-Ion batteries.

4.2 Propulsion Risks and Mitigations

The propulsion system is a source of several single point failures for the probe. A main engine failure, attitude control failure, or contamination of sample surfaces could greatly detriment the goals of the mission ranging from critical to catastrophic. Possible causes of failure for the main engine and attitude control are freezing in the tanks/lines, or a failure of the actuators and valves that allow propellant to flow from the tanks to their reaction site. To mitigate this, propellant has been selected with low freezing points as well as thermal insulation and heat will be provided by the RTG to ensure the health of the propellant system. Significant testing will be performed on the combustion chamber at a wide range of temperatures to ensure that adequate heating and cooling measures have been taken to allow for reliable operation. Lastly, the main engine will shut down at approximately two meters above the surface of Europa. The low specific gravity of the moon will limit the forces experienced by the landing gear on touchdown. The two-meter separation between exhaust gasses and the surface will provide some protection from contamination, however the deployable system will sample from just below the surface. This will further reduce the possibility of contamination from exhaust gasses.

4.3 Chassis Risks and Mitigation

The biggest risk to the chassis is structural failure of any of the components. This could be due to launch loads, landing loads, or deterioration from the environment. In order to best mitigate this sufficient designing and ground testing will be performed on the Minos Probe prior to launching.

4.4 Mechanisms/Deployables Risks and Mitigations

There are various risks involved with each mechanism/deployable described in section 3.4. As with all aspects of a spacecraft, these risks must be addressed in order to create a design that will minimize them to the best of its ability.

For the crushable legs and retro-rockets design for the landing mechanism/deployable system, the major risk comes with the crushable legs. The highest probability of failure that the legs will not be able to withstand the load applied when lander hits the surface after a 1-2-foot free fall. In order to mitigate this risk, a design was created with 6 legs. This not only provides for a distribution of the load across all 6 legs, but it also provides redundancy for the system. Should one leg fall, the lander should still be able to successfully touch down and complete its mission. Further analysis will be performed in conjunction with the structures engineer in order to make sure the design of the legs is suitable to withstand the loads to be applied on the landing.

Each piece of scientific equipment entails the risk of functionality. If the equipment does not work properly, then no data will be transmitted and the mission will be a failure. In order to mitigate this risk, space proven scientific equipment was held with the highest regard. Unfortunately, there were no space proven designs for the ice claw or the SUDA. Rensselaer's Aerospace Solutions is taking a risk by choosing to fly this equipment despite its lack of use in space as the company is confident in JPL and NASA's ability to manufacture high quality equipment. In Rensselaer's Aerospace Solutions professional opinion, the benefits outweigh the risks.

The biggest risk with the umbrella antenna design is the vibrations during launch. During the Galileo mission, the antenna was damaged due to vibrations from travel to Kennedy Space Center, and the antenna did not deploy. In order to mitigate this risk, a second "backup" antenna will likely be added to the Minos Probe. Further analysis will need to be conducted with the communications engineer to confirm this solution. If this solution is not implemented, Rensselaer's Aerospace Solutions is comfortable with the risk, as the umbrella method is highly proven in space, with few failures.

Table 16 displays the risk matrix used to determine the risk involved with each mechanism.

4.5 Command and Data Risks and Mitigations

The biggest risk to command and data will be the harsh environment of Europa and deep space. The severe cold will likely begin to deteriorate the CPU and electronics. In order to best mitigate this, a sufficient thermal control system will be implemented coupled with ground testing and proper design.

4.6 Communications Risks and Mitigations

Communications is a mission critical system and failure of the system would kill the mission. Component failure could render the communications system useless. Flight tested equipment that

has been used on past missions will be selected to help mitigate a component failure. Additionally, two frequency bands will be used with independent transceivers, each having multiple antennas. This will ensure that anything short of a catastrophic failure to the communications system, the probe will be able to communicate to the orbiter in some fashion.

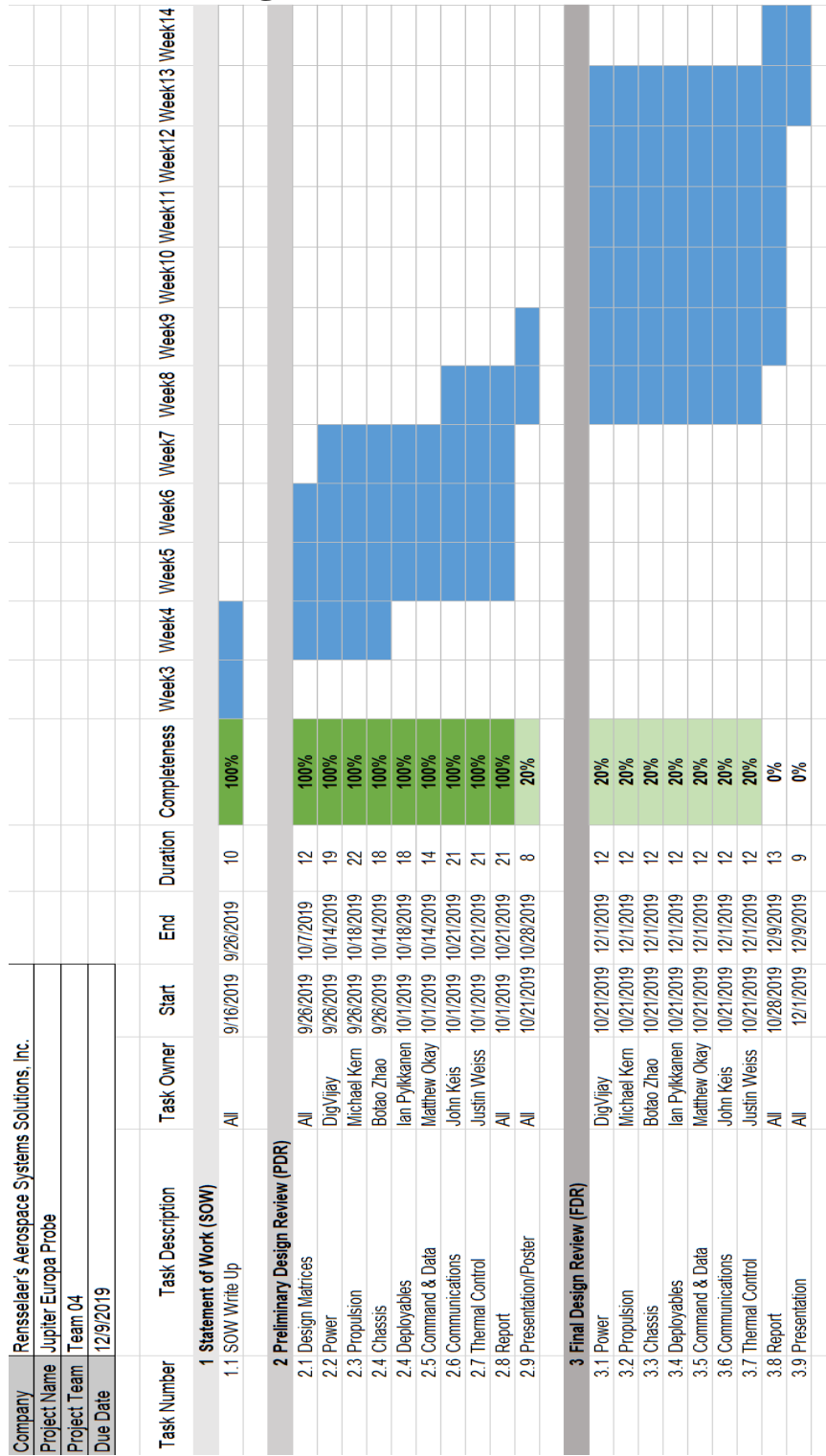
Europa is known to have an atmosphere and it is possible that frozen water droplets are present which could introduce interference to the communication system. To avoid any risks to the transmission of commands and data due to atmospheric interference, the frequencies selected are UHF and X-band, both of which are not known to be affected by this type of interference.

The orbiter's trajectory could also introduce a risk should it be out of range of the communication system. The landing site of the probe could also impose a communications risk if there is an object in-between it and the orbiter during the window of communications time. Proper mission planning and landing site selection will be critical to mitigate these risks.

4.7 Thermal Control Risks and Mitigations

Thermal Control is a critical subsystem of the probe. Failure to properly control the temperature of the probe's components could potentially result in their failure, which could be detrimental to the overall mission. Most risk mitigation will be accomplished by creating an accurate mathematical model for which to analyze the thermal properties of and the heat transfer through the probe. Most methods in the thermal control system are passive, so improper temperature control due to an inaccurate mathematical model won't be corrected by on-board computers. To mitigate the risk of excess heat building up, the radiator may be covered by a passive louvre that uses springs which open the louvre when their temperature rises. Mitigating the risk of components getting too cold can be accomplished by adding more RHUs than necessary and radiating away the excess heat created. More risk mitigation strategies will be explored and discussed in the final design report.

5 Timeline and Planning



6 Conclusion

This report outlines the preliminary design for the Minos Probe set to land on Jupiter's moon Europa. The Minos Probe will be a hexagonal plate structure lander made from 2219-T87 Aluminum Alloy carrying $\text{N}_2\text{O}_4 - \text{N}_2\text{H}_4$ fuel. A ^{238}Pu MMRTG with a lithium-ion battery will be used to supply and store power for the lander while an RHU and thermal straps system will be used to transfer heat and keep the Minos Probe warm in Europa's harsh climate. Crushable legs and retro-rockets will be used for landing the probe on Europa's surface where an ice claw, SUDA, SAM, and Mastcam-Z will be used to collect data samples. A UHF Omni and Low Gain antenna will be used to transmit this data to the RO over a Lower UHF band. With this equipment and design, the anticipated lifespan of the Minos Probe is around one year.

This design finds the perfect medium of ambition and reliability given its cutting edge and space proven technology. NASA and ESA have invested an immense amount of time and money in the pursuit of landing on Europa. This design of the Minos Probe provides opportunities to make unprecedented achievements and proved ground-breaking discoveries. NASA and ESA are embarking on a voyage decades in the making to find life elsewhere in this universe, and the Minos Probe will be the ship.

References

- [1] H. H. Haglund, "Surveyor III: Mission Report," JPL, 1 September 1967. [Online]. Available: <https://www.hq.nasa.gov/alsj/a12/Surveyor-III-MIissionRpt1967028267.pdf>. [Accessed 2019 October 18].
- [2] F. V. Bennett, "Apollo Lunar Descent and Ascent Trajectories," NASA, 19-21 January 1970. [Online]. Available: <https://www.hq.nasa.gov/alsj/nasa58040.pdf>. [Accessed 20 October 2019].
- [3] C. D. Brown, Elements of Spacecraft Design, Reston, VA: American Institute of Aeronautics and Astronautics, Inc., 2002.
- [4] T. Greicius, "NASA Tests Robotic Ice Tools," 30 March 2017. [Online]. Available: <https://nasa.gov/feature/jpl/nasa-tests-robotic-ice-tools>.
- [5] E. Howell, "Europa: Facts About Jupiter's Icy Moon and Its Ocean," Space.com, 22 March 2018. [Online]. Available: <https://www.space.com/15498-europa-sdcmp.html>. [Accessed 22 October 2019].
- [6] "SAM," [Online]. Available: <https://mars.nasa.gov/msl/spacecraft/instruments/sam/>.
- [7] "Mastcam-Z for Scientists," [Online]. Available: <https://mars.nasa.gov/mars2020/mission/instruments/mastcam-z/for-scientists/>.
- [8] P. L. Conley, Space Vehicel Mechanisms: Elements of Successful Design, New York: John Wiley & Sons, Inc., 1998.
- [9] "STS-34 Galileo processing at KSC's SAEF-2 planetary spacecraft facility," [Online]. Available: <https://science.ksc.nasa.gov/mirrors/images/images/pao/STS34/10063715.jpg>.
- [10] W. Rits, "A Multipurpose Deployable Membrane Reflector - A New Design Concept," November 1996. [Online]. Available: <https://www.esa.int/esapub/bulletin/bullet88/rits88.htm>.
- [11] "Cassini Mission History," [Online]. Available: <https://solarsystem.nasa.gov/missions/cassini/mission/spacecraft/huygens-probe/>.
- [12] H. H. M. V. P. C. G. H. M. K. C. CLAUSEN1, "THE HUYGENS PROBE SYSTEM DESIGN," ESA Science Directorate, Scientific Project Department, ESTEC, Postbus 299, NL-2200 AG, 2002.
- [13] "Mars 2020 Mission," [Online]. Available: <https://mars.nasa.gov/mars2020/mission/rover/brains/>.

- [14] B. Systems, "RAD750 3UCompactPCI Technical Specificaitons," 2018. [Online].
- [15] D. G. Gilmore, *Spacecraft Thermal Control Handbook*.
- [16] "Thermal Control," NASA, [Online]. Available: <https://sst-soa.arc.nasa.gov/07-thermal>. [Accessed 22 October 2019].
- [17] "Juno Armored Up to Go to Jupiter," NASA, 12 July 2010. [Online]. Available: https://www.nasa.gov/mission_pages/juno/news/juno20100712.html. [Accessed 22 October 2019].
- [18] M. D. Griffin and J. R. French, *Space Vehicle Design*.
- [19] K. C. Wu, J. Antol, J. J. Watson, R. J. Saucillo, D. D. North and D. D. Mazanek, "Lunar Lander Structural Design Studies at NASA Langley," National Aeronautics and Space Administration, Hampton, Virginia, 2006.
- [20] R. C. Wiens, "ChemCam: Laser Induced Remote Sensing for Chemistry and Micro-Imaging," Los Alamos National Laboratory, Santa Fe, New Mexico, 2004.
- [21] J. Taylor, A. Makovsky, A. Barbieri, R. Tung, P. Estabrook and A. G. Thomas, "Mars Exploration Rover Telecommunications," National Aeronautics and Space Administration, Pasadena, California, 2005.
- [22] J. Taylor, D. K. Lee and S. Shambayati, "Mars Reconnaissance Orbiter Telecommunications," National Aeronautics and Space Administration, Pasadena, California, 2006.
- [23] T. Reichhardt, "Legs, Bags, or Wheels? When choosing landing gear for Mars spacecraft, engineers have to weigh their options-literally.,," August 2007. [Online]. Available: <https://www.airspacemag.com/space/legs-bags-or-wheels-19349872/?no-ist>.
- [24] N. Narayanan, "Jupiter's watery moon Europa shares eerie similarity with earth's sea; Scientists puzzled," 13 June 2019. [Online]. Available: <https://www.ibtimes.sg/jupiters-watery-moon-europa-shares-eerie-similarity-earths-sea-scientists-puzzled-31261>.
- [25] J. Hsu, "DUAL DRILL DESIGNED FOR EUROPA'S ICE," 15 April 2019. [Online]. Available: <https://www.astrobio.net/news-exclusive/dual-drill-designed-for-europas-ice/>.
- [26] E. Howell, "Parachutes, Sky Cranes and More: 5 Ways to Land On Mars," July 2016. [Online]. Available: <https://www.space.com/33483-mars-landing-technology-viking-curiosity-rover.html>.
- [27] T. Greicus, "Electra Relay Radio on MAVEN Mission to Mars," 28 February 2014. [Online]. Available: <https://www.nasa.gov/jpl/maven/electra-relay-radio-pia17952/#.XbDOq-hKiUl>.

- [28] D. Brown, G. Webster, G. Diller and R. Jessica, "Mars Science Laboratory Launch," National Aeronautics and Space Administration, Washington D.C., 2011.
- [29] R. C. Anderson, "Mars Science Laboratory Participating Scientists Program Proposal Information Package," National Aeronautics and Space Administration, Pasadena, California, 2010.
- [30] "Step-by-Step Guide to Entry, Descent, and Landing," [Online]. Available: <https://mars.nasa.gov/mer/mission/timeline/edl/steps/>.
- [31] "Space Communications with Mars," [Online]. Available: <http://www.astrosurf.com/luxorion/qsl-mars-communication3.htm>.
- [32] "RADIO FREQUENCIES FOR SPACE COMMUNICATION," [Online]. Available: <http://www.spaceacademy.net.au/spacelink/radiospace.htm>.
- [33] "Radar for Europa Assessment and Sounding: Ocean to Near-Surface (REASON)," [Online]. Available: https://www.lpi.usra.edu/opag/meetings/aug2015/presentations/day-1/8_f_REASON.pdf.
- [34] "Properties of Aluminum Alloys at Cryogenic and Elevated Temperatures," [Online]. Available: <https://www.totalmateria.com/page.aspx?ID=CheckArticle&site=ktn&NM=23>.
- [35] "EUROPA FIRST," 20 February 2009. [Online]. Available: <https://www.astrobio.net/europa/europa-first/>.
- [36] "Communications With Earth," [Online]. Available: <https://mars.nasa.gov/msl/mission/communications/#data>.
- [37] "CheMin," [Online]. Available: <https://mars.nasa.gov/msl/spacecraft/instruments/chemin/>.
- [38] "ASM Aerospace Specification Metals," [Online]. Available: <http://www.aerospacemetals.com/contact-aerospace-metals.html>.

Appendices

Deliverables

Table 18: Course Deliverables

Date	Deliverable
21-Oct-19	Preliminary Design Report
28-Oct-19	Preliminary Design Presentation Poster
9-Dec-19	Final Design Report
9-Dec-19	Final Design Presentation Poster

Risk Tables

All risk tables were calculated using NASA's risk assessment matrix where severity is ranked as either negligible, marginal, critical, or catastrophic.

Table 19: Power System Risk Table

Risk	Potential Cause	Severity	Mitigation
Environmental Contamination	Radiation from RTG	Critical	Adequate Shielding
RTG Failure	Launch Vehicle/Spacecraft Crash or Explosion	Catastrophic	Extensive Ground Testing, Mission Control Design
Secondary Battery Failure	Environmental factors	Critical	Redundancy, Quality Control, Extensive Ground Testing
Radiation Damage	Radiation from RTG	Critical	Adequate Shielding

Table 20: Propulsion System Risk Table

Risk	Potential Cause	Severity	Mitigation
Engine Failure	Environmental factors	Catastrophic	Extensive research, Thermodynamic analysis of components at wide range of temperature bands
Attitude Control Failure	Actuator failure due to environmental factors	Catastrophic	System Redundancy, robust actuators
Environmental Contamination	Toxic products of combustion	Critical	Descent engine shutdown at an altitude of 2m, Drill into ice to collect samples

Table 21: Chassis Risk Table

Risk	Potential Cause	Severity	Mitigation
Landing Gears Release/Engage System Failure	Components Failure, Environmental Factors	Catastrophic	Manufacturing Quality Control, Extensive Ground Testing
Structural Failure	Engineering/Design Failures, Environmental Factors	Catastrophic	Extensive Ground Testing

Table 22: Mechanisms/Deployables System Risk Table

Risk	Potential Cause	Severity	Mitigation
Crushable Legs Failure Under Landing Loads	Component Failure, Environmental Factors	Marginal	Quality Design, Redundancy Manufacturing Quality Control, Extensive Ground Testing
Scientific Equipment Failure	Component, Failure, Environmental Factors	Catastrophic	Quality Design, Quality Control, Extensive Ground Testing
Antenna Deployment Failure	Component Failure, Structural Damage During Launch	Critical	Redundancy, Quality Control, Extensive Ground Testing

Table 23: Command and Data System Risk Table

Risk	Potential Cause	Severity	Mitigation
CPU Failure	Component Failure, Damage During Launch, Environmental Factor	Catastrophic	Parallel Processing Units
Software Bug	Human Error, Unforeseen Environmental Factors	Negligible-Critical (Depending on the Bug)	EEPROM access to fix bugs, parallel processing unit
Low Processing Speeds	Extreme Cold	Marginal	Thermal Control to uphold CPU's thermal specifications

Table 24: Communications System Risk Table

Risk	Potential Cause	Severity	Mitigation
Component failure	Gimbal failure, HGA deployment failure, Electronics failure of transceiver	Catastrophic	Use flight heritage equipment, extensive ground testing, redundancy
Communications Interference	Atmospheric conditions, obstruction by planetary object	Critical	Ensure RO trajectory is planned properly
Safety of Assembly and Test Technicians	Unsafe working conditions, care not taken while working on energized equipment	Critical	Adhere to electrical safety guidelines, Proper oversight while testing
Environmental, Cultural, Political, Social	N/a	Negligible	N/a

Table 25: Thermal System Risk Table

Risk	Potential Cause	Severity	Mitigation
Environmental Contamination	Radiation from RHU	Critical	Shielding on RHU
Overheating of Probe	Louver malfunction	Critical	Independently actuating each louver blade with bimetallic springs
Failure to Regulate Temperature Properly	Inaccurate mathematical model	Critical	Quality Control, Redundancy, Extensive Ground Testing

Table 26: MER X-band and UHF Mass and Input Power Summary

Assembly	Input Power, W	RF Power out, W	Mass, kg	Quantity	Mass Total, kg	Dimensions, cm
X-Band						
SDST each			2.682	1	2.682	$18.1 \times 11.4 \times 16.6$
Receiver (R) only	11.0					
R+exciter, two-way (coherent)	13.3					
R+exciter, one-way (aux osc)	13.8					
SSPA	58	16.8	1.300	2	2.600	$4.4 \times 17.2 \times 13.4$
Hybrid			0.017	1	0.017	2.5×1.0
WTS			0.378	1	0.378	$4.1 \times 9.65 \times 10.9$
CTS			0.062	3	0.187	$5.3 \times 3.0 \times 4.0$
Coax			0.057	4	0.228	
Diplexer			0.483	1	0.483	$27.7 \times 5.6 \times 7.9$
Attenuator			0.004	1	0.004	0.79×2.18
HGA			1.100	1	1.100	28.0 dia.
CLGA			0.431	1	0.431	10.0×2.3
BLGA			0.235	1	0.431	10.3×3.5
RLGA			0.775	1	0.431	60.2×3.1
PLGA			0.020	1	0.020	1.5×1.5
MGA			0.499	1	0.499	23.4×13.4 at rim
Terminations, dummy loads, etc.			0.006	4	0.026	
X-band totals	71.8 max	16.8	5.367		6.835	
UHF						
UHF transceiver	6 rx only 43 rx/tx	12 *	1.900	1	1.900	$5.1 \times 6.8 \times 3.7$
Diplexer			0.400	1	0.400	$2.9 \times 3.7 \times 1.3$
CTS			0.083	1	0.083	$5.3 \times 3.0 \times 4.0$
RUHF			0.100	1	0.100	$16.9 \times 1.9 \times 1.9$
DUHF			0.100	1	0.100	$16.9 \times 1.9 \times 1.9$
Coax			0.300	1	0.300	

* UHF RF power out is measured at diplexer output.

Table 27: MRO Telecom Mass and Power Summary

Assembly	Subtotal, kg	Total mass, kg	Spacecraft power input, W	RF power output, W	Note
X-band transponder		6.4	16		Orbit average power
SDSTs (2)	5.8				
x4 frequency multiplier+bracket	0.1				
Other microwave components	0.5				
Traveling-wave tube amplifiers		12.1			
X-band TWTA (2)	1.9		172	102	100 W nominal
Ka-band TWTA	0.8		81	34	35 W nominal
X-band electronic power converters	3.0				
Ka-band electronic power converter	1.5				
Diplexers and brackets	1.8				
Waveguide transfer switches	1.5				
Other microwave components	1.4				
Miscellaneous TWTA hardware	0.2				
X-band and Ka-band antennas		22.6			
HGA prime reflector	19.1				
Antenna feed assembly	1.6				
LGAs and polarizers	0.8				
Miscellaneous antenna hardware	1.1				
HGA gimbals and drive motors		45.0	14		Orbit average power
Waveguides and coax		8.3			
USOs (2)		1.7	5		Orbit average power
UHF subsystem		11.5			
Electra transceivers (2) (each transciever has an integral solid-state RF power amplifier)	10.1		71	5	On, full duplex (17.4 W standby)
UHF antenna and radome	1.4				
String switch (S)	0.1				
Telecom total		<u>107.7</u>	<u>359</u>		